The FoxA1/FoxA2-LIPG axis regulates breast cancer growth through changes in lipid metabolism

Juan Felipe Slebe Concha

Tesi Doctoral UPF - 2013

Directors

Joan Guinovart, PhD

And

Roger Gomis, PhD

Tutor

Miguel Ángel Valverde, PhD

Institute for Research in Biomedicine, Barcelona

Metabolic Engineering and Diabetes Laboratory

INSTITUTE FOR RESEARCH IN BIOMEDICINE

IRB BARCELONA

Experimental and Life Science Department

upf. Universitat Pompeu Fabra Barcelona

A mis padres y hermanos

Acknowledgements

Pensar que el doctorado está llegando a su fin y que estoy acá escribiendo los agradecimientos es total. Por supuesto que hay una mezcla de emociones y sensaciones, terminar un trabajo que comenzó hace 5 años con una idea vaga y sin sentido y que luego se ha convertido en un trabajo con base y resultados, es increíble. Sin embargo, también hay un sentimiento de tristeza ¿extraño no?, sí porque sin duda terminar la tesis significa cambiar de ciclo y de lugar. Dejar de una u otra manera a mucha gente que le da el verdadero valor a este tiempo fuera de casa. Y de esto se trata al final todo, de la gente que nos rodea y nos permite crecer, superar obstáculos y al final del día (frase típica de pancho) sentirnos parte de una familia. Es acá donde los agradecimientos se convierten en la sección más importante de la tesis.

Voy a comenzar por aquellas personas que han estado conmigo durante años, desde siempre. A mis padres y familia, son un pilar gigante y sí viejos, ustedes son mis héroes. Cada uno posee cualidades increíbles y espero poder imitarlas algún día (ser desordenado es genético, creo que no se puede cambiar ¿verdad?). Seguramente estoy simplificando al agradecer a los bomberos en general, no puedo colocar en palabras todo lo que he aprendido en la primera compañía, desde los incendios y rescates vehiculares hasta las tardes de camaradería y bautizos. A los amigos de siempre, duri, provo, figue, juanes, pollo, pancho, guardita, migri, tobi, malrro y calpani nada que decir, nos conocemos desde años y aún nos aguantamos, seguro seguiremos siendo excelentes amigos. A la Stefanía de Mónaco y la chini, cada año que pasa las quiero más. Hemos logrado crecer juntos y ahora más maduros nuestra amistad es impagable.

A mi director de tesis, muchas gracias Joan por haberme aceptado en tu laboratorio, por la confianza, apoyo y la libertad científica que me has dado. Sobre todo, por ser esa persona apasionada por la ciencia y el conocimiento. Por esas charlas científicas, casi de ficción, los viernes a las 9 o 10 PM. Algún día podríamos hacer un guión para Hollywood. Si bien es difícil hacer una tesis

en este laboratorio y muchas veces el camino se ve empantanado, me quedo con tu mejor cualidad (dentro de muchas; siiiii soy un pelota ajja): descubrir y lograr maravillarse en el camino. A mi segundo director, Roger Gomis, gracias por participar en este proyecto y por aportar con la planificación, ideas y sobretodo la calma necesaria a mis ideas locas, fueron muchas.

A la gente del laboratorio muchas gracias por todo, a Emma, Anna y Carol por hacer que el laboratorio funcione como lo hace. En este último capítulo de la tesis he encontrado en ustedes a grandes personas. En particular a Emma (siempre lo pronuncio mal), gracias por aguantar placas con nombres raros, cambios de planificación a última hora, el tampón para romper núcleos y cargar cien mil veces hasta que salga bien. Por ser una muy buena amiga, ojalá que Brad Pitt no sea muy llorón. Como olvidar a Mar, esos gritos de sinfonía por las mañanas o esas historias de risas por haber metido la pata en algún momento o con alguien. Mar, gracias por ser una persona preocupada por nosotros, en particular por la ayuda en el lab y por las conversaciones divertidas fuera de él. Iliana, mi compi de despacho, llevamos dos días y de seguro ya estas harta de mí, mis intentos de cantos y mis papeles. Siempre estás dispuesta a ayudar a todos e increíblemente con una gran sonrisa, el paper de PTG será un éxito. A Jordi, gracias por la ayuda con diseño de primers, sondas etc. A todos los ex miembros del laboratorio, Jordi, Carles, Joaquim, Carlos, Oscar, Delia, Susana y Adelaida hemos compartido muchos momentos buenos. Laura siempre me acuerdo del menú libre de químicas, y por supuesto toda la ayuda en el inicio del proyecto, desde la interpretación de datos hasta cómo hacer qPCR. Lo más importante, con el paso de los años he ganado a una amiga. A Isabel, gracias por la ayuda y apoyo dentro y fuera del lab, además por los buenos momentos en ellos. Espero que tengas mucho éxito en Köln.

A los del fútbol y/o básquet Johan, Jordi Lanuza y Marta (que grupo) siempre es bueno tener gente conocida, pero tener amigos como ustedes es mucho mejor. Espero que sigamos compartiendo mucho más. A Marta, por hablar como mejicana y ser la mejor de las catalanas, gracias por todo (siempre me acordaré: la mejor tesis jajaj). Lucho y Claire, ha sido un placer conocerlos.

Claire eres un amor, muchas gracias por ayudarme en las correcciones de la tesis y las mañanas de pitis cuando llegaste, me alegra mucho que estés en el lab. Giorgia, llegar al lab y encontrarte riéndote con esa risa exagerada italiana no tiene precio. Gracias por alegrarme los días, aunque sea con el ceño fruncido, y por recordarme a la ciencia tal como me gusta. Aunque no me creas, estoy seguro que serás una súper científica y que por supuesto, seguirás llegando en una bicicleta de 1810 a trabajar; espero disfrutar de tu alegría por mucho. A Valerie, nunca he comido mejores papas fritas, pero de lejos nuestras conversaciones de 3 horas sobre la vida y otros ha sido lo mejor. Espero encontrarnos en unos años más en chile junto con guapi. Ah, seguro serás seca en tu nuevo trabajo. A JP por todas esas charlas de ciencia y consejos de vida, se nota que ya eres medio viejujo pero me has ayudado muchísimo, nunca olvidaré esas salidas a comer de 50 euros.

A mis compis de piso, Mili y Adela, que me han aguantado este tiempo con el desorden y las cenas en las que la casa queda patas para arriba. Mili con tu balcánica personalidad has sabido aconsejarme súper bien, eres lo máximo (deberías descubrir el ajo sin olor jjj).

Por último, a mi familia en Barcelona, los Barrigas (Pancho, Javi, Anita, Pablo y Carlos). Gracias Javi y Pancho por brindarme su cariño y recibirme como a un miembro de su familia. Ustedes han sido una parte fundamental por la que he podido terminar esta tesis y por todos los buenos momentos que he tenido en Barcelona, de verdad son mis hermanos. No tengo la menor duda que en unos años haremos retreats juntos, solo para tener un pretexto y tomar piscolas.

Por último y como dijo Cerati (Soda Stereo) en su último concierto.

Gracias Totales.

Abstract

The Fox transcription factor family comprises FoxA1, FoxA2 and FoxA3, which regulate tissue development and metabolism. In breast cancer, FoxA1 together with estrogen receptor regulates tumor growth and luminal specification. However, it is still unclear whether other members of the FoxA family participate in breast cancer pathogenesis and whether they contribute to tumor metabolic dependence. Here we show that FoxA1 and FoxA2 expression is mutually exclusive across different human breast cancer cell lines. Although both transcription factors regulate different set of genes and biological responses, they promote *in vitro* and *in vivo* tumor growth through the expression of endothelial lipase (LIPG). LIPG is ubiquitously expressed across various breast cancer subtypes, as seen in human cell lines and primary tumors. Furthermore, it has the capacity to rescue the loss of FoxA factors regulating a network enriched in oncogenic and structural lipids known to mediate proliferation. These findings collectively reveal how the FoxA1/FoxA2-LIPG axis regulates a central hub of lipids required for the growth of breast cancer.

Resumen

La familia de factores de transcripción FoxA está compuesta por FoxA1, FoxA2 y FoxA3. Estos factores regulan el desarrollo y el metabolismo de diversos tejidos. En cáncer de mama, FoxA1 media la acción de estrógenos y andrógenos regulando la especificación y el crecimiento del subgrupo luminal. No obstante, aún es desconocida la participación de los otros miembros de la familia en el desarrollo tumoral o su posible función en la dependencia metabólica de éstos. En esta tesis se describió que la expresión de los factores de transcripción FoxA1 y FoxA2 es mutualmente exclusiva en diferentes líneas celulares de cáncer de mama humanas. A pesar de que FoxA1 y FoxA2 controlan diferentes programas génicos y diferentes respuestas biológicas, ambos promueven el crecimiento tumoral *in vitro* e *in vivo* regulando la expresión de la enzima lipasa endotelial (LIPG). LIPG se expresa ubícuamente en líneas celulares humanas y tumores primarios de diferentes subgrupos de cáncer de mama. Además, LIPG es capaz de rescatar la pérdida de los factores FoxA regulando una red de lípidos oncogénicos y estructurales que median proliferación. Estos hallazgos revelan colectivamente que el eje FoxA1/FoxA2-LIPG regula un nicho central de lípidos que son necesarios para el crecimiento de cáncer de mama.

Preface

During decades the main focus of cancer metabolism has been devoted to understand the importance of the Warburg effect, aerobic glycolysis. Several studies show how cancer cells adapt their glycolytic flux in order to survive and grow, generating metabolic intermediates to fulfill the synthesis of biomolecules. In this work we explored the contribution of FoxA1 and FoxA2 transcription factors in the metabolic dependence of breast cancer cells. We identified that FoxA factors were differentially expressed in breast cancer, showing a mutually exclusive pattern in cells, and contributing to breast cancer growth.

Because FoxA factors regulate the metabolic response in multiple tissues and the loss of one could be rescued by the other, we hypothesized that both factors were regulating similar metabolic pathways in breast cancer. In this sense we identified a common FoxA regulated enzyme, named endothelial lipase (LIPG). LIPG regulates the growth of breast cancer lines by controlling common lipids known to be contributors to cancer pathogenesis.

Our work contributes to the knowledge of breast cancer pathogenesis and cancer metabolism in several aspects. FoxA1 is a known factor involved in the estrogen response modulating luminal specification. First, we uncover the participation of the FoxA2 transcription factor as a new contributor of breast cancer pathogenesis. We observed that FoxA2 was overexpressed in a triple negative human breast cancer cell line and in patient samples. Furthermore, FoxA2 deletion drives tumor growth arrest, similar to what is observed for FoxA1. These observations make FoxA2 an attractive gene to evaluate in breast cancer subgroup specification and clinical outcome.

In terms of cancer metabolism we discovered a new enzyme necessary for breast cancer growth. This enzyme is named endothelial lipase (LIPG) and it is involved in lipid metabolism. LIPG deletion in breast cancer cells drove growth arrest and remarkably, LIPG overexpression rescued the FoxA depletion phenotype. It has been highlighted that the *de-novo* lipid biosynthesis plays a

major role in cancer pathogenesis, and that several enzymes involved in the pathway are overexpressed in tumors. Contrary to what has been described, LIPG emerges as an enzyme that regulates the hydrolysis of phospholipids and the uptake of lipids from the extracellular niche. In this context, we describe a new mechanism to fulfill the lipid demands of cancer growth.

Finally, LIPG is homogeneously distributed across breast cancer subtypes. This expression pattern gives rise to the question of whether LIPG can be an attractive target for breast cancer treatment. Furthermore, it would be interesting to understand whether LIPG modulates the lipid metabolism in a broader spectrum of cancer types.

Abbreviations

2HG	2-hydroxyglutarate
ACACA	CoA carboxylase
ACL	ATP-citrate lyase
ADP	Adenosine diphosphate
AKT	Protein Kinase B
AMPK	5' AMP-activated protein kinase
AR	Androgen receptor
ATP	Adenosine triphosphate
ATX/lyso PLD	Autotaxin
BC	Breast cancer
Bcl2	B-cell CLL/lymphoma 2
BRAF	Serine/threonine-protein kinase B-Raf
BRCA1	Breast cancer type 1 susceptibility protein
C1P	Ceramide 1-phosphate
CD36	Cluster of Differentiation 36
Cdh11 OB	Cadherin 11, type 2, OB-cadherin
DG	Diacylglycerol
Dox	Doxycycline
EMT	Epithelial to mesenchymal transition
ER	Estrogen receptor
FA	Fatty acid
FASN	Fatty acid synthase
FoxA1	Forkhead box protein A1
FoxA2	Forkhead box protein A2
FoxA3	Forkhead box protein A3
G6PD	Glucose-6-phosphate dehydrogenase
GATA3	GATA-binding protein 3
GFP	Green fluorescent protein
GLS	Glutaminase
GLUT	Glucose transporter
HDL	High-density lipoprotein
HER2	Human epidermal growth factor receptor 2
HIF	Hypoxia-inducible factor
HL	Hepatic lipase
HMEC	Human mammary epithelial cells
IDH	Isocitrate dehydrogenase
KRAS	V-Ki-ras2 Kirsten rat sarcoma viral oncogene homolog
LDL	Low-density lipoprotein
LIPG	Endothelial lipase

LKB1	serine–threonine kinase liver kinase B1
Lmx1/b	LIM homeobox transcription factor 1-beta
LPA	Lysophosphatidic acid
LPC	Lysophosphatidyl choline
LPE	Lysophosphatyl ethanolamine
LPL	Lipoprotein Lipase
MAGL	Monoacylglycerol Lipase
mTORC1	Mechanistic target of rapamycin complex 1
MYB	Transcriptional activator Myb
NADPH	Nicotinamide adenine dinucleotide phosphate reduced
NGn2	Neurogenin 2
PA	Phosphatidic acid
PAF	Platelet-activating factor
PC	Phosphatidyl choline
PCA	Principal Component Analysis
PDH	Pyruvate dehydrogenase
PDK1	Pyruvate dehydrogenase kinase 1
PDX	Pancreatic and duodenal homeobox 1
PE	Phosphatidyl ethanolamine
PGM	Phosphoglycerate mutase
PHGDH	Phosphoglycerate dehydrogenase
PI3K	Phosphatidylinositol 3-kinase
PKC	Protein kinase C
PKD	Protein kinase D
PPP	Pentose phosphate pathway
PR	Progesterone
RB1	Retinoblastoma 1
RFP	Red fluorescent protein
ROS	Reactive oxygen species
SM	Sphingomyelin
SRBP1	Sterol regulatory element-binding protein 1
TCA	Tricarboxylic acid cycle
TG	Triglycerides
TGFβ	Transforming growth factor beta
TIGAR	TP53-induced glycolysis and apoptosis regulator
TP53	Tumor protein p53
VLDL	Very-low-density lipoprotein
XBP1	X-box binding protein 1

Index

Introduction

1. Breast cancer

1.1 Epidemiology

Breast cancer (BC) is a malignant neoplasm originated in the mammary gland, mainly affecting women but also men in rare cases. BC is the most frequently diagnosed cancer and the leading cause of cancer death among female, accounting for the 23% of the total cancer cases and 14 % of cancer deaths in 2008. In general, incidence rates are high in Western and Northern Europe, Australia/New Zealand and North America. Breast cancer deaths rates have been decreasing in North America and several European countries over the past 25 years as a result of early detection through mammography and improved treatment (Jemal et al., 2008). Nevertheless, the American Cancer Society estimates that 232,340 new cases of invasive breast cancer and 64,640 cases of ductal carcinoma *in situ* will be diagnosed among woman in the United States in 2013. Worldwide, an estimated 1,383,500 new cases of breast cancer will be diagnosed among woman. In 2013 458,400 deaths will be expected worldwide and 40,030 in the United Stated making this disease a health care issue (Jemal et al., 2011; Siegel et al., 2013).

1.2 Structure and cellular composition of the mammary gland

The mammary gland is composed of a diverse variety of cell types that are in a continuous interplay, which is essential for its normal development and physiological function. The normal female mammary gland grows rapidly at puberty to produce an elaborate bilayer tree-like structure resembling a branching network of ducts that end in clusters of small ductules that constitute the terminal ductal lobular units (**Figure1**). This structure is composed of an inner layer of luminal cells surrounded by an outer layer of basal cells. The majority of the basal cells are differentiated myoepithelial cells, but this layer also includes the mammary stem cells. Mammary stem cells (MaSCs) are presumed to be important for both organ development and maintaining tissue homeostasis. These cells give rise to the mature epithelium of either the luminal

or myoepithelial lineage, via a series of lineage-restricted intermediates (Russo and Russo, 2004; Visvader, 2009). The luminal cells include differentiated milk-secreting cells (during lactation) but other functional luminal cell types can be found, such as hormone receptor-expressing cells. The luminal layer is also thought to contain a number of different classes of progenitors, including progenitors for the hormone receptor-expressing cells and secretory cells. Luminal epithelial cells display polarity as shown by the localization of sialomucin (MUC1), epithelial specific antigen (ESA), occludin on the apical membrane and integrin b4 on the basolateral membrane. In contrast, myoepithelial cells influence the differentiation, polarity, proliferation and invasion/migration of adjacent luminal epithelial cells and are responsible of the contractions of the organ. Another component of the mammary gland is the mammary stroma. The stroma is comprised of extracellular matrix and various cell types that not only provide a scaffold to the organ, but also regulate mammary epithelial cell function via paracrine interactions; and that include fibroblasts, adipocytes, blood vessels, nerves and various immune cells, all of which are important for normal mammary development and function.

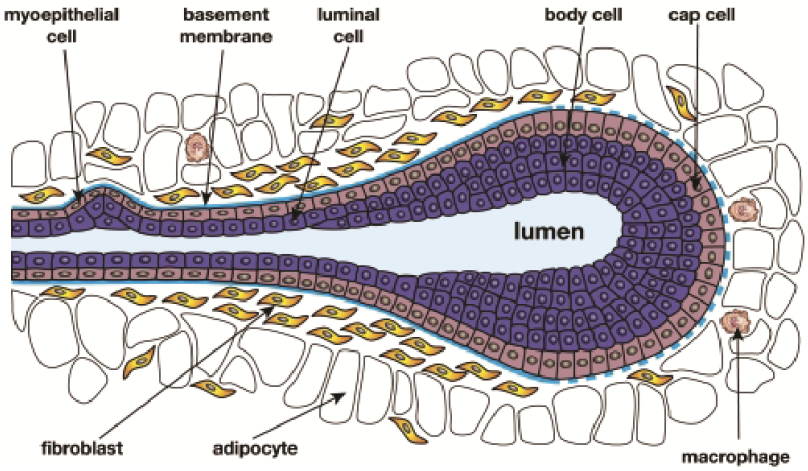

Figure 1.- Mammary gland morphology. Schematic representations of a terminal duct forming the breast, myoepithelial and luminal cells are represented. Figure adapted from (Visvader, 2009).

1.3 Breast cancer subtypes

Clinical breast cancer develops over a long period of time, and requires multiple molecular alterations. The development of BC involves the evolution of cellular

populations with increasingly aggressive phenotypic traits, characterized by variant pathological features, disparate response to therapeutics and substantial differences in long term patient survival. Considering this variability breast cancer is not just one disease with few variant subtypes, but instead represents a collection of distinct neoplastic disease of the breast and the cells composing the breast (Rivenbark et al., 2013).

Differential expression of biomarkers provides a clinical classification of BC and dictates therapeutic approaches for treatment due to their strong association with prognosis and outcome (Rakha et al., 2010; Rivenbark et al., 2013). BC are classified by their expression of estrogen receptor (ER), progesterone receptor (PR) and human epidermal growth factor 2 receptor (HER 2 or ERBB2) as well as human epidermal growth factor 1 (HER1) and various cytokeratines. Moreover samples are classified by Fluorescent in situ Hybridization (Fish) to determine ERBB2 gene amplification status.

Approximately 70% of invasive breast cancer express ER (Anderson et al., 2002) and the majority of ER expressing cancer also express PR (Cui et al., 2005; Rakha et al., 2007). Discrepant ER and PR expression patterns (ER+/PR-) and (ER-/PR+) are sometimes observed (Rakha et al., 2007). Collectively the ER+ malignant neoplasm are classified as luminal cancers. These cancers are further subclassified based on their HER2 status and proliferation rate giving rise to the ER+/PR+/HER2+ and ER+/PR+/HER2- subtypes. The ER- breast cancers are subclassified as HER2+ and triple-negative based on HER2 overexpression or gene amplification status, basal cytokeratin expression and HER1 expression, given rise to ER-/PR-/HER2+ (HER2-enriched) and ER-/PR-/HER2- (triple negative) subtypes. Triple negative breast cancer tumors are classified as basal-like tumors (Rivenbark et al., 2013).

The cell origin of the different molecular breast tumors is still under debate. Nevertheless upon gene expression profiles of the different breast cancers subtypes, human mammary stem cells (MaSC), luminal progenitors, mature luminal and stroma populations has provided insights in this issue. As predicted, the signature of differentiated luminal cells in breast tissue showed a profound

similarity with the luminal type of breast cancers indicating that many of these cancers may arise from progenitors within the luminal sublineages. Breast cancer containing mutations in BRCA1 gene frequently display a basal- like phenotype. Interestingly, deleting Brca1 in mouse mammary epithelial luminal progenitors produces tumors that resemble the majority of sporadic basal like breast cancer. Contrary, deletion of Brca1 in basal stem cells does not generate tumors that resemble the histological characteristic of human BRCA1 tumors or human basal breast cancers (Molyneux et al., 2010). Moreover, analysis of breast tissue from BRCA1 mutation shows an expanded luminal progenitor population. Gene expression analysis of breast tissue heterozygous for a BRCA1 mutation and basal breast tumors were more similar to normal luminal progenitor cells that any other subpopulation isolated (Lim et al., 2009). This evidence may indicate that the origin of this breast cancer type derived from luminal progenitors and not from stem cell as presumed before. **Figure 2A** shows a schematic representation of human breast epithelial hierarchy and potential relationships with breast tumors subtypes.

1.4 Molecular classification of breast cancer

As the expression status of ER, PR and HER2 is able to classify breast cancer tumors, early studies of transcription profiles using DNA microarrays identified several molecular subtypes of breast cancer. Gene expression profiles generated for individual breast cancer among large cohorts of breast cancer samples identified clusters based on common gene expression patterns driven by overexpressed genes. Perou et al proposed four major molecular subtypes: ER+/luminal, HER2+ (HER2-enriched), basal like and normal like. Subsequent transcription profiles determined that these classifications were reproducible among different breast cancer cohorts (Perou et al., 1999; Perou et al., 2000). Currently this classification is recognized as molecular portraits of human breast tumors and is constituted by luminal A, luminal B, HER2+, basal like, normal like and claudin low breast cancer subgroups (**Figure 2B**). Moreover there is a new group named as apocrine like (Doane et al., 2006; Farmer et al., 2005). Interestingly, although the gene expression profiling classification system was not initially developed to predict clinical outcome, the different molecular breast

cancer subtypes were found to be associated with distinct overall and relapse-free survival rates (Sorlie et al., 2001). In fact, the breast cancer subtypes not only express particular molecular markers and are associated differently with prognosis but they also display different physiopathological and histological grade, and respond differentially to treatment. Basal like and HER2+ subtypes are associated with shortest survival times. Although breast cancer classification methods show good reproducibility, suggesting that these are robust biological subtypes, breast cancers that are not classifiable are identified with regular frequency (Prat and Perou, 2011).

A

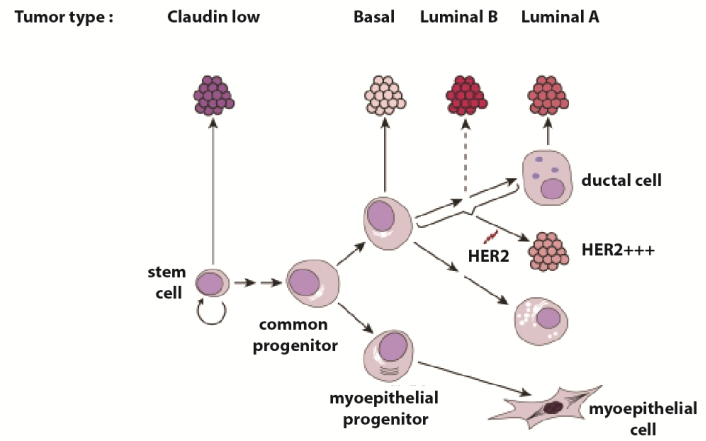

B

	Expression markers	Common features	Clinics
Luminal A	ER/GATA3/ FOXA1/XBP1/MYB	retain RB and TP53 activities	long term survival
Luminal B	ER/GATA3/FOXA1/ XBP1/MYB and HER2	TP53 mutations ATM loss MDM2 amplification	long term survival
HER2+++	ER-/HER2	CD4/CD1 amplification	poor overal survival
Basal	Triple negative ER-/PR-/HER2-	myoepithelial features mutations in TP53/BRACA1/RB	poor overal survival
Claudin low	Triple negative ER-/PR-/HER2-	EMT/stem cell markers enrichment	poor overal survival

Figure 2.-. Most representative BC Molecular subtypes A) Schematic model of the human breast epithelial hierarchy and potential relationships with breast tumor subtypes. The five different tumor types are with their closet normal epithelial counterpart based on gene expression analysis. Figure adapted from (Visvader, 2009). **B)** Molecular classification BC with their remarkable features

1.4.1 Luminal A and Luminal B Breast Cancers

ER+ breast cancers occur most frequently and comprise two major molecular classifications: luminal A and luminal B. The expression status of proliferation-associated genes is one major discriminator between Luminal A and Luminal B breast cancer. Both groups are associated with a good prognosis and excellent long term survival (80% to 85% 5-years) (Prat and Perou, 2011). They have a luminal expression signature which contains overexpression of ESR1, GATA3, FOXA1, XBP1 and MYB. Moreover analysis comparing luminal versus basal subtypes emphasized the FOXA1-ER complex as a critical network hub in this tumor group ((CGAN), 2012).

Luminal A tumors are ductal in situ low grade carcinomas with a frequency of 28-31% being the most common carcinomas. They are indolent and sensitive to anti-estrogen therapy (Tamoxifen) (Rivenbark et al., 2013). They retain more activities of tumor suppressor genes as RB1 and TP53 that Luminal B type ((CGAN), 2012). Luminal B breast cancer represent approximate the 20% of patients in any given data base and express the estrogen receptor accompanied by amplification and/or overexpression of HER2 gene (Prat and Perou, 2011). Luminal B subtype is more aggressive, display higher grade of lesions and present higher frequency of TP53 mutations. In addition they show ATM loss and MDM2 amplification and moreover cyclin D1 amplification. MYC and FOXM1 associated proliferation is hyperactivated in this subtype ((CGAN), 2012). Luminal B subtype show worst respond to the anti-estrogen therapy compared to Luminal A breast cancer subtype, however targeted HER2 therapy with trastuzumab and adjuvant chemotherapy has improve their survival (Baselga et al., 2006).

1.4.2 Basal-like carcinomas and Claudin-Low Breast Cancers

Together represent subsets of triple negative breast cancers, lacking expression of ER, PR and HER2 (Rivenbark et al., 2013). Basal-like tumors exhibit some characteristics of breast myoepithelial cells moreover represent the 15% of all breast cancers and have high rates of cell proliferation and extremely poor clinical outcomes (Prat and Perou, 2011). This subtype of tumors show high frequency of TP53 mutations (80%), which when inferred with

TP53 pathway activity suggest that loss of TP53 function occurs in almost all basal like cancers. In addition loss of BRCA1 and RB tumor suppressor are basal like features. Many of the components of the PI3K pathway activity and RAS-RAF-MEF pathway as well as EGFR are amplified. Keratins 5, 6 and 17 are common characteristic of basal-like subtypes. Others RKT receptors that are amplified include FGFR1, FGFR2, IGFR1, KIT, MET and PDGFRA ((CGAN), 2012). These tumors carry a great degree of genomic instability and often metastasize to visceral organs. Despite being very aggressive most of them are sensible to chemotherapy.

Claudin-low breast cancers represent the 10% of all breast cancers. They are enriched for markers of epithelial to mesenchymal transition and stem cell-like and /or tumor initiating cell features. As basal-like tumors patients this breast cancer subtype has poor recurrence free survival and overall survival outcomes (Prat et al., 2010).

1.4.3 HER2+ Breast Cancers

This sub-type of breast tumors account for the 17% of all breast cancers cases and are classified as high grade tumors (Prat and Perou, 2011). As expected, this group has HER2 overexpression or DNA amplification with overexpression of multiple HER2 amplicon associate genes. CDK4 and cycline D1 is amplified. Data comparison between HER2+ breast cancers with luminal HER2+ subgroup identified higher expression in FGFR4 and EGFR and higher mutations in TP53. Moreover, they have higher pSRC and pS6 protein expression as well ((CGAN), 2012). HER2+ breast cancers have worst clinical outcomes, nevertheless the trastuzumab treatment has improved the long term outcomes for these patients (Baselga et al., 2006).

1.4.4 Normal like Breast Cancers

The normal-like breast cancers are so designated because they tend to cluster closely with normal breast epithelium in microarrays studies and show strong expression of basal epithelial genes (Perou et al., 2000)

1.4.5 Apocrine Breast Cancers

Apocrine tumors have strong apocrine features on histological examination, and at molecular levels they express the androgen receptor (AR) without estrogen receptor. Moreover they commonly have ERBB2 receptor amplification. They growth through the androgen signaling and they represent the 8-14 % of breast cancer subtypes (Farmer et al., 2005).

2. FoxA1 and FoxA2 transcription factors

2.1 FoxA1 and FoxA2 function and regulation

The FoxA protein sub-family belongs to the major family of transcription factors named forkhead box (Fox). Over 100 Fox genes have been identified and classified into subfamilies and many have been shown to have important biological functions. Several have been identified as genes mutated in human disease, with phenotypes ranging from defective T cell differentiation to speech impediments (Carlsson and Mahlapuu, 2002). FoxA subfamilies comprises FoxA1, FoxA2 and FoxA3 transcription factors and have been proven to be critical in a variety of processes, both during development of organs such as liver, pancreas lungs and prostate and in postnatal life controlling metabolism through the regulation of multiple targets in multiple tissues. FoxA factors work as pioneer factors whose binding to promoters and enhancers enable chromatin access for other tissue-specific transcription factors. The subfamily of transcription factors was initially discovered on the basis of DNA binding activity present in liver nuclear extracts which was specific for promote of the transthyretin (Ttr), alfra1-antitrypsin (Serpina1) and albumin (Alb1) genes. For these reason the genes were originally named hepatocyte nuclear factor-3 (HNF-3) α, β and γ (Friedman and Kaestner, 2006; Kaestner, 2000).

Interestingly FoxA1 and FoxA2 transcription factors cooperate in many biological processes (**Table I**). For instance when both genes are missing from the foregut endoderm, hepatic specification is blocked completely (Lee et al., 2005). In contrast, embryos retaining either FoxA1 or FoxA2 protein in foregut endoderm specified the liver normally, indicating overlapping functions and

targets for the two genes (Kaestner et al., 1999). A similar behavior is observed during branching morphogenesis in lungs. This process is blocked when both factors are missing, but not by ablation of either factor alone (Wan et al., 2005).

FoxA transcription factors act in multiple stages of development, in different time frames and in multiple organs. FoxA1 and FoxA2 control several phases of dopaminergic neuronal development, form the earliest specification of progenitors via activation of the transcription factor Ngn2 and Lmx1a/b, to the expression of tyrosine hydroxylase, an enzyme required for the conversion of tyrosine to dopamine, a function of mature dopaminergic neuron (Ferri et al., 2007; Lin et al., 2009). Strikingly, mice heterozygous for FoxA2 null allele show age-dependent motor behavior abnormalities, which correlate with progressive loss of dopaminergic neurons (Kittappa et al., 2007). Using conditional alleles for both FoxA1 and FoxA2, it was shown that FoxA1/FoxA2 activate PDX gene; the master gene of pancreas development (Gao et al., 2008). In addition, in the mature β-cell, both factors cooperate to control insulin secretion and to repress a neuronal transcription program. Moreover both factors control the expression of carbohydrate response element-binding protein (ChREBP) and doing so regulate the carbohydrate metabolism in pancreas development and as well as in mature islets (Gao et al., 2010). As mentioned before, ablation of just one factor has little effect on early pancreatic development. Remarkable, in dopaminergic neuronal and pancreas development, FoxA proteins act during organ specification, linage differentiation and mature function of the organ, controlling different set of gene in each time frame (Kaestner, 2010).

There are still questions regarding on how FoxA factors can have such a broad effect. One possibility is that FoxA factors are able to work with cell specific cooperators or inhibitors. During earliest endoderm development, prior to liver specification, Groucho co-repressor protein (Grg3) is co-expressed with FoxA transcription factors and is able to repress the hepatic gene expression program generated by FoxA1/FoxA2 (Santisteban et al., 2010). On the other hand, FoxA factors play a major role in gene activation by glucocorticoids. Glucocorticoids and glucagon regulate gluconeogenic genes in the liver in fasting situations in cooperation with FoxA2. Liver specific abolition of FoxA2 decreases Tyrosine

Aminotransferase (TAT), Phosphoenolpyruvate Carboxykinase (PEPCK) and Insulin Growth Factor Binding Protein 1 (IGFBP-1) *in vivo* (Zhang et al., 2005). Not only gluconeogenic enzymes are regulated during fasting by FoxA2, fatty acid β-oxidation is increased as well as fatty acid secretion. This phenomenon is co-regulated with PPARγ co-activator β (Pgc-1β) (Wolfrum et al., 2004; Wolfrum and Stoffel, 2006). In a similar way and highlighting the redundancy of FoxA factors, FoxA1 is a potent inhibitor of liver fatty acid synthesis and an activator of fatty acid β-oxidation. Nevertheless contrary to FoxA2, FoxA1 inhibits fatty acid liver secretion (Moya et al., 2012). Remarkably, the targets regulated by FoxA2 in the liver not only depend on fasting situations, upon an acute liver injury for example, FoxA2 regulates in cooperation with different transcription factors the transcription of genes involved in lipid metabolism, stress response and molecular transport (Bochkis et al., 2009).

While the functions of FoxA1/FoxA2 appear to be compensatory in a variety of systems, striking examples exist wherein FoxA1 alone appears to be the master regulator of tissue specific differentiation and function. These are mainly associated with tissues dependent on sex hormones signaling, such the breast and prostate glands. Here FoxA1 co-regulates a set of genes to mediate specific organ differentiation with the Androgen receptor (AR) in the prostate (Gao et al., 2003) and Estrogen receptor (ER) in breast, specifically the estrogen-induce mammary duct expansion (Bernardo et al., 2010). Furthermore in MCF7 cancer cell lines ER response is almost total dependent on FoxA1 co-activation and therefore FOXA1 is a major determinant of estrogen-ER activity and endocrine response (Hurtado et al., 2011).

FoxA factors are regulated at mRNA levels. In adipocytes, FoxA1 and FoxA2 can block the differentiation progress of undifferentiated pre-adipocytes to adipocytes *in vitro*. In this model FoxA1 expression is controlled by CCAAT-enhancer-binding protein β (C/EBP) and FoxA2 expression is controlled by the Growth hormone (GH). Additionally, FoxA1 and FoxA2 suppress adipogenic genes and lipid accumulation and FoxA2 alone induces the expression of genes involved in glucose metabolism such as hexokinase (HK) and glucose transporter 2 (GLUT2) (Fujimori and Amano, 2011; Wolfrum et al., 2003).

Another way to regulate the factors is by post translational modifications. FoxA2 is phosphorylated by the insulin/PI3K/AKT pathway leading to nuclear exclusion in the liver in fed states. Contrary during fasting, FoxA2 is acetylated by glucagon signaling inducing an increase in the transcriptional activity of the factor (von Meyenn et al., 2013).

Another model for stage-specific gene regulation has been shown in *Caenorhabiditis elegans*. Here the homologue of FoxA, PHA-4 is thought to bind only to high affinity sites when is at low levels and later to lower affinity sites once the levels of the factor have risen sufficiently (Gaudet and Mango, 2002).

Table1. Targeted deletions of FoxA family members in mice

FoxA genotype	Cre transgene	Phenotype
$FoxA1^{loxp/loxp}$;$FoxA2^{loxp/loxp}$	Pdx1CreERT2	Glucose homeostasis and insulin secretion impaired
$FoxA1^{-/-}$;$FoxA2^{loxp/loxp}$	SP-C-rTA;$(tetO)_7$Cre	Abnormal branching morphogenesis and epithelial differentiation of lung
$FoxA1^{-/-}$;$FoxA2^{loxp/loxp}$	FoxA3-cre	Death at E9.5-10.5 Loss of liver specification

2.2 FoxA1 and FoxA2 in cancer

As FoxA1/FoxA2 factors are critical effectors of tissue development and function it is not striking to find them playing roles in human malignancy. Actually, FoxA1/FoxA2 factors exert pro and anti-tumorigenic properties. For example, in pancreatic cancer FoxA1 and FoxA2 expression inversely correlates with disease progression and or aggressiveness. Both are expressed in normal epithelium and in precancerous lesions but are commonly lost in poorly differentiated disease (Song et al., 2010). FoxA2 is expressed in metastatic samples of colorectal liver metastasis and in neuroendocrine lung cancers (Khoor et al., 2004; Lehner et al., 2007). The expression of the factor in

lung cancer cells has been shown to inhibit epithelial to mesenchymal transition and invasion (Tang et al., 2011). Functional analysis of FoxA2 should be done in liver colorectal metastasis in order to evaluate their implication in the disease.

As mentioned above FoxA factors can induce pro-tumorigenic features. For example, in prostate cancers FoxA1 expression has a strong association with tumor size, extraprostatic extension, invasion and metastasis, and it is found to be amplified in metastatic samples (Jain et al., 2011; Robbins et al., 2011). Moreover, prostate neuroendocrine adenocarcinomas, prostate cancer subtype with poor prognosis and androgen independency, express high levels of FoxA2. Here, cooperation of FoxA2 and HIF-1α enables a transcriptional program required for the development of neuroendocrine differentiation promoting malignancy and metastasis (Qi et al., 2010a).

In breast cancer high FoxA1 expression is found in luminal type of tumors and is associated with good prognosis and overall outcome. Antagonistically, low FoxA1 expression correlates with high grade, increased tumor size, basal tumors and nodal metastasis (Rutika J Metha et, al 2012). FoxA1 is expressed additionally in a subgroup of breast cancer expressing androgen receptor instead of estrogen receptor named molecular apocrine subtype (Farmer et al 2005). This type of cancer is enriched in HER2 amplification but in many ways has features remaining prostate cancer (Doane et al., 2006).

Luminal and apocrine breast cancer cell types and prostate cancer lines need FoxA1 to proliferate. In these cells FoxA1 co-regulate the hormonal response and doing so the proliferation of cells. Chip seq experiments reveal that 50% ER binding sites and 70 % AR binding events occur at regions also co-occupied by FoxA1. FoxA1silencing in ER+ MCF7 human breast cancer lines induce a significant loss of ER binding at more than 90% of all ER binding sites. For AR, silencing of FoxA1 in prostate cancer cells result in loss of 50% AR binding events, with the remaining 50% of AR sites still present independently of FoxA1.

3. Cancer Metabolism

3.1 Metabolic fate of cancer cells

In order to sustain the rapid proliferation and to counteract the hostile environment observed in tumors, cells must increase the rate of metabolic reactions to provide the adenosine triphosphate (ATP), lipids, nucleotides and amino acids necessary for cell division. Most tumor cell types share common requirements to acquire a transformed phenotype. Ten years ago Hanahan and Weinberg reviewed what they considered the hallmarks of cancer. They suggested that the vast catalog of cancer cell genotypes is a manifestation of six essential alterations in cell physiology that collectively dictate malignant growth (Hanahan and Weinberg, 2000). Recently, this model has been revised and updated including two new emerging hallmarks (Hanahan and Weinberg, 2011). The growing evidences indicating the importance of metabolism reprograming in cancer malignancy has positioned this trait, named as reprograming of energy metabolism, as a new cancer hallmark.

The first metabolic alteration described in cancer cells can be traced to the pioneering work of Otto Warburg which highlighted that cancer cells tend to ferment glucose into lactate even in the presence of oxygen; aerobic glycolysis (Koppenol et al., 2011). In the presence of oxygen, most non-proliferating, differentiated cells depend on the efficiency of ATP production to preserve their integrity maintaining homeostatic processes. To fulfill this requirement cells metabolize glucose to pyruvate through glycolysis, and then completely oxidized a large fraction of the generated pyruvate to carbon dioxide in the mitochondria, were oxygen is the final acceptor in an electron transport chain that generates an electrochemical gradient facilitating ATP production. Under anaerobic conditions, normal differentiated cells redirect glycolytic pyruvate away from mitochondria oxidation and instead largely reduce it to lactate. In contrast, rapidly proliferating cells metabolize glucose to lactate regardless of the availability of oxygen. Considering that proliferating cells must not only generate enough energy to support cell replication, but also satisfy the anabolic demands of macromolecular biosynthesis and maintain cellular redox homeostasis in response to escalated production of toxic reactive oxygen

species, behind the Warburg effect several other metabolic pathways are deregulated (Cantor and Sabatini, 2012; Koppenol et al., 2011; Ward and Thompson, 2012).

3.2 Metabolic regulation in rapid proliferating cells

Mammalian cells typically rely upon growth factor-mediated stimulation of specific signaling cascades, which in turn trigger a transcriptional response driving the expression of genes that promote proliferative adaptations. In these terms, cancer cells and normal proliferating cells share a similar collection of metabolic demands and adaptations (**Figure 3**). Accordingly, the signaling and transcriptional circuitry that modulates cell growth is largely conserved across proliferating cells in general. However, whereas normal cells possess a variety of checkpoints that enable correct maintenance of this system, various tumorigenic lesions impart cancer cells with the ability to fracture proper regulation and as a consequence affecting the expression of metabolic genes which in turn will have a direct impact on the deregulation of metabolic pathways (Cantor and Sabatini, 2012). It is known that oncogenes regulate the metabolic adaptations of cancer cells in order to proliferate and grow. As well, tumor suppressors will maintain a non-proliferative metabolic state to control and avoid cell division. **Figure 4** summarizes oncogenes and tumor suppressor genes controlling specific metabolic pathways that are increased to proliferate.

For instance, PI3K/Akt pathway, which is affected in a variety of human tumors, including glioblastomas, breast, colon and endometrial cancer is a major player in tumor initiation and growth (Hirsch et al., 2013). And when it is activated leads to enhanced glucose uptake and aerobic glycolysis. Akt moreover, is sufficient to induce the Warburg effect in non-transformed cells or cancer cells (Elstrom et al., 2004)

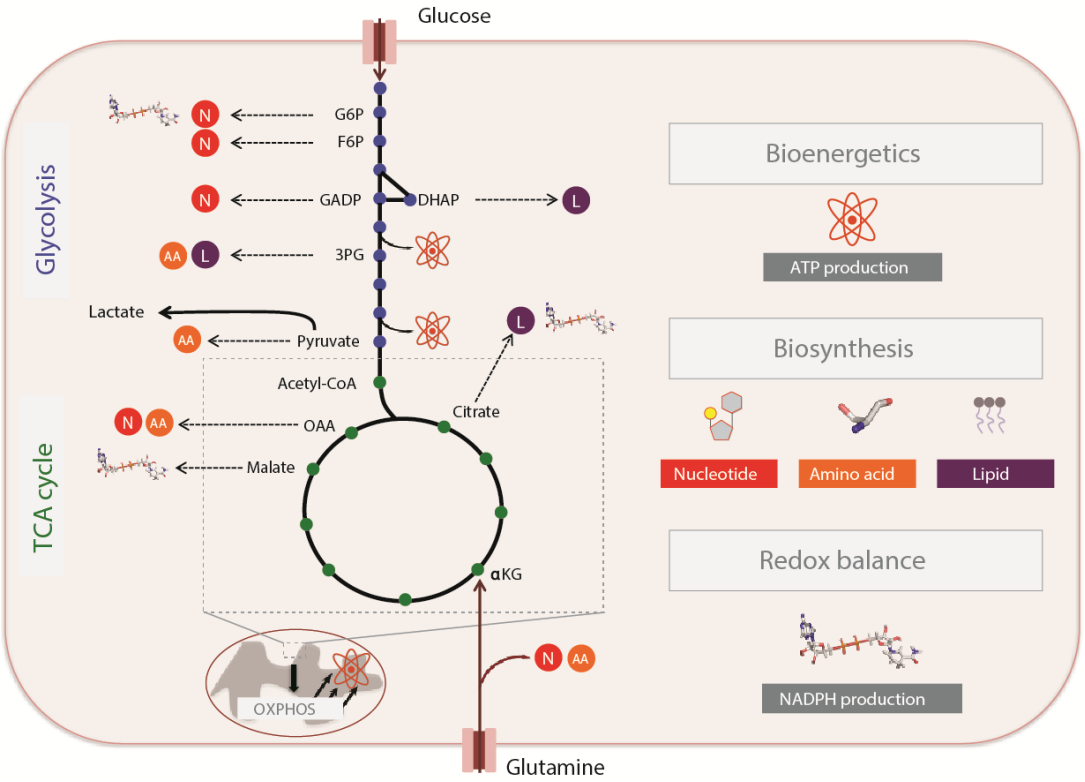

Figure 3.- Metabolic demands in rapid proliferating cells. Proliferating cells take glucose and glutamine as principal carbons donators in order to satisfy the 3 indispensible metabolic demands; bioenergetics, macromolecular biosynthesis and redox maintenance. Glucose trough aerobic glycolysis generates the necessary intermediates (blue dots) to nucleotides, amino acids and lipid synthesis whereas glutamine serves as nitrogen source for nucleotides synthesis and various non-essential amino acids. In addition, glutamine is a carbon source for the replenishment of TCA cycle intermediates (green dots) which are diverted into various anabolic pathways (Cantor and Sabatini, 2012).

ATP-citrate lyase (ACL), enzyme responsible for the inter-conversion of citrate to acetyl-CoA in the cytosol (Srere, 1972; Sullivan et al., 1974), is phosphorylated and activated by the PI3K/Akt pathway promoting lipid synthesis. Activation of ACL promotes cell growth and transformation. Furthermore, inhibition of the enzyme suppresses tumor growth (Bauer et al., 2005; Hatzivassiliou et al., 2005). Another member of the PI3K/Akt pathway is the cell growth regulator mechanistic target of rapamycin complex1 (mTORC1). Activation of mTORC1 allows cells to increase the surface expression of nutrient transporters, enabling cells to increase glucose, amino acids and other nutrients uptake (Edinger and Thompson, 2002; Roos et al., 2007; Xu et al., 2005). Moreover it is able to enhance the protein translation through direct phosphorylation of the translational regulators 4E-binding protein 1 and S6 kinase (Gingras et al., 2001; Laplante and Sabatini, 2012). Among the downstream targets of mTORC1-dependent translation are a number of

transcription factors that coordinate metabolic gene expression as HIF1α, MYC, and SREBP-1(Cantor and Sabatini, 2012). SREBP-1 induces the expression of several genes involved in fatty acid and sterol biosynthesis in response to growth factors and sterol levels (Duvel et al., 2010). LKB1 is a tumor suppressor gene responsible for the inherited cancer disorder Peutz-Jeghers syndrome (Hemminki et al., 1998) and is the second most commonly mutated tumor suppressor in sporadic human lung cancer after TP53 (Sanchez-Cespedes et al., 2002). The LKB1-AMPK pathway is the energy sensor and modulator of cell growth and metabolism that is activated under conditions of low intracellular ATP. Activated AMPK regulates growth in part through inhibition of mTORC1 signaling and by targeting defective mitochondria for autophagy and control of fatty acid metabolism (Egan et al., 2011; Inoki et al., 2003; Jeon et al., 2012).

Myc oncogene regulates genes involved in glutaminolysis, which results in enhanced cell viability and proliferation. In the same way, regulates mitochondrial glutaminase (GLS) protein, an enzyme involved in promoting lymphoma and prostate cancer cell growth (Gao et al., 2009; Wise et al., 2008). As ACL, pharmacological inhibition of GLS reduces cell proliferation and xenograft growth (Le et al., 2012). On the other hand, mutations in KRAS (colorectal, pancreatic and some forms of lung cancers) or mutations in BRAF (melanomas and colorectal tumors without KRAS mutations) (Davies et al., 2002; Rajagopalan et al., 2002) enhanced GLUT1 expression with commitment of glucose uptake and glycolysis driving cell survival in low-glucose conditions (Yun et al., 2009). Moreover, for Ras-mediated tumorigenesis, processes such as autophagy, mitochondrial metabolism and ROS production are essential to induce anchorage –independent growth of colorectal cancer cells as well as *in vivo* tumor growth (Guo et al., 2011; Weinberg et al., 2010).

Another well-known tumor regulator which has been shown to regulate metabolism is the tumor suppressor protein p53. P53 plays a critical role in responding to cellular stress and inhibiting malignant development (Vousden and Lu, 2002; Vousden and Ryan, 2009). P53 can inhibit the expression of the glucose transporters GLUT1 and GLUT 4 (Fabiana Schwartzenberg-Bar-Yoseph F, 2004) decrease the phosphoglycerate mutase enzyme (PGM)

expression (Kondoh et al., 2005) and induce the expression of TIGAR, a glycolytic regulator (Bensaad et al., 2006). Silencing of PGM reduces cell proliferation and tumor growth by a decrease of glycolysis and pentose phosphate pathway (PPP) flux and biosynthesis (Hitosugi et al., 2012). Further, p53 regulates the PPP flux as it can inhibit, through its direct binding, glucose-6-phosphate dehydrogenase (G6PD) protein; rate limiting enzyme in PPP flux. Doing so p53 is able to reduce glucose consumption, NADPH production and as a consequence decrease nucleotide biosynthesis (Jiang et al., 2011).

Finally, one of the most important transcription factors in the regulation of metabolic adaptations to hypoxia are HIF1 and HIF2 complexes. Both complexes are the major transcription factors that are responsible for gene expression changes during cellular response to low oxygen conditions. They are heterodimers that are composed of the constitutively expressed HIF1β subunit and either HIF1α or the HIF2α subunits, which are rapidly stabilized on exposure to hypoxia. HIF1α can also be stabilized under normoxic conditions by oncogenic signaling pathways. Once activated, HIF1 induces the expression of glucose transporter genes and most of the glycolytic enzymes, increasing the capacity of the cell to carry out glycolysis (Cairns et al., 2011). HIF1 also regulates the expression of pyruvate dehydrogenase kinase 1 (PDK1) (Papandreou et al., 2006). PDK1 is responsible for the inhibition of pyruvate dehydrogenase (PDH) activity, enzyme that catalyzes the conversion of pyruvate into Acetyl-CoA (Holness and Sugden, 2003; Sugden and Holness, 2003). Inhibition of PDH will drive the conversion of pyruvate into lactate and thereby will reduce glucose carbon incorporation into mitochondrial citrate (Lum et al., 2007; Papandreou et al., 2006). Doing so, it favors the Warburg effect and the generation of biomolecules.

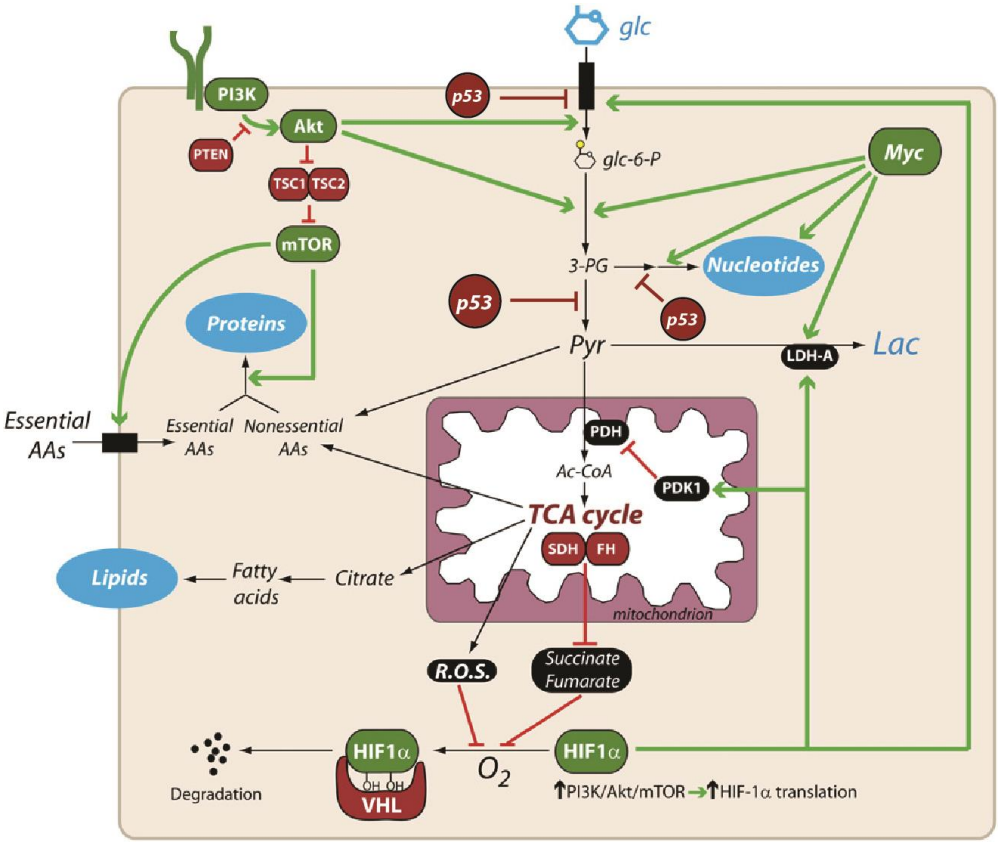

Figure 4.- Oncogenes or tumor suppressor genes controlling metabolism in proliferation. Metabolic circuits increased in cancer cells due deregulation in tumor suppressor genes or activation of oncogenes such us glycolysis; lactate production; the use of TCA cycle intermediates; and the biosynthesis of proteins, nucleotides and lipids. Mutation in the PI3K/AKT pathway will induce the synthesis of proteins and the uptake of essential amino acids; moreover it will induce the uptake of glucose and the flux through glycolysis. Second, it will enhance HIF-1α translation. During normoxia HIF-1α protein is degraded, but hypoxia, mutation in VHL tumor suppressor, the increase and accumulation of reactive species of oxygen (ROS) and the TCA intermediates Succinate or Fumarate impair HIF-1α degradation. That allows HIF-1α enter into the nucleus to engage their transcriptional activity. Transcriptional targets are glucose transporter, LDH-A and PDK1. The transcription factor MYC increases the expression of many metabolic enzymes including glycolytic enzymes and several enzymes required for nucleotide biosynthesis. Last tumor suppressor p53 inhibits glucose uptake, glycolysis and nucleotide synthesis by inhibiting the expression of glucose transporters and glycolytic enzymes. Moreover it can bind glucose-6-phosphate dehydrogenase (G6PD) protein to further inhibit it suppressing carbon flux through nucleotides synthesis. Figure adapted from (DeBerardinis et al., 2008).

3.3 Metabolic circuits in cancer cells

3.3.1 Glucose and the Warburg effect

During growth, glucose is used to generate biomass as well to produce ATP. Although ATP hydrolysis provides free energy for some of the biochemical reactions responsible for the replication of biomass, these reactions have additional requirements. For instance, synthesis of palmitate, a major

constituent of cellular membranes, requires 7 molecules of ATP, 16 carbons from 8 molecules of acetyl-CoA and 28 electrons from 14 molecules of NADPH. In oxidative glycolysis one molecule of glucose can generate up to 36 ATPs, or 30 ATPs and 2 NADPHs (if diverted into the pentose phosphate shunt), or provide 6 carbons for macromolecular synthesis. Thus to generate a 16 carbon fatty acyl chain, a single molecule of glucose can provide five times the ATP required, whereas 7 glucose molecule are needed to generate the NADPH required. Moreover 3 glucose molecules are consumed to acetyl-CoA production to satisfy the carbon requirement of the acyl chain itself. It is clear that in order to proliferate; the bulk of the glucose cannot be committed to carbon catabolism for ATP production. Last, if this were the case, the resulting rise in the ATP/ADP ratio would severely impair the flux through glycolytic intermediates, limiting even more the production of acetyl-CoA and NADPH required for macro-molecular synthesis. Taken into count that glucose and glutamine supply most of the carbon, nitrogen free energy and reducing equivalents for cell growth and division, it becomes clear that converting all of the glucose to CO2 via oxidative phosphorylation to maximize ATP production runs counter of cancer cells (Vander Heiden et al., 2009). Under these observations, glycolysis is not a metabolic vacuum in which a single input (glucose) is converted through a multistep process into a single output (pyruvate). Rather, this module of central carbon metabolism is highly interconnected with several other metabolic pathways, particularly those associated with the *de novo* synthesis of cellular buildings blocks, within which various glycolytic intermediates serve as substrates (**Figure 5**) (Cantor and Sabatini, 2012).

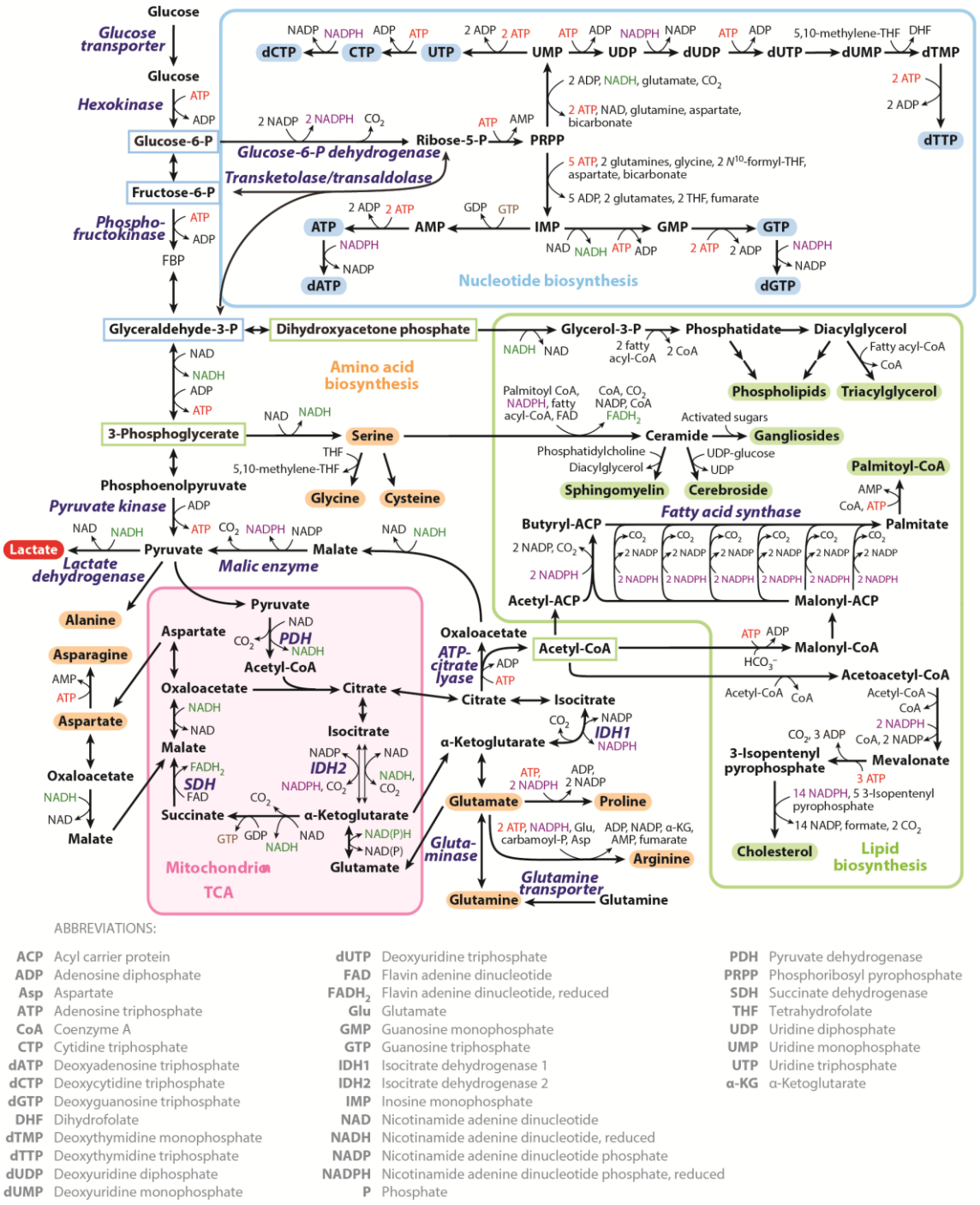

Figure 5.- Metabolic pathways active in proliferating cells. Enzymes that are often overexpressed or mutated in cancer cells are shown in dark blue. Nucleotides are highlighted in light blue, representative lipids are highlighted in green and nonessential amino acids are highlighted in orange. Key metabolites that serve as important precursors for biomass production are boxed. Figure adapted from (Lunt and Vander Heiden, 2011).

Thus there are known glycolytic intermediaries that are utilized by anabolic pathways. For example, half of the purine nucleotide carbons are derived from 5-phosphoribosyl-α-pyrophosphate (PRPP), an activated version of ribose-5-phosphate, which derives from glycolytic intermediates. 3-phosphoglycerate, another glycolytic intermediate can be converted to glycine, which can donor

two more carbons in the synthesis of purines. Glycolysis is also a major source of carbons for biosynthesis of pyrimidine nucleotides (CTP,UTP,dCTP,and dTTP), as 5 out of 9 carbons to generate them comes from PRPP. In addition to support nucleotide biosynthesis, glycolysis is also a source of carbons for lipid precursors. Dihydroxyacetone phosphate is the precursor to glycerol-3-phosphate, which is crucial for the biosynthesis of phospholipids and triacylglycerols that serve as major structural lipids in cell membranes as well as cardiolipin, an important component of mitochondrial membranes. 3-phosphoglycerate is the precursor of sphingolipids, another major class of lipids in cells, playing roles in growth, differentiation, senescence, apoptosis and cancer. The carbons for the synthesis of fatty acyl chains of various lipid classes are provide by acetyl-CoA. Oxidative decarboxylation of pyruvate to acetyl-CoA occurs in mitochondria and subsequently is transformed to citrate which can follow the TCA cycle or be exported to cytosol to be reconverted to acetyl-CoA which is used to generate lipids. Last but not least glycolysis throw 3-phosphoglycerate provides the carbons for cysteine, glycine and serine and pyruvate the carbons for alanine (Lunt and Vander Heiden, 2011). Serine and glycine have been shown to be necessary for melanoma and breast cell lines growth. In this cell lines Phosphoglycerate dehydrogenase (PHGDH) protein is the responsible to divert glycolytic carbons to serine and glycine synthesis using 3-phosphoglycerate as substrate. The overexpression of PHGDH is induced by gene amplification in cancer cell lines and in human melanoma samples (Locasale et al., 2011).

As we can imagine there should be a coordinated regulation of the metabolic enzymes of glycolysis to induce the Warburg effect and to generate the metabolic intermediates for biosynthetic pathways. Gene expression analysis have shown that genes of the glycolysis pathway are overexpressed in the majority of clinically relevant cancers and particularly glyceraldehide-3-phosphate dehydrogenase, enolase and pyruvate kinase are overexpressed ubiquitously in 24 cancer types (Altenberg and Greulich, 2004). The embryonic Pyruvate Kinase M2 isoform play a pivotal function in controlling aerobic glycolysis (Warburg effect). PKM2 is overexpressed in cancer cells controlling the fate of glucose and thus facilitating the shunting of glucose carbon/glycolytic

intermediates into branching anabolic pathways. Cancer cells which swap the expression to the M1 (adult) isoform have less lactate production, and more oxygen consumption *in vitro* and show delay in tumor development and smaller tumor mass (Chaneton and Gottlieb, 2012; Christofk et al., 2008). PKM2 is unique among pyruvate kinase isoforms as it has the ability to switch between a low and high activity state that confers cancer cells the ability to regulate in time and space the production of glycolytic intermediaries or carbons going to TAC cycle. In addition, PKM2 has non metabolic roles in cancer proliferation. PKM2 can interact with HIF-1α subuntit and promote transactivation of glycolytic genes to promote glucose metabolism. In another fashion PKM2 can regulate the expression of cyclin D1 and myc for cell proliferation and tumorigenesis (Luo et al., 2011; Yang et al., 2012).

3.3.2 Beyond the Warburg effect

As glucose, glutamine is another carbon source that is highly required for cancer cell growth and proliferation. Once in the cell glutamine can be converted to α-ketoglutarate and enter into the TCA cycle. As glycolysis; the TCA cycle, and as a consequence glutamine, serves as an important source of biosynthetic precursors. In this way glutamine provides carbons to TCA intermediates that serve as precursors of many nonessential amino acids and fatty acids, as acetyl-CoA can be derived from glutamine. In the same way glutamine anaplerotic flux may also be important for mitochondrial production of NADH and FADH2 which are important for the integrity of the mitochondria. Glutamine can be used as a nitrogen source for nucleotides, amino acids and hexosamines such as glucosamine, a precursor to glycosylated proteins and lipids (Lunt and Vander Heiden, 2011). As described before, glutaminolysis is regulated by oncogenes. MYC regulates genes involved in glutamine uptake and metabolism. Moreover, human glioma cells render to growth arrest when are deprived of glutamine in presence of glucose. 14C-glutamine is used as carbon source for phospholipid synthesis demonstrating the capacity of glutamine as the precursor (Wise et al., 2008).

Glycolysis and glutaminolysis are heavily regulated by cancer cells, nevertheless there are more metabolic pathways necessary for cancer pathogenesis and growth. For example fatty acids, lipids and phospholipids are emerging metabolites regulating cancer cell survival, growth, malignancy and migration. Fatty acid synthase (FASN) is responsible for the endogenous synthesis of long-chain fatty acids by using acetyl-CoA as a primer, malonyl-CoA as a two-carbon donor, and NADPH as a reducing equivalent. Interestingly, various tumors and their precursor lesion unexpected undergo exacerbated endogenous fatty acids biosynthesis. FASN is not the only enzyme overexpressed in cancer cells, as mentioned before ATP citrate lyase is also overexpressed. CoA carboxylase (ACACA) is the rate-limiting enzyme for the long chain fatty acids synthesis that catalyzes the ATP dependent carboxylation of acetyl-CoA to malonyl-CoA. ACACA has been shown to be overexpressed in advanced breast carcinomas and in pre-neoplastic lesions with increased risk for the development of infiltrating breast cancer (Menendez and Lupu, 2007). Interestingly pharmacological inhibition or silencing of the above-mentioned enzymes in breast and prostate cancer models impairs cell viability and tumor growth (Brusselmans et al., 2005; Chajes et al., 2006; De Schrijver et al., 2003; Pizer et al., 2000; Pizer et al., 1996; Vazquez-Martin et al., 2007). A novel enzyme Monoacylglycerol Lipase (MAGL) was described to play roles supporting malignant behavior. More aggressive cancer lines as well as high grade primary tumors contained elevated fatty acid levels, which could be reduced by pharmacological inhibition or silencing of MAGL. This inhibition reduces cell migration, invasion and tumor growth. On the same way the overexpression of MAGL in cells with low levels of it induce an increased malignant phenotype. Lipidomic approach reveals that an increase of MAGL activity not only decreases monoacilglycerols and increase fatty acids but it also leads to an increase in fatty acid derived lipid signals, such as lysophosphatidic acid (LPA), phosphatidic acid (PA) and prostaglandins E2 (PGE2) among others (Nomura et al., 2010). The relationship between the synthesis, storage and use of fatty acids in cancer is poorly understood (Yecies and Manning, 2010). In this model, the authors propose that free fatty acids generated in cancer cells are rapidly converted into neutral lipids stores such as monoacylglycerols and that MAGL release fatty acids from them in order to

generate a broad type of phospholipids for β-oxidation, membrane generation and signaling lipids as LPA, **Figure 6**.

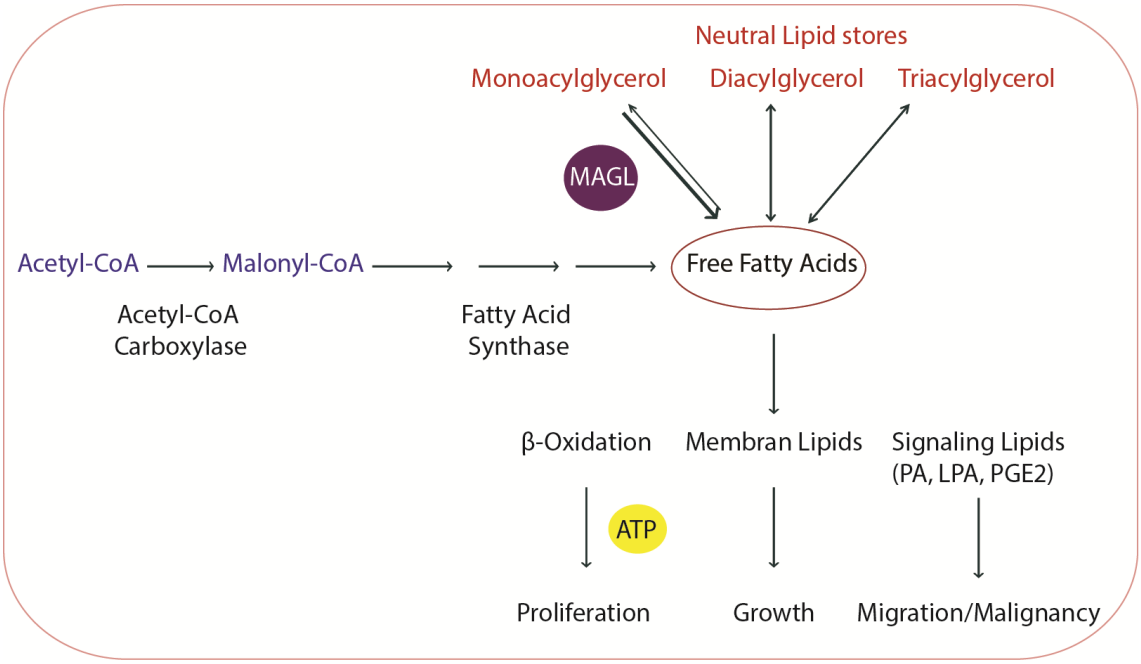

Figure 6.- Destiny of lipids in cancer cells. Newly fatty acids synthesis by the overexpressed fatty acid synthase in cancer cells are believed to be converted into neutral lipids as mono-, di-, or triacylglicerols. MAGL catalyzes the lypolitic release of monoacylglycerols in aggressive cancer lines. MGAL matins free fatty acids levels to be converted in pro tumoral signaling lipids, cell membranes lipids or to be used for β-oxidation. The last pathway generates ATP. FFA remodeling and utilization contribute to tumor cell proliferation, growth and migration (Yecies and Manning, 2010)

It is thought that fatty acids and lipids are generated in cancer cells mainly endogenously by FASN using carbons from glucose or glutamine (Menendez and Lupu, 2007). Recent report has been shown that cancer cells can incorporate exogenous fatty acids (Louie et al., 2013). Cancer cells are able to incorporate isotopic palmitic acid into cells. Moreover, using metabolomic profiling the investigators realized that the palmitic acid was used to generate a high range of phospholipid molecules such as phosphatidyl cholines (PC) lysophosphatidyl cholines (LPC) phosphatidic acids (PA) lysophosphatidic acids (LPA) phosphatidyl ethanolamines (PE) lysophosphatyl ethanolamines (LPE); sphingolipids such as Ceramides, sphingomyelin (SM) and Ceramide 1-phosphate between others. Furthermore, comparing aggressive cancer cells with their non-aggressive counterparts, they found a common signature of altered lipid molecules (**Figure 7**).

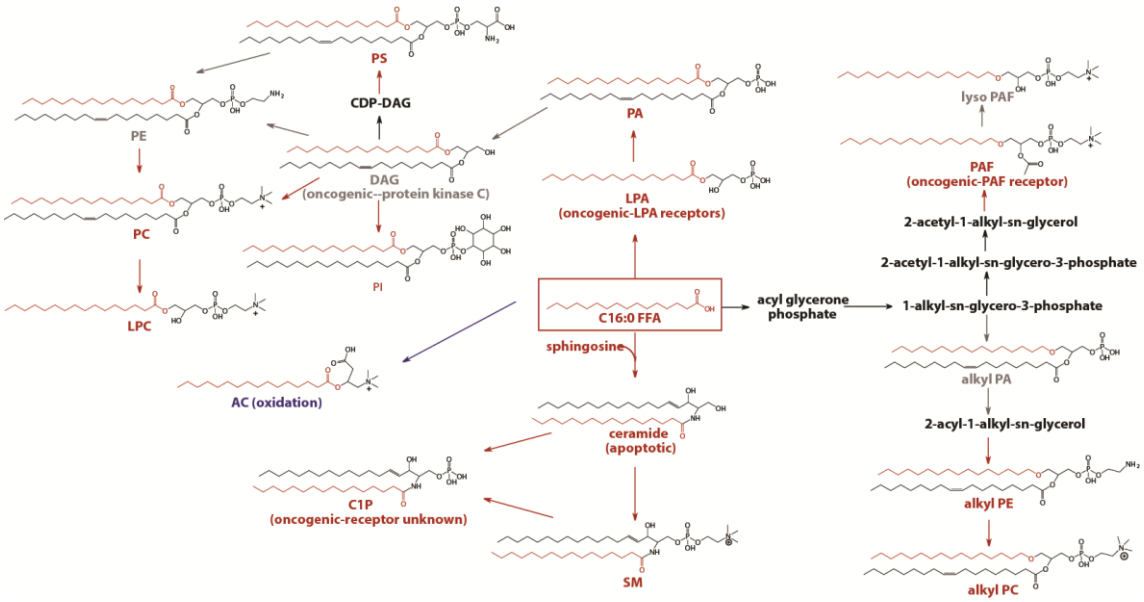

Figure 7.- Lipid signature in aggressive cancer lines. Lipids metabolic map generated from d_4-palmitic acid (d_4-C16:0 FFA) tracing in non and aggressive cancer cell lines. d4C16:0 FFA incorporation into lipid structures is represented in red. Arrows and metabolites in red (increased), in blue (decreased) and in gray (unchanged) when aggressive versus non aggressive lines were compared. Metabolites and arrows in black were not detected by the analysis (Louie et al., 2013).

Increased levels of isotopicaly labeled phospholipids such as PA, PS, PC and PI; sphingolipids such as Ceramide and SM; ether lipids such as alkyl PE and alkyl PC, as well as oncogenic signaling lipids such as PAF, LPA and C1P were found (Louie et al., 2013). The exact function of the whole range of fatty acids or lipids found in cancer cells is unknown. Fatty acids for example can be used to produce energy trough β-oxidation as an alternative route for glycolysis in certain situations of energetic stress such as matrix detachment or oxidative stress (Buzzai et al., 2005; Schafer et al., 2009). Fatty acids and lipids are also necessary in proliferating cells for the production of newly synthesized membranes for daughter cell generation (DeBerardinis et al., 2008; Kroemer and Pouyssegur, 2008).

Of note, specific lipids can contribute to oncogenesis providing intracellular and extracellular lipid-derived signals (Wymann and Schneiter, 2008). One known signal-lipid is lysophosphatidic acid (LPA) and is an inducer of cell proliferation, migration and survival exerting effects in the initiation and progression of malignant disease as well as being a key contributor to the metastatic cascade

(Mills and Moolenaar, 2003). For example, LPA induces invasion of T-lymphoma cells trough the activation of RhoA-like GTPase and phospholipase C signaling pathways. On the other hand LPA induces ovarian and breast cancer cell proliferation activating MAPK pathway (Stam et al., 1998; Xu et al., 1995). Ceramide metabolism is altered in several cancer models since ceramide induces apoptosis and cell cycle arrest. For instance, several enzymes involved in the clearance of ceramide are overexpressed in cancer cells. This is the case for sphingosine kinase1 overexpressed in prostate cancer cells and prostate cancer samples, acid ceramidase overexpress in prostate, breast and liver cancer or ceramide kinase which is overexpressed in human tumor samples and human tumor cell lines from breast and lung cancer and of leukemia (Morad and Cabot, 2013). Another well-known lipid messenger is phosphatidylinositol-3,4-triphosphate which activates PKB/Akt to promote cell proliferation and survival or prostaglandins which support migration and tumor-host interactions. Cyclooxygenase (COX2) which generate prostaglandins, is able to mediate vascular remodeling in conjunction with metalloproteinase 1 and 2 and growth factor receptor ligand epiregulin to seed pulmonary metastasis (Gupta et al., 2007).

3.3.3 Oncometabolites

Tumors and proliferating cells share common metabolic pathways to allow them to grow; in these terms there is an overexpression of certain enzymes that will favor the direction of metabolic intermediates into specific pathways that are not necessarily specific to cancer. The strongest evidence to date that altered metabolism is selected for by cancer cells during tumorigenesis has come with the elucidation of somatic mutations in metabolic enzymes. Mutations in the cytosolic NADP-dependent isocitrate dehydrogenase 1 gene (IDH1) were first found in glioma and acute myeloid leukemia (AML) through whole genome sequencing (Mardis et al., 2009; Parsons et al., 2008). Now it is known that mutations in R132 in IDH1 and R172 or R140 in IDH2 gave to the enzymes the activity to convert α-ketoglutarate to 2-hydroxyglutarate (2HG) instead to isocitrate (Ward et al., 2010; Yan et al., 2009). 2HG is a metabolite found in trace in mammalian samples but overproduced in glioblastomas and AML

samples. Collective evidence stemming from several reports have highlighted that pathophysiological role of 2HG is, at least in part, the competitive inhibition of various αKG-dependent dioxygenases, including TET2 DNA hydroxylases and JmjC histone demethylases. Therefore, the tumorigenic effect of 2HG appears to be at level of epigenetic deregulation. High levels of 2HG clock the differentiation of non-transformed cells through inhibition of histone demethylation. Furthermore, the introduction of mutant IDH1 into primary human astrocytes can trigger remodeling of the DNA methylome in a fashion that recapitulates pattern similarly observed in mutant IDH-harboring glioma cells. Similarly, exogenous expression of the mutant enzymes, or treatment with 2HG, is sufficient to reprogram epigenetics, impair differentiation and promote malignant features in cultures erythroleukemic cells (Cantor and Sabatini, 2012; Ward and Thompson, 2012). There are two other oncometabolites regulated in cancer cells among 2HG. Loss of function of Succinate Dehydrogenase (SDH) and Fumarate Hydratase (FH) occur in pheochrocytoma, paraganglioma, leiomyoma and renal carcinoma. Accumulation of Fumarate or Succinate were found to enable aberrant stabilization of HIF1α through competitive inhibition of PHD2 (Isaacs et al., 2005; Selak et al., 2005), which otherwise suppresses this stabilization in normoxia.

3.4 Metabolic targets in cancer therapy

As mentioned before there are several metabolic enzymes overexpressed by oncogenes or by DNA amplification in cancer. On the other hand, some cancers preferentially express a metabolic enzyme that is mutated to generate a by side product such 2GH or to generate loss of function mutants to accumulate a special metabolite, as in the case of fumarate or succinate. In addition, some tumors express a selective enzyme isoform such as PKM2 or HK2. All these metabolic adaptations confer to cancer cells growth and malignancy advantages. These adaptations allow a wide range of possibilities to design new therapeutic agents against cancer. Still, there are key issues to be considering in other to target cancer cell metabolism as a reliable therapeutic possibility. For example all cells rely on the same metabolic pathways to generate ATP, and it is often assumed that drugs that target metabolic

pathways would have detrimental effects on normal tissue, especially in normal proliferating cells. Although this is true for some metabolites the success of cytotoxic agents that target the folate metabolism and DNA synthesis illustrate that a therapeutic window can exist for metabolic anticancer drugs. The same idea is applicable for the specific differences in metabolic circuits among several cancer types. Understanding why some cancers are addicts to some metabolic pathways and metabolites will give a therapeutic window to treat them without having severe toxic effects in normal cells. Several pathways often exist to generate the same metabolic end product, and redundant pathways that are present in normal cells but absent in cancer cells may provide another window (Vander Heiden, 2011). There are some potential metabolic targets described in the literature. Targeting nutrients uptake could have a huge impact on cancer growth. The glucose transporter 1 (GLUT1) is expressed in almost all tissues but is present at much higher levels in cancer cells than in normal ones. In these case a direct inhibition of GLUT1 will have unwanted effects in normal cells, but a partial inhibition may sensitize cancer cells to other drugs (El Mjiyad et al., 2011). GLUT3 may give another therapeutic window as cancer cells express it at high levels but most normal cells do not (Yamamoto et al., 1990). PKM2 isoform is another interesting enzyme to be targeted. Peptide aptamers that promote a less active form of PKM2 have been shown to cause energy stress and cell death in cultured cancer cells (Spoden et al., 2008). Activation of the enzyme is another intelligent strategy to use an isoform–specific-small-molecule activators of PKM2 have been reported to inhibit tumor growth in xenograft models (Jiang et al., 2010; Walsh et al., 2010). Beside targeting glycolysis, cancer cells rely in the generation of NAD+ and NADH cofactors for metabolic oxidation-reduction reactions or to be substrates for enzymes such as NAD-dependent deacetylase sirtuins and poly(ADP-ribose) polymerases. Cells that are treated with NAMPT inhibitors, enzyme involved in regenerating NAD+ from nicotidamine and phosphoribosyl pyrophosphate via salvage pathway, die as a result of NAD+ depletion. Moreover NAMPT inhibition has shown to be an anticancer agent in preclinical models of cancer (Garten et al., 2009). One interesting target is the generation of 2HG. The development of small molecules that inhibit the production of 2HG may be a good model to treat glioblastoma and other cancer types that are dependent on this metabolite. Inhibitors

targeting mutated IDH2 or IDH1 are able to reduce cancer cell growth, promote differentiation and delay xenograft growth (Rohle et al., 2013; Wang et al., 2013). Interestingly, inhibitory action against IDH1 mutant does not drive changes in genome wide DNA methylation state of tumors suggesting that the growth promotion of the enzyme may be done by other mechanisms beyond the epigenetics. The inhibitors effect against mutated IDH1 and IDH2 are cytostatic rather than cytotoxic, in line with the idea that they stimulate cell differentiation and not cell death. For this reason it is necessary to determine if the therapeutics effects of the drugs will persist over long time frames (Kim and DeBerardinis, 2013).

Many cancer cells need de novo fatty acid synthesis to generate new membranes for cell growth and the enzymes that are involved directly in fatty acid synthesis have been suggested as cancer treatment (Vander Heiden, 2011). Lipids and lipases have been recently show to have important roles in the regulation of oncogenic signals, MAGL inhibitors have been shown to reduce cancer cell proliferation and xenograft growth of aggressive cancer cell lines (Mulvihill and Nomura, 2013; Nomura et al., 2010). The diabetes therapeutic biguanide compounds metformin and phenformin have been show to inhibit complex I of the mitochondria (Dykens et al., 2008; El-Mir et al., 2000; Owen et al., 2000), resulting in increases in intracellular AMP and ADP that bind to the gamma regulatory subunit of AMPK and trigger LKB1-dependent phosphorylation of AMPK (Hawley et al., 2010). Interestingly metformin or phenformin treatment has been found to reduce tumor growth in xenograft, transgenic mice and carcinogen-induced mouse cancer models (Algire et al., 2011; Anisimov et al., 2005; Huang et al., 2008; Memmott et al., 2010; Shackelford et al., 2013). Epidemiological studies reveal that diabetic patients taking metformin show a statistically significant reduced tumor incidence and given the safety of metformin use, it is an interesting target as anticancer agent (Dowling et al., 2012; Taubes, 2012).

It is clear that a better understanding of how metabolism is altered in specific genetic context that lead to cancer will provide an insight into which enzyme, or combination of them, represent promising targets in certain cancers, and this

understanding will arise from the analysis of cancer metabolism that extends beyond the levels of expression of various enzymes in a metabolic pathway. In this moment efforts to target several enzymes involved in cancer metabolism are in their infancy, yet as targets become better defined, the use of these enzymes could result in the delivery of better therapies (Vander Heiden, 2011).

4. Endothelial Lipase (LIPG) and lipoprotein metabolism

4.1 Lipoprotein metabolism

Fatty acids (FAs) are essential molecules with multiple biological functions; they are integral components of membrane lipids, efficient energy substrates and potent second messengers. To prevent deleterious effects of high extracellular or intracellular FA concentrations, long chain FAs are detoxified by esterification to glycerol forming triglycerides (TGs). FAs are transported through the blood in HDL, chylomicrons, VLDL and other molecules as TGs. In response to metabolic demand, TGs can be hydrolyzed to FAs and glycerol by lipolysis, which involves the enzymatic activity of TG hydrolasas (lipases). TGs cannot move across cell membranes without first being degraded by lipases. Intestinal enterocytes package dietary lipids into chylomicrons, which enter the lymphatic vessels and then quickly reach the bloodstream. Chylomicrons transport TGs to adipose tissue for storage and to vital tissues such as heart and skeletal muscle for use as fuel. The liver synthesizes and secretes VLDL, which serves to redistribute TG to adipose tissue, hart and muscle between others. In the capillaries lipoprotein lipase (LPL), which is attached along the luminal surface of endothelial cells, hydrolyze TGs from the lipoproteins to liberate FAs. Hepatic lipase (HL) has 40% homology with LPL and is expressed highly in hepatocytes and is located mainly in at the surface of those cells and surrounding endothelial cells. HL exhibits low TG hydrolase activity against chylomicrons substrates and instead hydrolyzes TGs chylomicron remnants, intermediate density lipoproteins (IDL) and TG-rich high-density lipoproteins (HDLs) (Young and Zechner, 2013).

4.2 Endothelial Lipase

Endothelial Lipase (LIPG) protein was first described and characterized as a protein member of the triacylglycerol (TG) lipase family by two laboratories trying to determine gene expression patterns in different models. One of them searched for genes up or down regulated in an *in vitro* model of tube development using human umbilical vein endothelial cells (HUVEC) cells (Hirata, 1999). The second study sought to determine genes that were differentially regulated in macrophage like cells (THP-1) treated with oxidized low density lipoprotein (oxLDL) (Jaye et al., 1999). Human LIPG amino acid sequence identity is 44% to human lipoprotein lipase (LPL) and 41% to human hepatic lipase (HL), with considerable conservative substitutions of non-identical residues. The mature human and mouse LIPG proteins consist of 482 amino acids encoding a 55 kDa protein. LIPG has common features with LPL and HL; for example, LIPG alignment with human LPL and HL amino acid sequences revealed conservation of catalytic residues serine (Ser169), aspartic acid (Asp 193) and histidine (His 274). Moreover the LIPG lid region, which forms an amphipathic helix covering the catalytic pocket of the enzyme and confers substrate specificity to the TG-lipase family, is three residues shorter and less amphipathic than LPL and HL. LIPG has a heparin binding region, five potential glycosylation sites and a secretion signal sequence in the amino-terminus region. Once LIPG is secreted, it binds to cell surface heparin-sulfate proteoglycans, where it has been shown to exert part of its action (Hirata, 1999). HUVEC cells and human coronary artery endothelial cells (HCAEC) express LIPG mRNA and three LIPG protein isoforms. This isoforms are detected in the cultured media of the cells and when stimulated with phorbol ester (PMA) they expression is increased. LIPG is detected as a 55 kDa protein corresponding to the predicted molecular mass of the mature protein, an isoform of 68 kDa considered to be the glycosylated and an immune reactive band of 40 kDa representing a proteolytic product of the native protein (Jaye et al., 1999).

Northern blot analysis and in situ hybridization analysis show LIPG mRNA expression in placenta, lung, liver, kidney, testis, thyroid and ovaries; brain, heart and muscle did not express LIPG mRNA. Interestingly, LPL shows a

different expression pattern and has been found to be expressed in muscle, heart, mammary gland, brain and macrophages (Hirata, 1999; Jaye et al., 1999).

LIPG has a high activity level of phospholipase A1, the ratio of triglyceride activity to phospholipase activity of LIPG is of 0,65 compared with 24,1 for HL or 139,9 for LPL. LIPG has primary phospholipase A1 activity, hydrolyze the sn-1 fatty acids from phospholipid substrates, with minimal triglyceridase activity. (McCoy et al., 2002). LIPG efficiently cleaves fatty acids (FA) form HDL-phospholipids, supplying FA in LIPG expressing cells. It has been observed that LIPG not only is able to hydrolyze phospholipids, moreover, the enzyme promotes lipoprotein incorporation as acting as a bridge between lipids and endothelial cells, showing a non-catalytically function (Fuki et al., 2003). Regarding this function LIPG is able to uptake HDL-C in vitro and in vivo (Broedl et al., 2003; Strauss et al., 2002). Mass spectrometry analysis in LIPG overexpressing HAEC cells incubated with HDL show an increase in various Lysophosphatidylcholine (LPC) and lysophosphatidylethanolamine (LPE) species in cell culture supernatants. When lipid content was analyzed, cellular phosphatidylcholine (PC), LPC and triglycerides levels were increased. LIPG overexpressing HADEC cells incubated with (^{14}C)-PC or (^{14}C)-LPC further accumulate 14C-LPC indicating that LIPG mediate the LPC supply in cells (Riederer et al., 2012).

The main LIPG physiological function known so far is the regulation of plasma HDL cholesterol (HDL-C) levels. It has been reported that LIPG overexpression resulted in significantly decreased HDL cholesterol plasma levels by increasing the catabolic rate of HDL apolipoproteins (Maugeais et al., 2003) whereas inhibition (Jin et al., 2003a) or genetic ablation of LIPG (Ishida et al., 2003; Ma et al., 2003) raise plasma HDL cholesterol (HDL-C), phospholipids and apoA-I due to a slower catabolic rate. Moreover it has been described that catabolism and hepatic cholesterol uptake by LIPG is done through scavenager receptor class B type I. As a result LIPG promotes the remodeling and elimination of HDL-C particles and by doing so HDL plasma levels are reduced and hepatic cholesterol content is increased (Nijstad et al., 2009; Wiersma et al., 2009).

As mentioned before there is a link between LIPG expression and inflammation. LIPG expression is regulated by a variety of factors. Tumor necrosis factor α, interleukin1β (IL1β) and biomechanical forces can induce LIPG mRNA expression in human endothelial cells (Hirata et al., 2000). Although phospholipase and TG lipase activities are barely detected in endothelial cells without stimulation, cytokine treatment induces phospholipase and TG lipase activities with concomitant increase in the protein expression (Jin et al., 2003b). Lipopolysaccharide induces LIPG expression via activation of toll-like receptor 4 in macrophages *in vitro* and *in vivo* (Wang et al., 2007).

LIPG activity is also regulated trough posttranscriptional mechanisms. LIPG forms a homo-dimer that is essential to maintain LIPG activity. LIPG activity is shown to be regulated by protein convertases (PCs). PCs induce site specific proteolysis, which play a crucial role regulating many biological pathways, including the sequential initiation of activation of blood coagulation factors and activation of caspases and digestive enzymes. LIPG is proteolitically processed into 40 and 28 kDa fragments and inactivated by PCs. Overexpression of porfurin, an inhibitor of PCs, inhibits the cleavage of LIPG and increases plasma phospholipase activity (Jin et al., 2005). Mice overexpressing profurin in livers by adenovirus infection present decreased levels of plasma HDL-C and phospholipids with reduction in plasma content of LIPG 40 kDa isoform and increase of 68 kDa isoform. Moreover plasma phospholipase activity was increased in Adenovirus-porfurin treated mice demonstrating that hepatic PCs regulate LIPG function through LIPG cleavage which inhibits the protein (Jin et al., 2007).

4.3 Lipolysis and cancer

We have revised cancer metabolism in the previous section, nevertheless there are some evidences that lipolysis could have an impact in cancer growth. LPL expression in rapidly proliferating cancer cells could affect the delivery and uptake of lipids nutrients to those cells. Immunohistochemical studies have demonstrated the presence of LPL and CD36 (a FA transporter) in the majority of breast cancer, liposarcoma and prostate cancer samples. Interestingly, LPL is frequently overexpressed in invasive cervical squamous cell carcinomas.

Most impressively, patients with chronic lymphocytic leukemia whose leukemia cells express high levels of LPL transcripts have lower survival rate. Little is known about the role of intracellular lipases in carcinogenesis and tumor proliferation but for example MAGL (described before) has a potent pro-tumorigenic activity. Still a profound study is necessary to address whether lipases play pivotal roles in cancer pathogenesis (Young and Zechner, 2013).

Objectives

Metabolic reprograming is known to be a major event in cancer cells. Here we addressed whether breast cancer cells relay on particular metabolic pathways to allow proliferation. We sought to study the contribution of FoxA transcription factors to breast cancer metabolic dependence.

The present work sought to fulfill the following objectives:

1. To identify FoxA regulated genes in breast cancer associated with metabolic function.

2. To understand how metabolic genes downstream of FoxA transcription factors contribute to breast cancer.

3. To explore the regulated metabolites under the control of our selected candidate.

Results

1. Breast cancer retain FoxA1 or FoxA2 transcription factors for cancer growth

1.1 Expression of FoxA transcription factors in breast cancer

For decades it has been known that cancer cells change their metabolism from oxidative phosphorylation to aerobic glycolysis, a process termed the Warburg effect. Nevertheless, the change in the glycolytic pathway is not the only metabolic modification in cancer cells. In this scenario, several efforts have been undertaken to elucidate to what extent the modification on metabolic pathways supports cancer growth and pathogenesis in a tumor specific context. It is currently accepted that alterations in metabolic pathways or metabolic genes provide advantages in terms of tumor progression, growth and malignancy. For example, monoacylglycerol lipase (MAGL) promotes cell migration, invasion, survival and *in vivo* tumor growth through the regulation of pro-oncogenic lipids (Nomura et al., 2010).

In this regard, we explored differentially expressed transcription factors that may regulate breast cancer progression or growth through the regulation of metabolic genes. For this purpose, and in order to find deregulated transcription factors, we interrogated the gene expression of Human Mammary Epithelial cells (normal cells) and the human breast cancer cell lines MCF7 (ER+) and MDA-MB-231 (ER-).

Principal Component Analysis (PCA) was applied to the normalized data of all cell lines to reveal the main components that explained the variance in the data. PCA is a mathematical procedure that uses orthogonal transformation to convert a set of observations of possibly correlated variables into a set of values of uncorrelated variables called principal components (PC). This transformation is defined in such a way that the first PC preserves as high variance as possible. PCA was able to highlight the differences in the genetic background between HMEC, MDA-MB-231 and MCF7 cells, emphasizing the differences between them at molecular levels (**Figure 8A**). The heatmap generated on

samples showed expressed genes at the same level and differentially expressed genes in all assessed cells. Moreover, there were common differentially expressed genes in both tumor cell lines compared with the non-tumor cell line. Lastly, we observed differentially expressed genes just in one breast cancer subtype compared with the non-tumor cells and the other breast cancer line (**Figure 8B**).

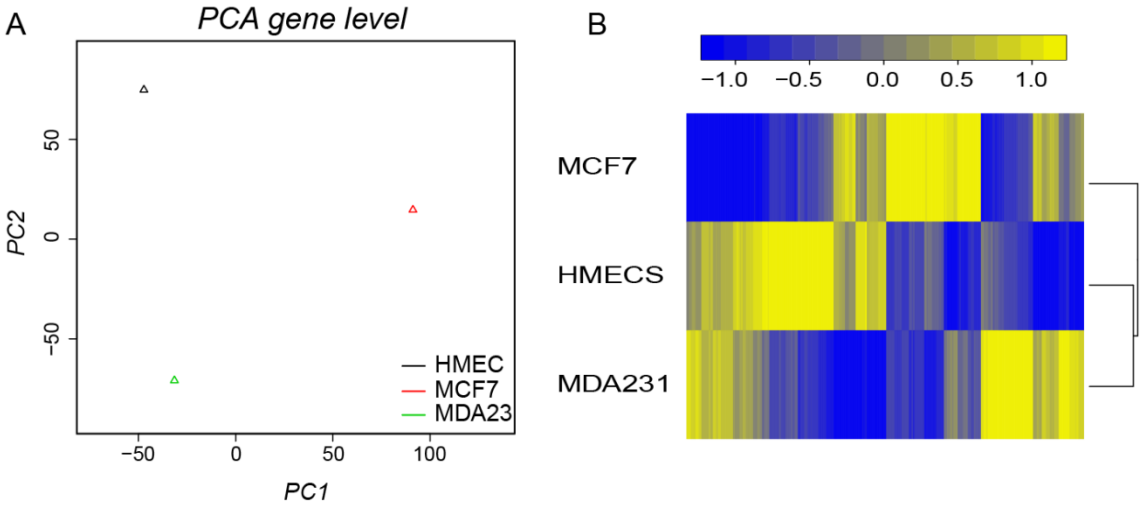

Figure 8.- Analysis of HMECS, MCF7 and MDA231 gene expression patterns. A) PCA plot from HMEC, MCF7 and MDA-MB-231 cells. Samples were positioned along the first (PC1) or the second (PC2) principal component according to their gene expression similarity. B) Hierarchical cluster diagram of samples from cells.

We next generated three lists of differentially expressed genes comparing the above mentioned cells. The first list contained up- or down- regulated genes in both cancer cell lines compared with the non-tumor cells; the second and third lists included genes that were up- or down- regulated in MCF7 or MDA-MB-231 cell lines, independently, compared with the non-tumor cells. These lists are referred to **Tumor expression**, **ER+ expression** and **ER- expression**, respectively. Next, we identified transcription factors in the three lists using two annotated gene ontology pathways (transcription factor complex and transcription factor binding). We identified six transcription factors deregulated in both cancer cell lines and ten differentially expressed transcription factors in the **ER+** list. Lastly, we found five deregulated transcription factors in the **ER-** list (**Figure 9**). From the analysis, we were interested in transcription factors that regulated metabolic pathways in different tissues. Among the 21 deregulated transcription factors, FoxA1 emerged as an attractive candidate to

evaluate its contribution to breast cancer pathogenesis through the regulation of metabolic pathways.

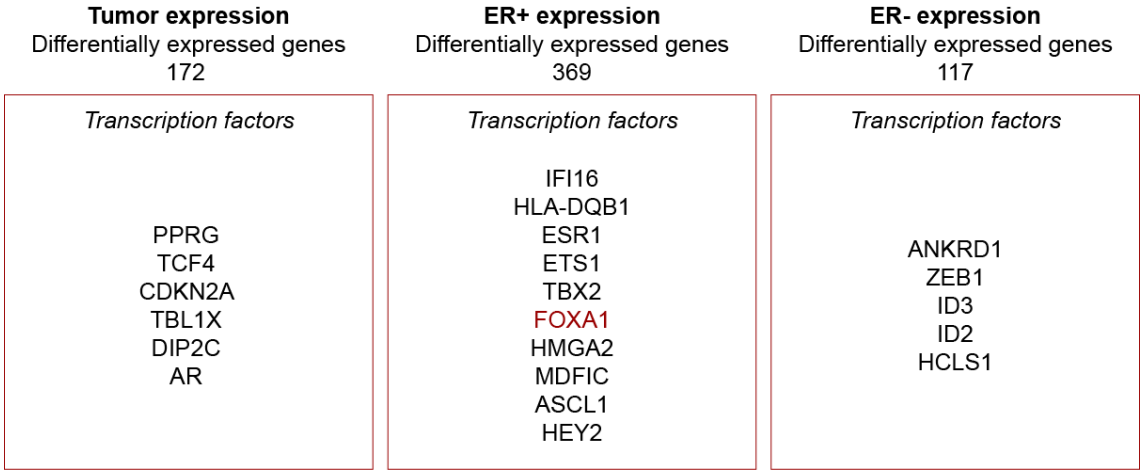

Figure 9.- Transcription factors deregulated in breast cancer tumor cells. Transcription factors deregulated in both breast cancer cell lines (Tumor list). Transcription factors deregulated in MCF7 cells compared with MDA-MB-231 cells and HMEC (ER+ list). Finally, transcription factors deregulated in MDA-MB-231 cells compared with MCF7 and HMEC.

FoxA1 is a member of the FoxA family of transcription factors, which regulates tissue development and metabolism in several adult tissues. In this context, FoxA1 regulates gluconeogenesis and lipolysis in the liver and insulin secretion and metabolism in the pancreas, among others. More specifically, FoxA1 regulates the estrogen response in breast cancer and is therefore necessary for luminal specification.

Interestingly, there are compensatory functions between members of the FoxA family. For this reason, we evaluated whether other transcription factors of the FoxA family were expressed in breast cancer. We first, determined the expression of FoxA1, FoxA2 and FoxA3 in HMEC, MDA-MB-231 and MCF7 cells using Affymetrix derived data (**Figure 10**). FoxA1 was overexpressed in MCF7 cells compared with both cell types, as we previously detected. Remarkably, we found overexpression of FoxA2 in MDA-MB-231 cells. For FoxA3, there were no differences in the expression across the three cell types.

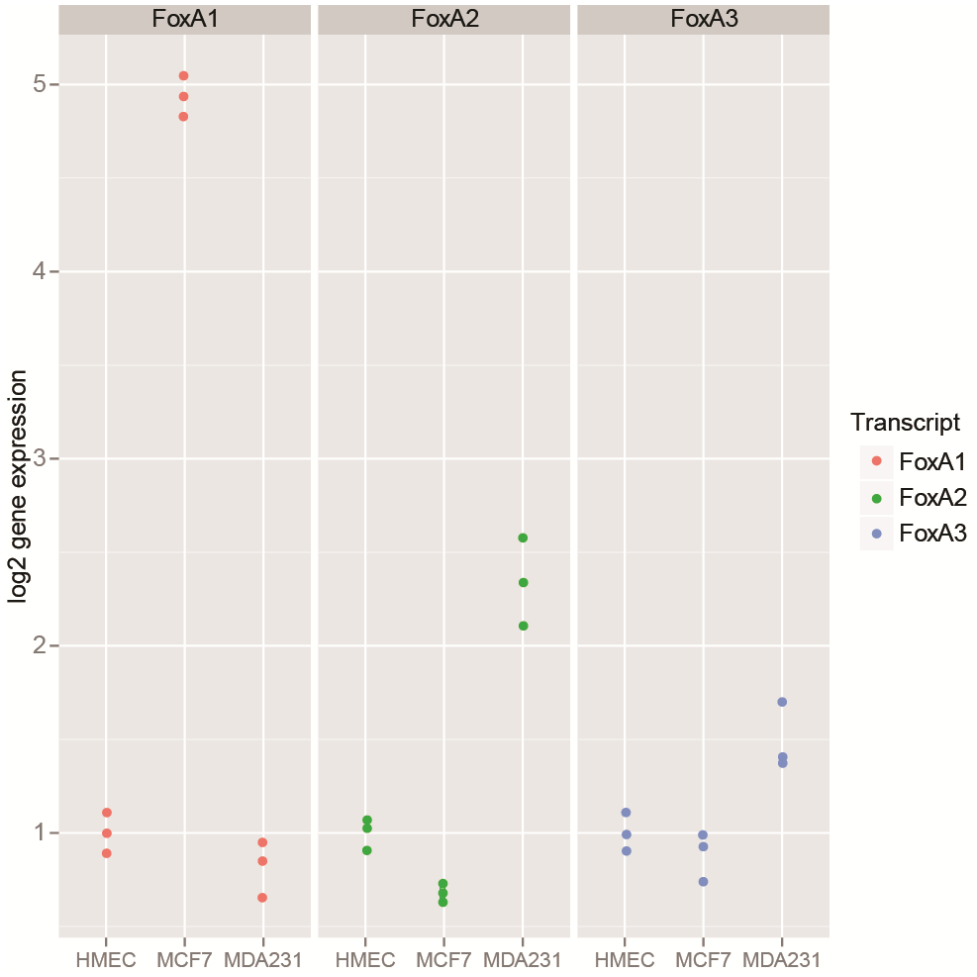

Figure 10.- Analysis of HMECS, MCF7 and MDA-MB-231 gene expression. A) FoxA1, FoxA2 and FoxA3 expression in breast cancer cell lines. Data is derived from Affymetrix expression analysis.

Next, we used kernel density estimation to evaluate the probability density function of FoxA1 in three cohort of primary breast cancer tumors (MSKCC/EMC). When using all samples (ER+ and ER- breast cancer samples), the data is represented as a bimodal curve showing two populations of patients with low and high FoxA1 expression (**Figure 11A**). As expected, FoxA1 expression is distributed as a monomodal curve in estrogen positive breast cancer samples (**Figure 11B**), whereas ER- samples presented a bimodal distribution (**Figure 11C**).

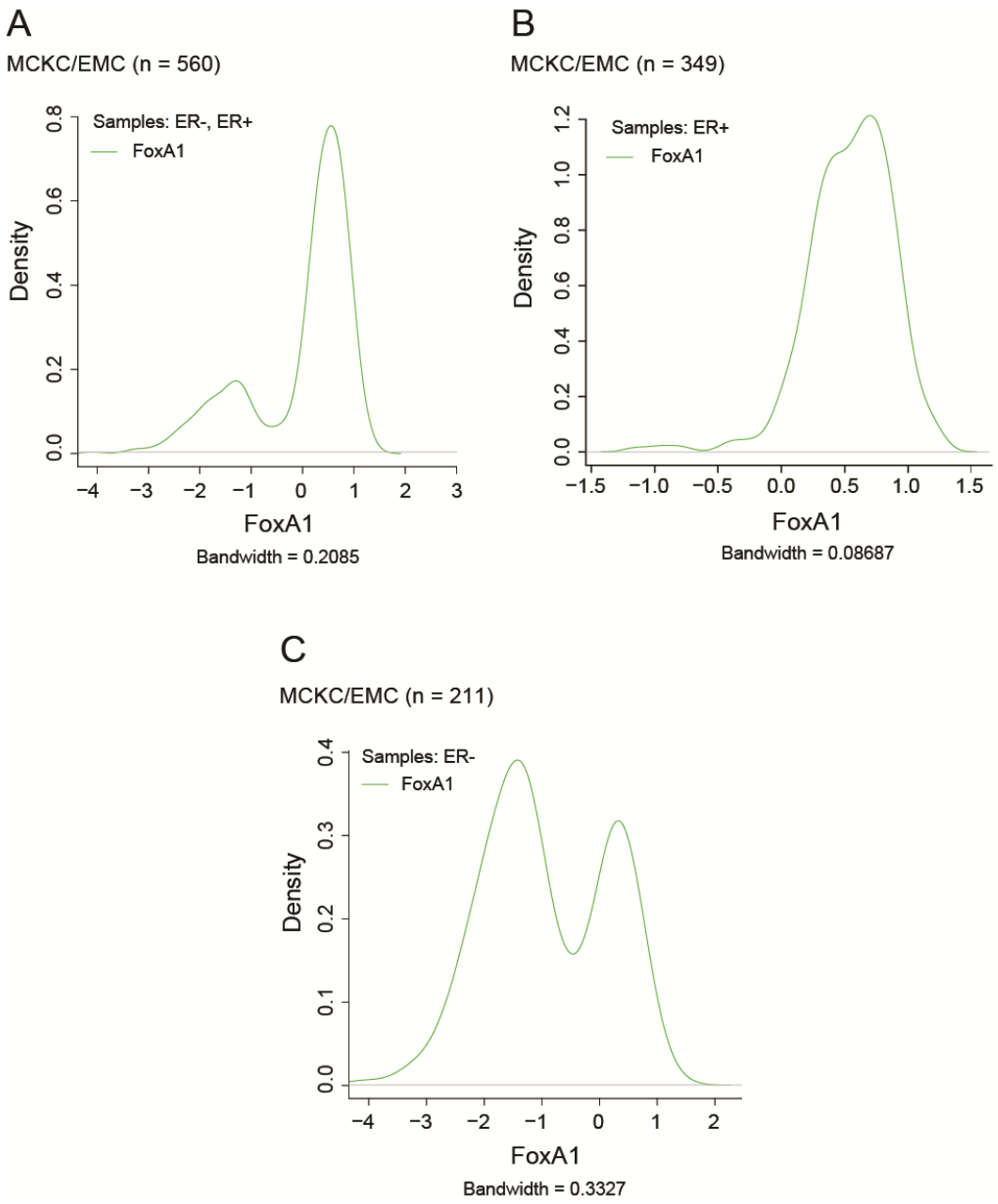

Figure 11.- FoxA1 in breast cancer patients. Kernel density plots of FoxA1 mRNA expression in human breast cancer samples. **A**) All samples, **B**) ER+ samples and **C**) ER- samples.

To further analyze the expression of FoxA factors in human samples, we correlated FoxA1 gene expression levels to FoxA2 mRNA expression (**Figure 12)**. FoxA2 was expressed in human breast cancer samples independently of FoxA1 expression in both ER- and ER+ breast cancer samples.

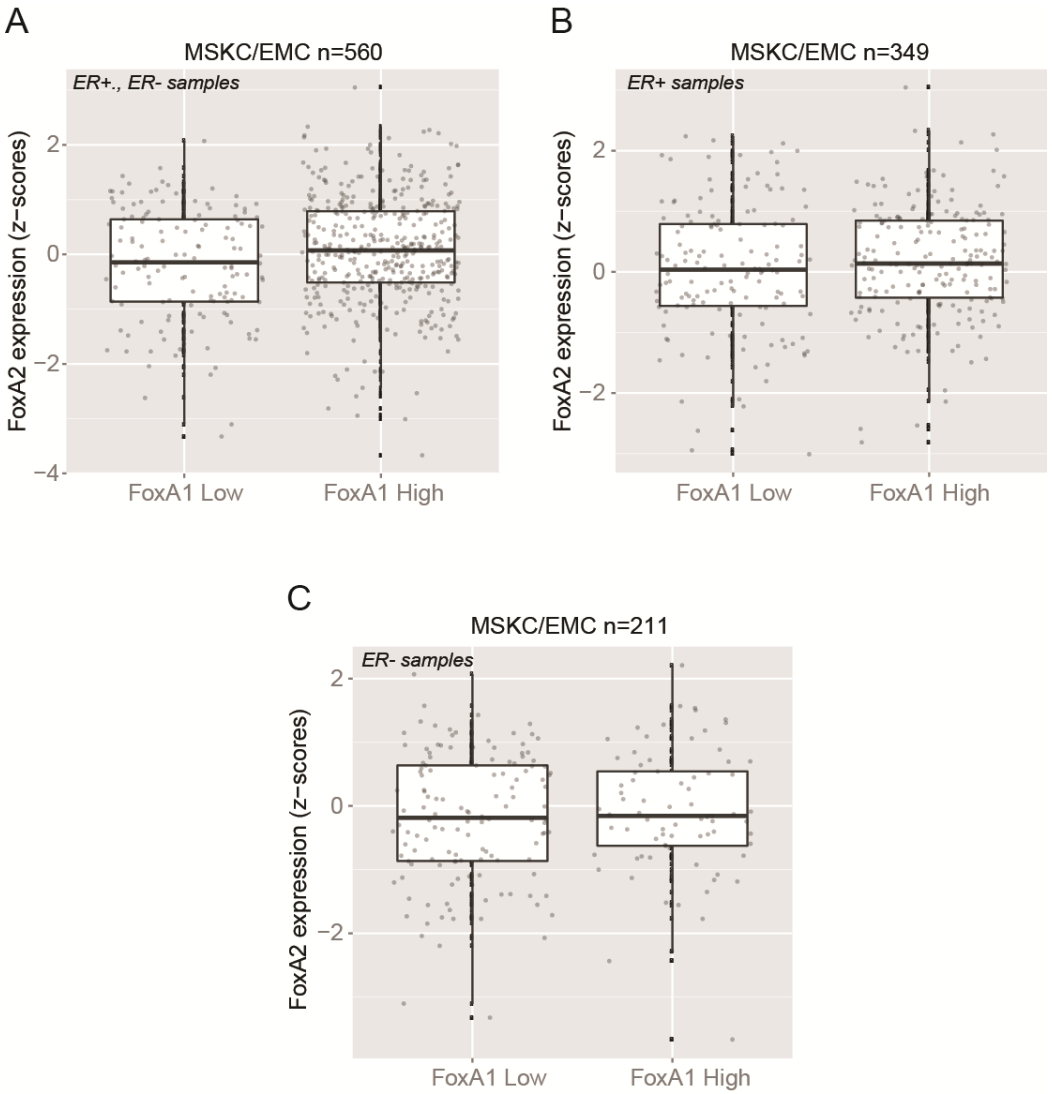

Figure 12.- Correlation of FoxA1 and FoxA2 expression levels in breast cancer samples.

We showed that FoxA1 mRNA levels were able to separate breast cancer patients in two groups, those with high or low levels of FoxA1 expression. Most striking was the fact that ER- patients have the same bimodal curve, meaning that FoxA1 was expressed, in part, in samples without ER expression. Furthermore, FoxA2 was expressed in breast cancer samples. Yet, we wondered whether FoxA1 and FoxA2 functions were retained in breast cancer cell lines. To this end, we evaluated FoxA expression in different human breast cancer cell lines, one which expresses ER, while the other does not.

We assessed FoxA1 expression by real time PCR and western blot analysis in several breast cancer lines **(Figure 13 A and B, respectively)**. We compared three ER + breast cancer cell lines (MCF7, T47D and BT474) and five ER-

breast cancer cell lines (SKBR3, MDA-MB-231, MDA-MB-468, MDA-MB-435 and BT20) to human mammary epithelial cells (HMEC). Among the ER+ and ER- breast cancer cell lines two were HER2+ (BT474 and SKBR3). We noted that all ER positive cells (MCF7, T47D and BT4747) expressed FoxA1 mRNA levels over 100 times higher than in HMEC cells. Furthermore, SKBR3 cells also express FoxA1, as do the ER positive lines. This is in agreement with the previous observation in ER negative breast cancer patients. Protein expression analysis using an antibody against FoxA1, showed a molecular band of 50 KDa in MCF7, T47D, SKBR3 and BT474 cell lines, in agreement with mRNA levels. Out of the four ER- cell lines, BT20 and MDA-MB-468 cells overexpressed FoxA1 mRNA levels compared with HMEC. This expression was not found at the protein level. Finally, MDA-MB-231 (ER-) and MDA-MB-435 (ER-) cells expressed similar FoxA1 mRNA levels compared with HMEC.

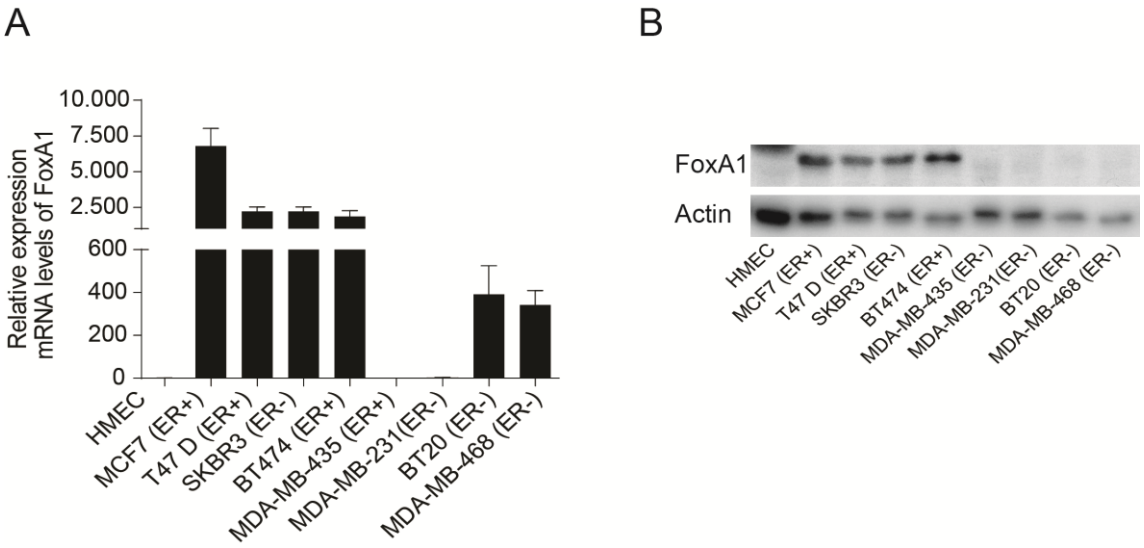

Figure 13.- FoxA1 mRNA and protein expression in breast cancer cell lines. A) Total RNA was probed by qRT-PCR with FoxA1 TaqMan probe and normalized to 18S expression levels in 8 breast cancer cell lines compared with Human Mammary Epithelial cells, data is normalized to non-tumor cells, data are mean +/- SD (n=3). **B)** Extract of 8 breast cancer cell lines and Human Mammary Epithelial cells were immunobloted using a FoxA1 antibody

In the same panel of breast cancer lines, we assessed the expression of the FoxA2 transcription factor. To our surprise, MDA-MB-231 cells, the most common triple negative breast cancer cell line, expressed FoxA2 instead of FoxA1 (**Figure 14 A and B, respectively**). FoxA2 mRNA levels were over 100

times higher in these cells than in HMEC. Of note, FoxA1 and FoxA2 expression was mutually exclusive in breast cancer cells.

In summary, FoxA1 and FoxA2 were overexpressed in patient samples and breast cancer lines, and we noted that FoxA1 expression levels stratified breast cancer tumor samples. Similarly, FoxA1 was expressed in a subset of breast cancer cell lines usually displaying luminal features. In the case of FoxA2, it did not correlate with low or high FoxA1 expression levels in tumor samples. However, FoxA2 was found to be expressed in the triple negative MDA-MB-231 cells. A striking observation was that FoxA factors showed a mutually exclusive expression pattern.

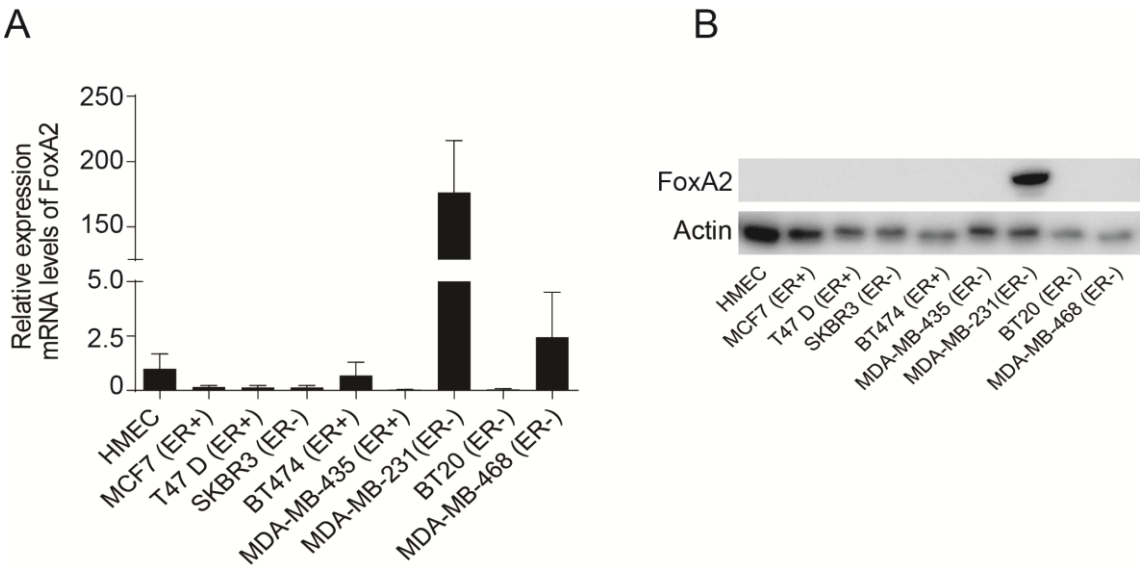

Figure 14.- FoxA2 mRNA and protein expression in breast cancer cell lines. A) Total RNA was probed by qRT-PCR with FoxA2 TaqMan probe and normalized to 18S expression levels in 8 breast cancer cell lines compared with Human Mammary Epithelial cells, data is normalized to non-tumor cells, data are mean +/- SD (n=3). **B)** Extract of 8 breast cancer cell lines and Human Mammary Epithelial cells were immunobloted using a FoxA2 antibody.

1.2 FoxA transcription factors control pivotal genes for breast cancer growth.

FoxA transcription factors were overexpressed in breast cancer cell lines and patients samples, including FoxA1 and FoxA2. Next, we aimed to explore whether breast cancer rely on FoxA transcription factors for growth. To this end, we engineered cells bearing a doxycycline-inducible shRNA vector targeting

either FoxA1 or FoxA2 (**Table II and III**). Furthermore, upon doxycycline treatment, there was concomitant expression of Turbo RFP (tRFP) to track shRNA induction. As controls, we used cells transduced with the same expression system carrying a shRNA sequence that did not target any specific mRNA upon doxycycline administration (sh Control (Dox+)), and cells containing the doxycycline–driven FoxA1 or FoxA2 shRNA expression system without doxycycline treatment (**Table II and III**). All cells constitutively expressed GFP and cells with the doxycycline–driven shRNA expression system expressed tRFP, as indicated above.

Table II and III.- FoxA1, FoxA2, tRFP and GFP expression in MCF7 and MDA-MB-231 engineered cells

Table II

MCF7 (ER+) cells	**FoxA1**	**FoxA2**	**tRFP**	**GFP**
Sh Control (Dox+)	**yes**	**no**	**yes**	**yes**
Sh FoxA1 (Dox-)	**yes**	**no**	**no**	**yes**
Sh FoxA1 (Dox+)	**no**	**no**	**yes**	**yes**

Table III

MDA-MB-231 (ER-) cells	**FoxA1**	**FoxA2**	**tRFP**	**GFP**
Sh Control (Dox+)	**no**	**yes**	**yes**	**yes**
Sh FoxA2 (Dox-)	**no**	**yes**	**no**	**yes**
Sh FoxA2 (Dox+)	**no**	**no**	**yes**	**yes**

Doxycycline addition to the culture media for 72 hrs induced the expression of tRFP and the concomitant short hairpin sequence of interest. As expected, all sh-inducible populations showed red fluorescence (**Figure 15A**). Next, we performed a doxycycline treatment time course in MCF7 and MDA-MB-231 cells, in order to confirm FoxA depletion. Doxycycline treatment in MCF7 cells for 48, 96 and 144 hrs induced a sequential drop of FoxA1 mRNA levels, reaching almost 60% of reduction at 144 hrs. Similarly, doxycycline treatment in MDA-MB-231 cells decreased FoxA2 mRNA levels at all tested time points.

Control cells did not show differences in FoxA levels (**Figure 15B**). Of note, cells maintained factors down-regulation only in the presence of doxycycline.

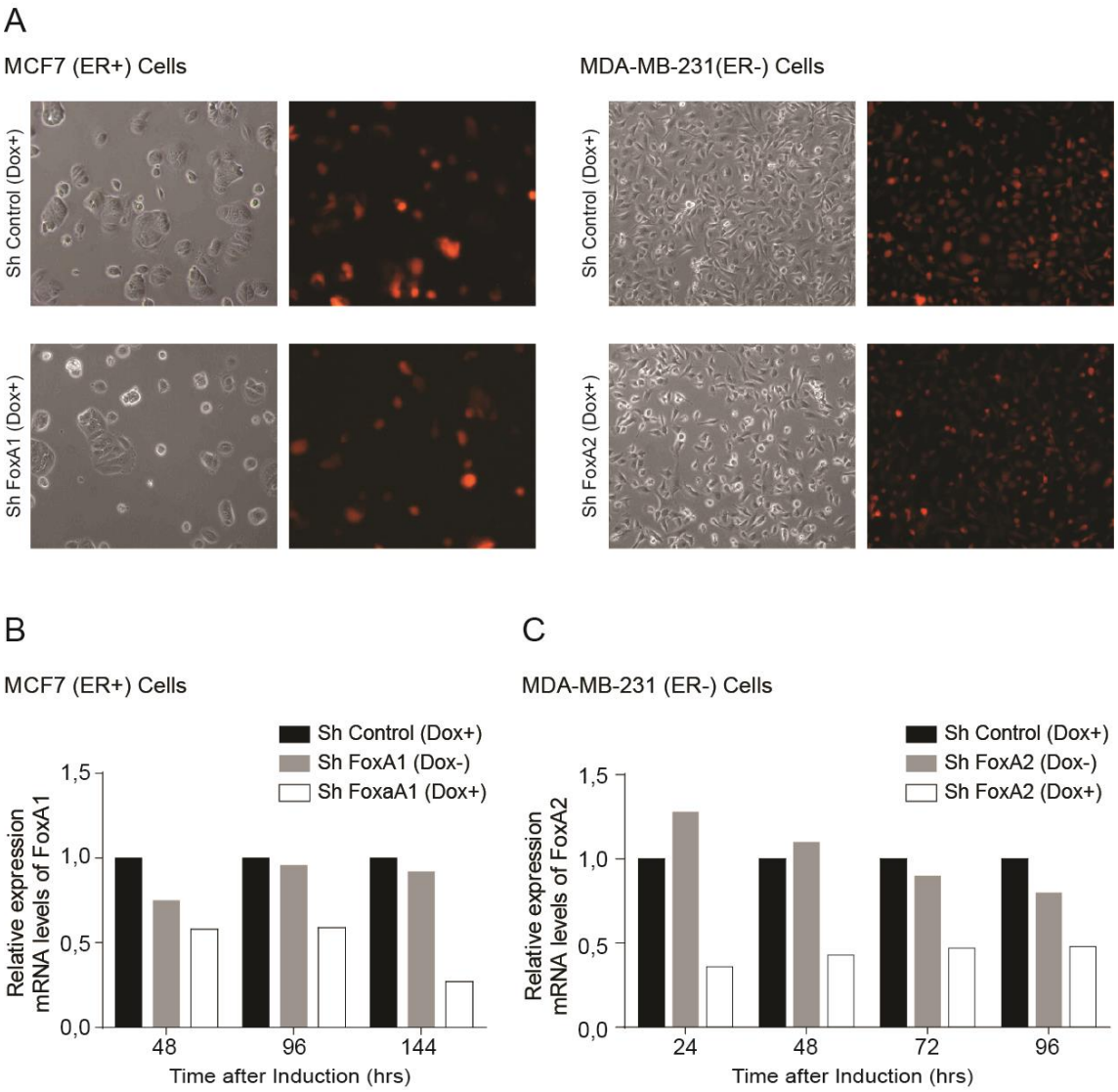

Figure 15.- Doxycycline treatment induces the expression of FoxA1 and FoxA2 short hairpins with the concomitant FoxA transcription factors mRNA reduction. MCF7 and MDA-MB-231 cells, transduced with a non-targeting mRNA sequence or with an inducible FoxA1 and FoxA2 short hairpin sequence were grown in complete media with 2µg/mL doxycycline (Dox+) or without doxycycline (Dox-) for 48, 96, 144 hrs and 24, 48, 72, and 96 hrs, respectively. **A)** Microscopy images of cells at 96 hrs of Doxycycline treatment. **B**) Total RNA was probed by qRT-PCR with FoxA1 and FoxA2 TaqMan probes and normalized to 18S expression levels, data is normalized to cells containing the non-targeting sequence at 48 hrs for MCF7 cells and 24 hrs for MDA-MB-231 cells, n=1 for each time point and for each cell genotype.

Deeper analysis of cells at 144 hrs of doxycycline treatment demonstrated that FoxA2 was not induced in FoxA1 depleted MCF7 cells, and similarly, FoxA1 was not induced in FoxA2 depleted MDA-MB-231 cells. These observations

were determined by protein expression (**Figure 16 A and B**). Interestingly, FoxA1-depleted MCF7 cells displayed morphological changes (**Figure 17A**) and showed a significant growth arrest *in vitro* (**Figure 17B**). As in MCF7 cells, FoxA2-depleted MDA-MB-231 cells phenocopied FoxA1-depleted cells, which included, morphological changes and *in vitro* growth reduction (**Figure 17 A and B**).

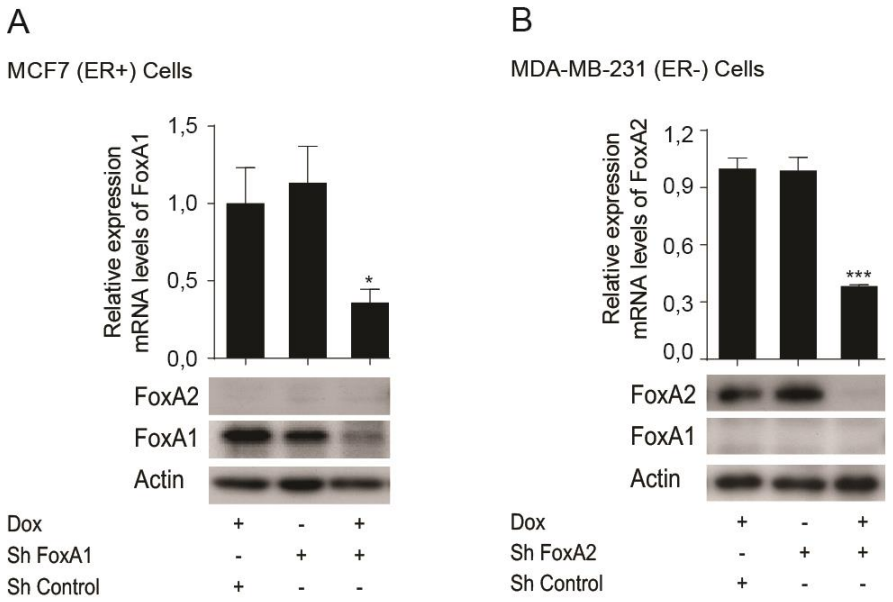

Figure 16.- 144 hrs of doxycycline treatment induces the down-regulation of FoxA1 and FoxA2. MCF7 and MDA-MB-231 cells containing sh control sequences and an inducible FoxA1 or FoxA2 short hairpin sequence were incubated for 144 hrs with 2µg/µL doxycycline (Dox+) and without doxycycline (Dox-). **A)** Total MCF7 cells RNA were probed by qRT-PCR with the corresponding TaqMan probes and normalized to 18S expression levels, data is normalized to cells containing the sh control sequence incubated with doxycycline, data are mean +/- SD (n=3). MCF7 cell extracts were immunobloted with corresponding antibodies. **B)** Total MDA-MB-231 cells RNA were probed by qRT-PCR with the corresponding TaqMan probes and normalized to 18S expression levels, data is normalized to cells containing the non-targeting sequence incubated with doxycycline, data are mean +/- SD (n=3). MDA-MB-231 cell extracts were immunobloted with corresponding antibodies.

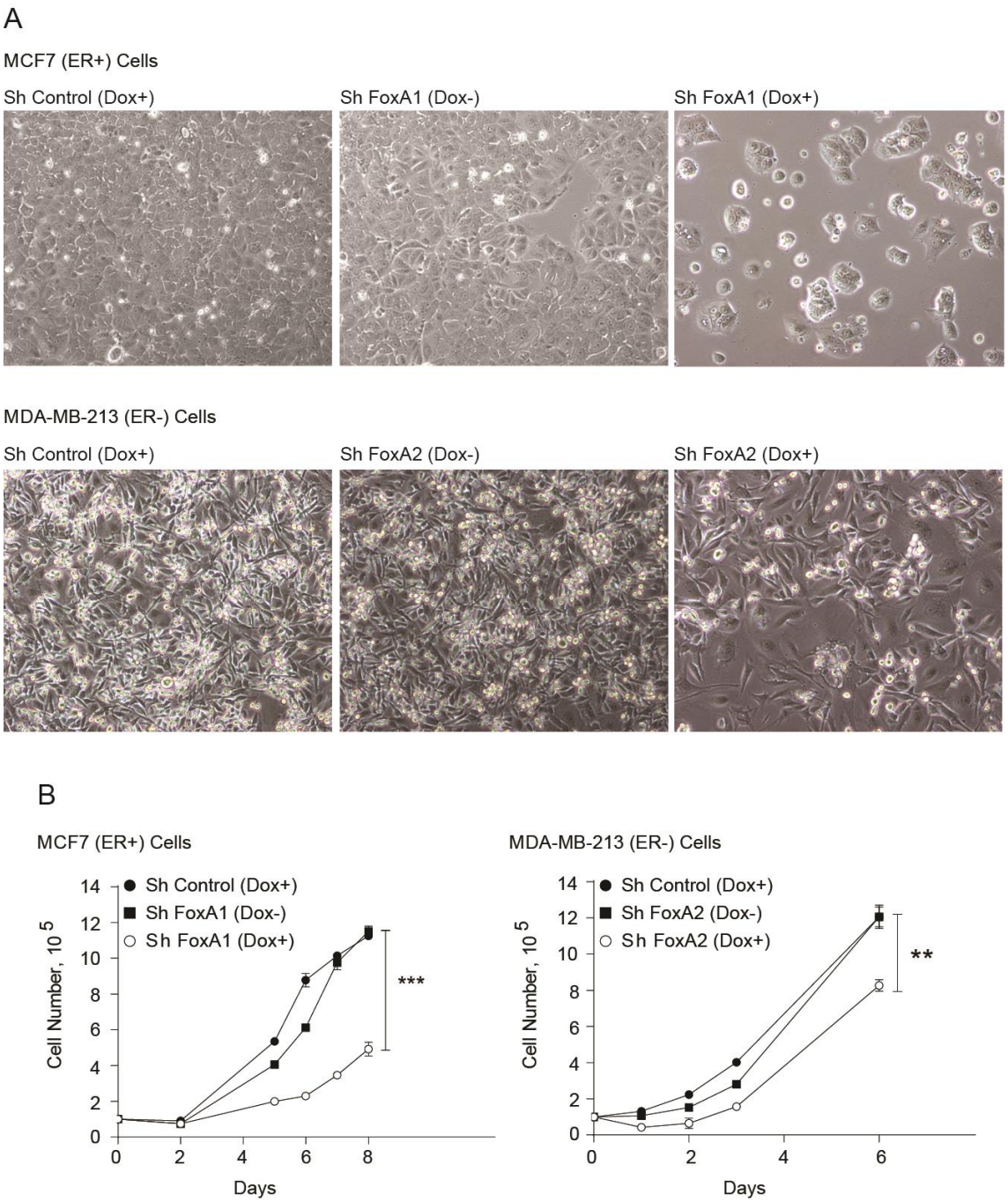

Figure 17.- FoxA1 and FoxA2 are necessary for cancer cell growth *in vitro*. MCF7 and MDA-MB-231 cells transduced with doxycycline inducible system were treated without Doxycycline (Dox-) or with 2µg/µL (Dox+) for 8 days and then plated to assess *in vitro* cell growth. **A)** Microscopy pictures of transduced cell post-doxycycline treatment. **B)** *In vitro* growth, 4 days (MDA-MB-231) or 8 days (MCF7), data are mean +/- SD (n=3) and T-test was calculated for the last point of the curve using cells carrying the sh control (Dox+) cell lines as control.

Finally, we assessed the *in vivo* influence of FoxA factors in breast cancer growth. To this end, we subcutaneously injected human MDA-MB-231 and MCF7 cells bearing the inducible shRNA system against FoxA1 or FoxA2 and

their corresponding controls. 1X10^6 cells cultured without doxycycline (sh RNAs were not expressed) were inoculated subcutaneously in nude mice treated with or without doxycycline for 2 weeks, and maintained with this regime for the duration of the experiment (**Figure 18A**). Fluorescence at 23 days post inoculation showed tRFP expression only in animals treated with doxycycline, indicating that the shRNAs were expressed *in vivo* (**Figure 18B**). FoxA1 or FoxA2 *in vivo* depletion induced a sustained tumor growth reduction in MCF7 and MDA-MB-231 cells (**Figure 19 A and B**). Growth inhibition was not observed in control tumors, however.

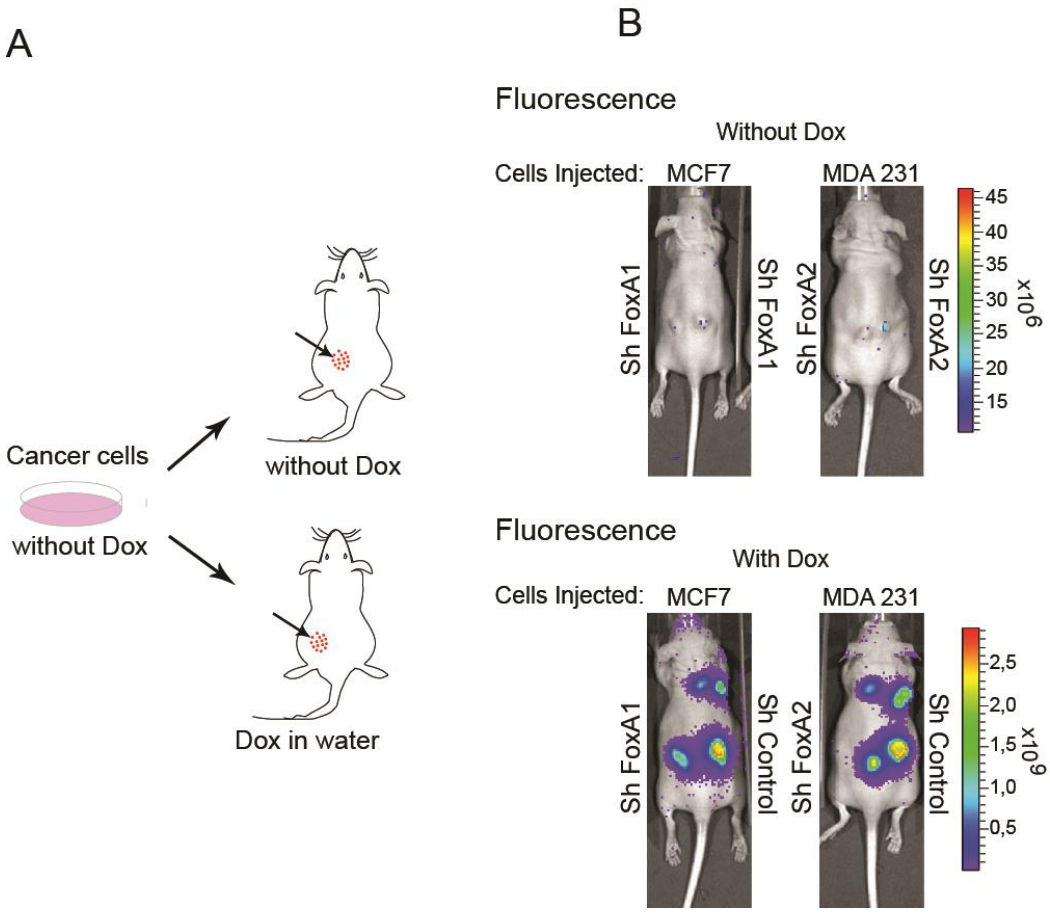

Figure 18.- ***In vivo*** **growth of transduced tumor cells. A)** Schematic representation, 1 X10^6 MDA231 and MCF7 transduced cells injected subcutaneously in NUD mice. Cells were grown without doxycycline (**short hairpin not expressed**) and inoculated in mice treated with or without doxycycline. **B)** Pictures of fluorescence recordings at 533 nm excitation wavelength for animals with and without doxycycline treatment.

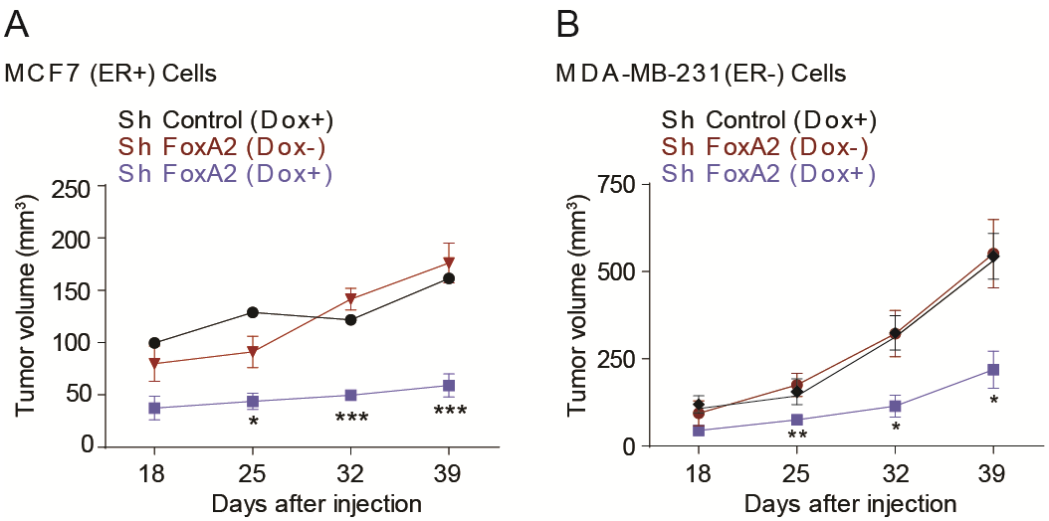

Figure 19.- FoxA1 and FoxA2 transcription factors are necessary for breast cancer growth *in vivo*. Tumor growth curves of cells subcutaneously injected in NUD mice with or without doxycycline administration for 39 days. **A)** MCF7 cells; sh control (Dox+) (**black line**), Sh FoxA1 (Dox-) (**red line**), Sh FoxA1 (Dox+) (**blue line**). **B)** MDA-MB-231cells; sh control (Dox+) (**black line**), Sh FoxA2 (Dox-) (**red line**) and Sh FoxA2 (Dox+) (**blue line**). Each data point represents the mean tumor volume +/- SEM (n=3-8) and T-test was calculated at each point using sh FoxA (Dox-) as controls in both cell types.

1.3 Compensatory roles of FoxA1 and FoxA2 in breast cancer.

Luminal and basal breast cancer types grow through different mechanisms. The luminal subgroup has a transcriptional program mediated by estrogen, where FoxA1 plays a key role. The basal subgroup, on the other hand, grows through mutations in tumor suppressor and oncogenes with hormone independency. Interestingly, it is known that FoxA1 and FoxA2 can regulate common genes in some tissues and that the loss of one factor is compensated by the other one. For this reason, we sought to evaluate whether in MCF7 cells and MDA-MB-231 cells (i.e. a ER+ breast cancer and triple negative breast cancer) FoxAs control a common set of genes to sustain *in vivo* growth.

In order to better understand the compensatory roles of FoxA1 and FoxA2 in breast cancer pathogenesis, we attempted to rescue the growth reduction phenotype of FoxA depleted tumors by expressing FoxA2 in MCF7 cells and FoxA1 in MDA-MB-231 cells.

To achieve this, we used doxycycline–driven shFoxA1 MCF7 cells with exogenous FoxA2 expression and doxycycline–driven shFoxA2 MDA-MB-231 cells with exogenous FoxA1 expression (**Table IV and V**).

Table IV and V.- FoxA1 and FoxA2 expression in MCF7 and MDA-MB-231 engineered cells

Table IV

MCF7 cells	FoxA1	FoxA2	tRFP	GFP
Sh Control (Dox+)	**yes**	**no**	**yes**	**yes**
Sh FoxA1 (Dox-)	**yes**	**no**	**no**	**yes**
Sh FoxA1 (Dox+)	**no**	**no**	**yes**	**yes**
Sh FoxA1+FoxA2 (Dox-)	**yes**	**yes**	**no**	**yes**
Sh FoxA1+FoxA2 (Dox+)	**no**	**yes**	**yes**	**yes**

Table V

MDA-MB-231 (ER-) cells	FoxA1	FoxA2	tRFP	GFP
Sh Control (Dox+)	**no**	**yes**	**yes**	**yes**
Sh FoxA2 (Dox-)	**no**	**yes**	**no**	**yes**
Sh FoxA2 (Dox+)	**no**	**no**	**yes**	**yes**
Sh FoxA2+FoxA1 (Dox-)	**yes**	**yes**	**no**	**yes**
Sh FoxA2+FoxA1 (Dox+)	**yes**	**no**	**yes**	**yes**

The addition of doxycycline to the cell culture medium induces FoxA1 depletion in FoxA2 expressing MCF7 cells and FoxA2 depletion in FoxA1 expressing MDA-MB-231 cells (**Figure 20 A and B**). Next, $1X10^6$ cells cultured without doxycycline were subcutaneously inoculated in nude mice. These mice were previously treated with or without doxycycline for 2 weeks prior to inoculation. Exogenous FoxA2 and FoxA1 expression in MCF7 or in MDA-MB-231 cells, respectively, rescued the growth reduction phenotype of FoxA depletion (**Figure 21 A**). MCF7 and MDA-MB-231 cells with simultaneous FoxA1 and FoxA2 expression grew in similar fashion as control tumors (**Figure 21 B**).

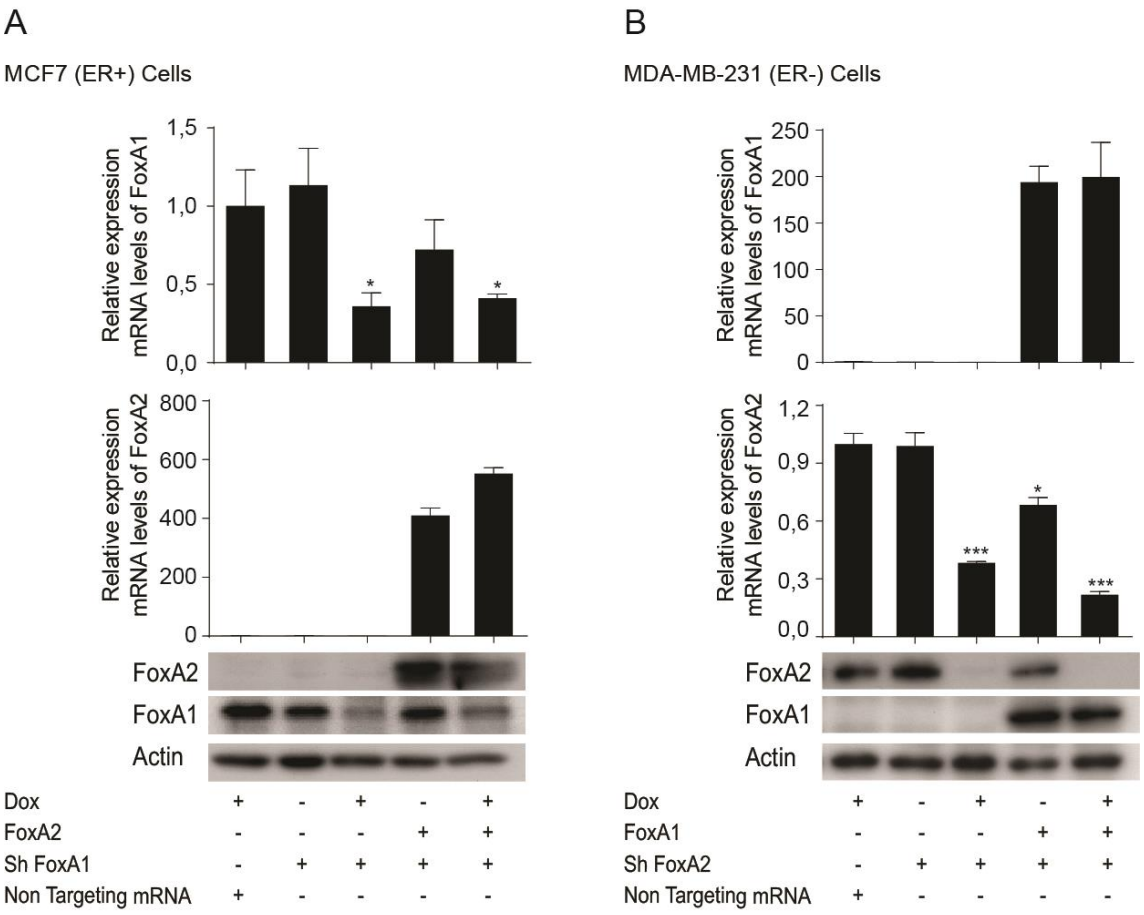

Figure 20.- 144 hrs of doxycycline treatment induces down-regulation of FoxA1 and FoxA2. MCF7 and MDA-MB**-**231 cells containing a non-targeting mRNA sequence, an inducible FoxA1 or FoxA2 short hairpin sequence or an inducible FoxA1 or FoxA2 short hairpin sequence with Foxa2 cDNA for MCF7 cells and FoxA1 cDNA for MDA231cells incubated for 144 hrs with 2µg of doxycycline (Dox+) and without doxycycline (Dox-). **A)** Total MCF7 cells RNA were probed by qRT-PCR with the corresponding TaqMan probes and normalized to 18S expression levels, data is normalized to cells containing the non-targeting sequence incubated with doxycycline, data are mean +/- SD (n=3); MCF7 cell extracts were immunobloted with the corresponding antibodies. **B)** Total MDA-MB-231 cells RNA were probed by qRT-PCR with the corresponding TaqMan probes and normalized to 18S expression levels, data is normalized to cells containing the non-targeting sequence incubated with doxycycline, data are mean +/- SD (n=3); MDA-MB-231 cell extracts were immunobloted with the corresponding antibodies.

To validate our results, we performed gene expression analysis of the different tumor populations (**Figure 22 A and B**)**.** MCF7 and MDA-MB-231 shFoxA tumors with doxycycline treatment showed reduced levels of FoxA1 or FoxA2, respectively. Moreover, FoxA2 was not induced in FoxA1-depleted MCF7 tumors. Similarly, FoxA1 was not induced in FoxA2-depleted MDA-MB-231 tumors. Lastly, we observe higher amounts of exogenous FoxA2 in MCF7 cells and exogenous FoxA1 in MDA-MB-231 cells in the FoxA overexpressing tumor populations.

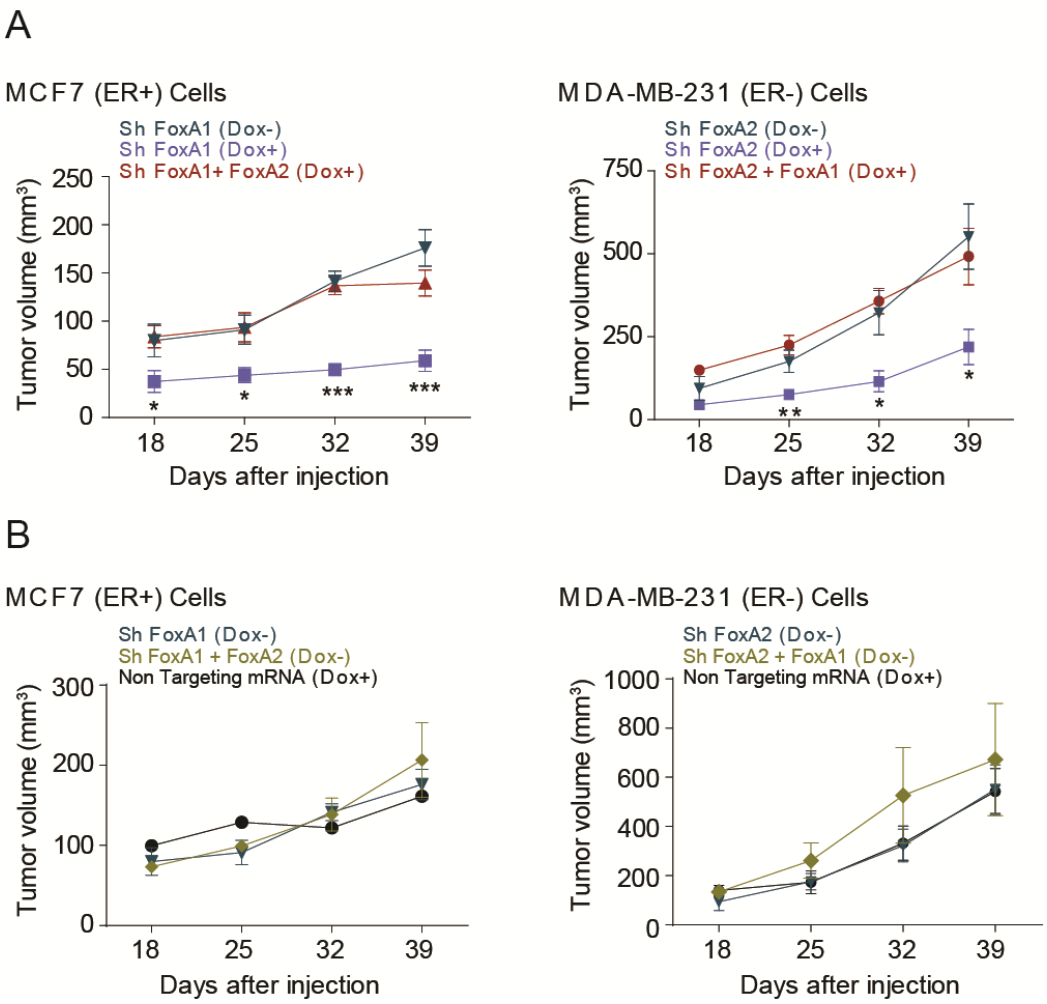

Figure 21.- FoxA1 and FoxA2 transcription factors are necessary for MDA-MB-231/MCF7 *in vivo* growth. Tumor growth curves of cells injected subcutaneously in NUD mice with or without doxycycline administration. A) MCF7 Sh FoxA1 and MDA-MB-231 Sh FoxA2 (Dox-) control tumors (**red lines**); MCF7 Sh FoxA1 and MDA-MB-231 Sh FoxA2 (Dox+), FoxA transcription factors short hairpins expressing tumors (**blue lines**); and MCF7 ShFoxA1+FoxA2 and MDA-MB-231 ShFoxA2+FoxA1 (Dox+), FoxA transcription factors short hairpins expressing tumors with overexpression of FoxA2 for MCF7 cells and FoxA1 for MDA-MB-231 cells (**green lines**). B) MCF7 Sh FoxA1 and MDA-MB-231 Sh FoxA2 (Dox-) control tumors (**red lines**); and MCF7 ShFoxA1+FoxA2 and MDA-MB-231 Sh FoxA2+FoxA1 (Dox-), cells overexpressing FoxA2 for MCF7 cells and FoxA1 for MDA-MB-231 cells (**green lines**) and MCF7 and MDA-MB-231 Non targeting mRNA (Dox+), non-targeting mRNA sequence expressing tumors (**black lines**). Each data point represents the mean tumor volume +/- SEM (n=3-8) and T-test was calculated in each point using sh FoxA (Dox-) as controls in both cell types.

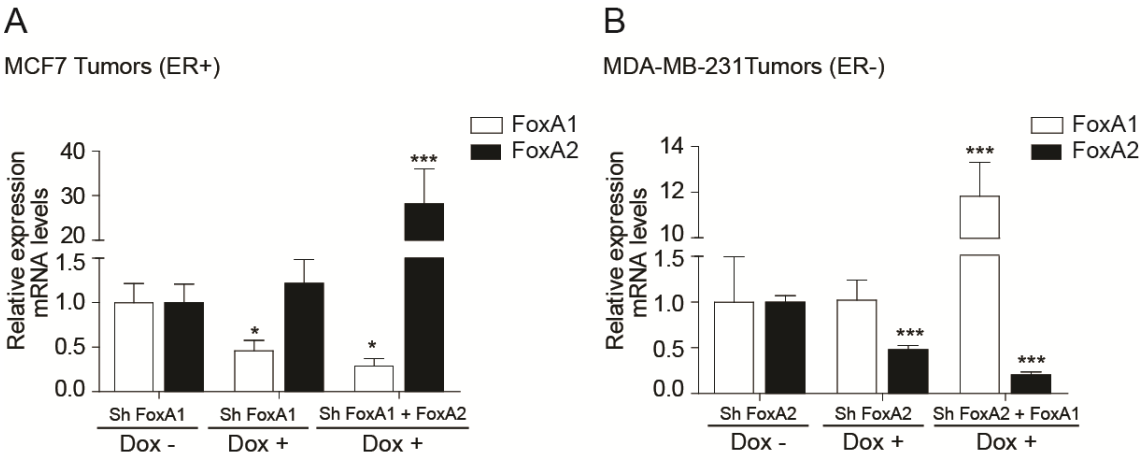

Figure 22.- ***Ex vivo*** **analysis of tumor at 39 days of growth.** Total RNA of MCF7 or MDA-MB-231 tumors at day 39 were probed with FoxA1 or FoxA2 TaqMan probes and normalized to 18S expression levels. **A)** MCF7 Sh FoxA1 (Dox-), control tumors; MCF7 Sh FoxA1 (Dox+), FoxA1 short hairpin expressing tumors; MCF7 Sh FoxA1+FoxA2 (Dox+), FoxA1 short hairpin expressing tumors with overexpression of FoxA2. Data is normalized to tumors MCF7 Sh FoxA1 (Dox-), data are mean +/- SD (n=3-5). T-test was calculated for each group using MCF7 Sh FoxA1 (Dox-) as control group. **B)** MDA-MB-213 Sh FoxA2 (Dox-), control tumors; MDA-MB-231 Sh FoxA2 (Dox+), FoxA2 short hairpin expressing tumors; MDA-MB-231 Sh FoxA2+FoxA1 (Dox+), FoxA2 short hairpin expressing tumors with overexpression of FoxA1. Data is normalized to tumors MDA-MB-231 Sh FoxA2 (Dox-), data are mean +/- SD (n=3-8). T-test was calculated for each group using MDA-MB-231 Sh FoxA2 (Dox-) as control group.

2. Endothelial Lipase, a novel regulator of breast tumor growth

2.1 Gene expression analysis of isolated tumor cells highlight Endothelial Lipase (LIPG) as a FoxA regulated target for tumor growth

To study FoxA1 and FoxA2 regulated genes involved in tumor growth, we isolated cells derived from MCF7 Sh FoxA1 (Dox-) and MDA-MB-231 Sh FoxA2 (Dox-) tumors (**control group**), MCF7 Sh FoxA1 (Dox+) and MDA-MB-231 Sh FoxA2 (Dox+) tumors (**FoxA depleted group**), and MCF7 Sh FoxA1+FoxA2 and MDA-MB-231 Sh FoxA2 + FoxA1 tumors (**rescued group**). Using GFP (all cancer cells) and tRFP expression (sh FoxA1 and sh FoxA2 expressing cells), we isolated pure human cancer cells while excluding mouse stroma cells. We selected cells with the highest short hairpin expression levels by sorting cells with the strongest tRFP signal, and then analyzed their gene expression profiles (**Figure 23A and B).**

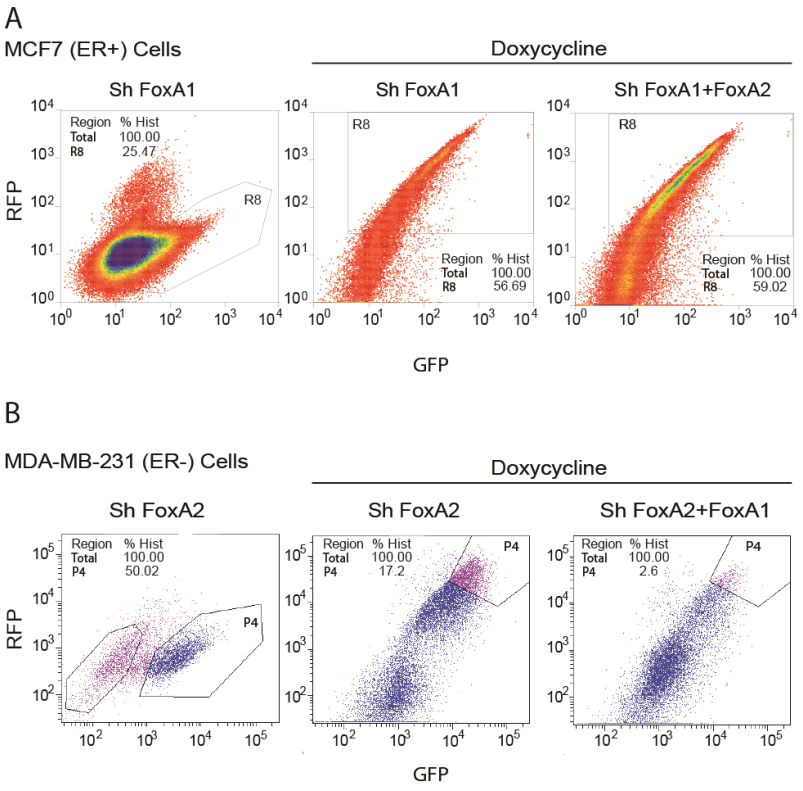

Figure 23.- Isolation of MDA-MB-231 and MCF7 cells expanded as subcutaneous xenografts. FACS profiling of **A**) MCF7 and **B**) MDA-MB-231 cells derived from MCF7 Sh FoxA1 and MDA231 Sh FoxA2 (Dox-), control tumors; MCF7 Sh FoxA1 and MDA-MB-231 Sh FoxA2 (Dox+), knockdown tumors and MCF7 ShFoxA1+FoxA2 and MDA-MB-231

ShFoxA2+FoxA1 (Dox+), rescues tumors, isolated by the expression of GFP (control groups) or GFP and RFP (Knockdown and Rescue groups).

We determined the differences in global gene expression between the different stable lines generated. PCA analysis highlighted differences between populations, showed that they could be classified on the PC coordinates depending on their molecular backgrounds (**Figure 24**). This suggests that the modulation of FoxA factors in breast cancer cells affects gene expression patterns.

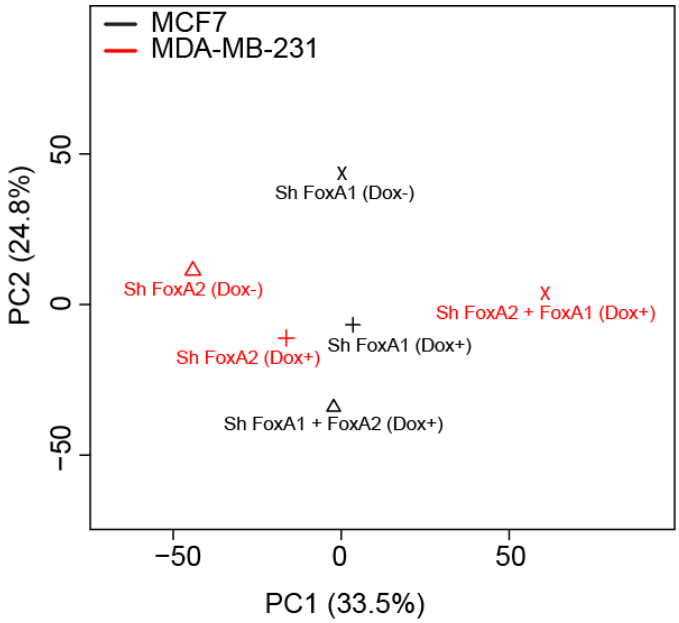

Figure 24.- Analysis of MCF7 and MDA-MB-231 gene expression patterns. PCA plot from MCF7 Sh FoxA1 (Dox-), Sh FoxA1 (Dox+), Sh FoxA1+FoxA2 (Dox+), (**black**); MDA-MB-231 Sh FoxA2 (Dox-), Sh FoxA2 (Dox+), Sh FoxA2+FoxA1 (Dox+), (**red**). Samples were positioned along the first (PC1) or the second (PC2) principal component according to their gene expression similarity.

After the initial sample analysis we sought to classify genes as **positively** and **negatively** regulated by FoxA1 and FoxA2 factors, in both cells lines. In order to classify as a FoxA **positively** regulated transcript, a gene probe must show a fold change of ± 2 and a Bayesian false discovery rate below 5%, and meet the following criteria: (1) decrease in MCF7 and MDA-MB-231 **FoxA-depleted** cells versus MCF7 and MDA-MB-231 **control** cells; (2) increase in MCF7 and MDA-MB-231 **FoxA-rescued cells** versus MCF7 and MDA-MB-231 **FoxA-depleted** cells. On the other hand, to classify as a FoxA **negatively** regulated transcript, a gene probe must show a fold change of ± 2 and a Bayesian false discovery rate below 5%, and meet the following criteria: (1) increased in MCF7 and MDA-MB-231 **FoxA-depleted** cells versus MCF7 and MDA-MB-231 **control** cells; (2) decreased in MCF7 and MDA-MB-231 **FoxA-rescued** cells versus MCF7 and MDA-MB-231 **FoxA-depleted** cells. We represented positive and negative

FoxA-regulated genes Venn diagram (**Figure 25 A and B**). Strikingly, out of 1520 differentially expressed genes in MCF7 cells and 1466 in MDA-MB-231 cells only 3 met our criteria.

The positively regulated genes found in our selection process were endothelial lipase (LIPG) and B-cell lymphoma 2 (Bcl2). On the contrary, we only found one negatively regulated gene Cadherin 11 OB (Cdh 11 OB) (**Supplementary Table V**). Bcl2 is implicated in cancer survival by exerting anti-apoptotic functions (Kelly and Strasser, 2011), whereas Cdh11 OB is known to induce apoptosis (Li et al., 2012). Contrary to Bcl2 and Cdh 11 OB, there are no known tumor growth functions for LIPG.

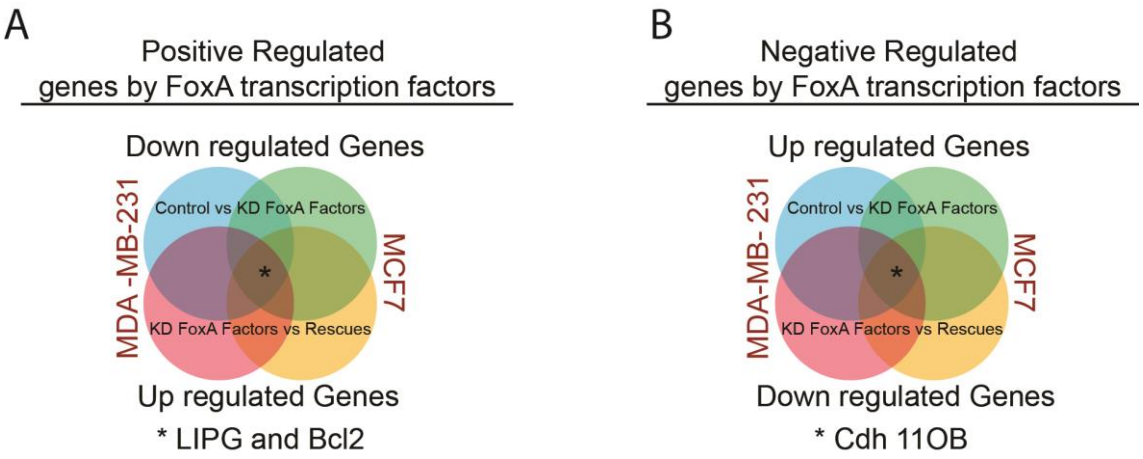

Figure 25.- A Genomic approach to identify FoxA1-FoxA2 regulated transcripts in MCF7 and MDA-MB-231 cells . Venn diagrams of data obtained from the gene expression analysis of sorted tumor cells from controls, knockdowns and rescues tumors groups. **A)** Positively regulated genes and **B**) negatively regulated genes. FoxA1-FoxA2 regulated transcripts were classified as those that met all four requirements with a statistical cut of FDR below 5% and a Fold Change ± 2.

We corroborated the results from the Affymetrix analysis by testing LIPG, Bcl2 and Chd11 OB transcript levels in tumor samples. The only gene that recapitulated the classification criteria was LIPG, its transcript levels were reduced in MCF7 and MDA-MB-231 cells when FoxA1 or FoxA2 were depleted, respectively. Moreover, LIPG transcript levels were reestablished to basal levels upon exogenous FoxA1 or FoxA2 expression in FoxA depleted tumors (rescued group). In contrast, Bcl2 and Cdh 11 OB did not follow the classification criteria (**Figure 26 A and B**).

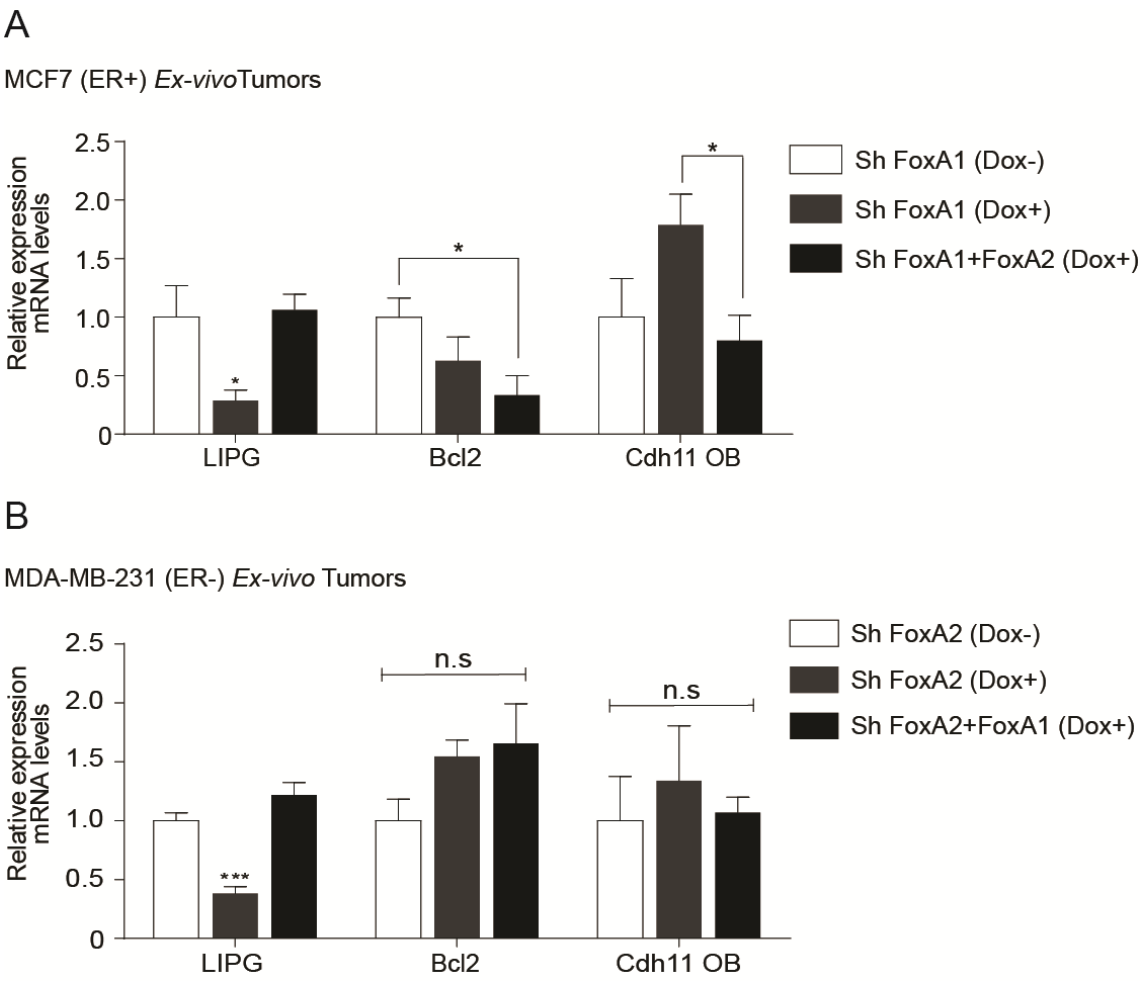

Figure 26.- Real time analysis of LIPG, Bcl2 and Cdh11OB mRNA levels in tumors. Total RNA of MCF7 and MDA-MB-231 tumors at day 39 were probed with corresponding TaqMan probes and normalized to 18S expression levels. **A)** MCF7 Sh FoxA1 (Dox-), control tumors; MCF7 Sh FoxA1 (Dox+), FoxA1 short hairpin expressing tumors; MCF7 Sh FoxA1+FoxA2 (Dox+), FoxA1 short hairpin expressing tumors with overexpression of FoxA2. Data is normalized to tumors MCF7 Sh FoxA1 (Dox-), data are mean +/- SD (n=3-5). T-test was calculated for each group using MCF7 Sh FoxA1 (Dox-) as the control group. **B)** MDA-MB-213 Sh FoxA2 (Dox-), control tumors; MDA-MB-231 ShFoxA2 (Dox+), FoxA2 short hairpin expressing tumors; MDA-MB-231 Sh FoxA2+FoxA1 (Dox+), FoxA2 short hairpin expressing tumors with overexpression of FoxA1. Data is normalized to tumors MDA-MB-231 Sh FoxA2 (Dox-), data are mean +/- SD (n=3-8). T-test was calculated for each group using MDA-MB-231 Sh FoxA2 (Dox-) as the control group.

2.2 LIPG expression in breast cancer

After finding that LIPG mRNA expression was regulated by FoxA1 and FoxA2, we wanted to assess the implication of LIPG in breast cancer pathogenesis. We first analyzed LIPG expression in the MSKCC/EMC cohort (**Figure 27**), which LIPG showed expression in all breast cancer types subtypes, suggesting that LIPG action could be necessary across breast cancers.

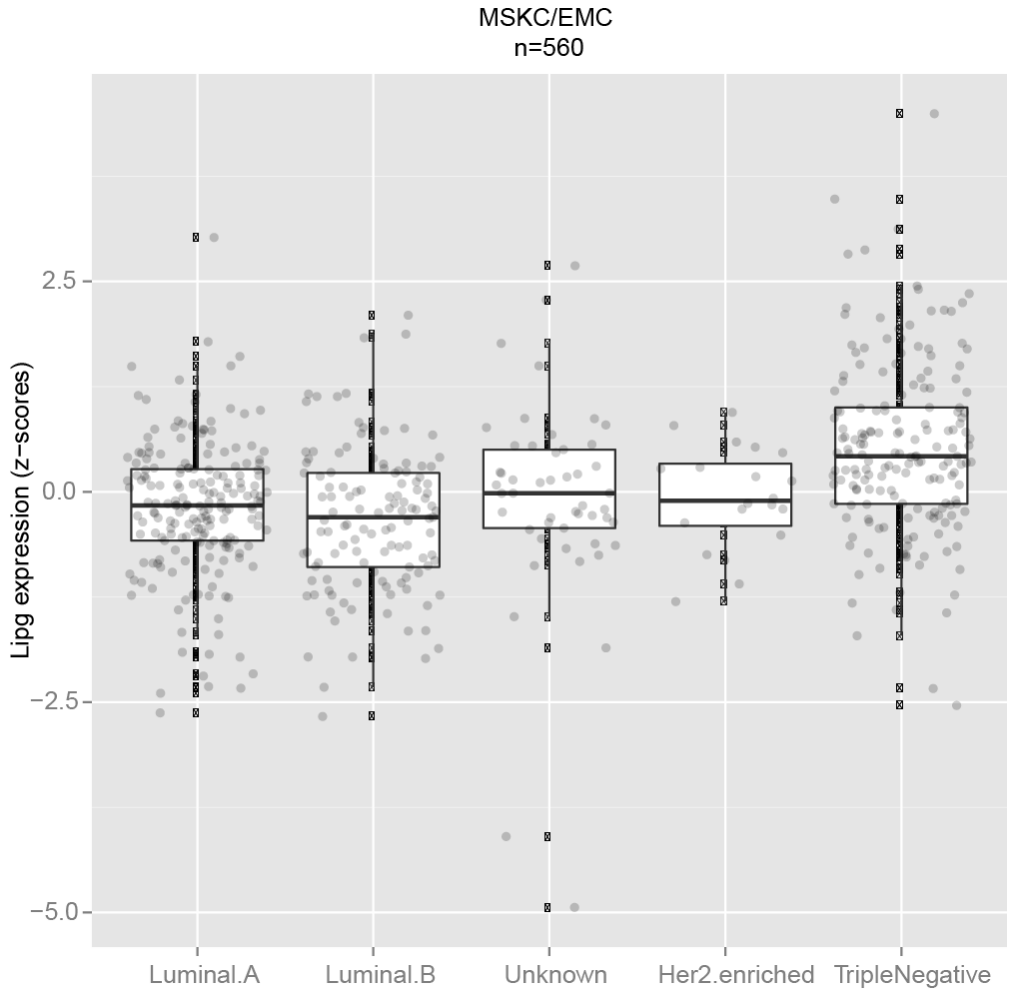

Figure 27.- LIPG expression in different breast cancer subtypes. Patient samples were divided into different breast cancer subtypes based on their gene expression signatures, and LIPG expression level was then assessed.

Once we observed that LIPG was expressed in clinical samples, we evaluated LIPG protein expression using MCF7 and MDA-MB-231 cells with LIPG gain or loss of function. We used sh control expressing cells to evaluate endogenous LIPG levels. LIPG is expressed in endothelial cells, as well as in other cell types, with a molecular weight of 55 kDa. The protein has two post-translational modifications: first it is glycosylated, generating a 68 kDa isoform and secondly, LIPG is proteolyzed to generate a 40 kDa isoform. Exogenous 55 kDa expressed LIPG is glycosylated by tumor cells and then is proteolyzed, generating the 40 kDa form (**Figure 28A**). We only detected a 40 kDa band in sh control cells, suggesting that this isoform is predominant in cell homogenates. The same band decreased in LIPG-depleted cells confirming antibody specificity (**Figure 28A**). Next, we analyzed a set of breast cancer cells

(used in section 1.2) to detect LIPG expression. Out of 8 breast cancer lines, 7 lines had high levels of the 40 kDa LIPG isoform compared with non-tumor cells (HMEC). The only breast cancer line that had reduced, but detectable, levels of 40 kDa isoform was MDA-MB-435 (**Figure 28B**). The aforementioned results suggest that LIPG is expressed across different breast cancer subtypes, represented among patient samples and established human cell lines.

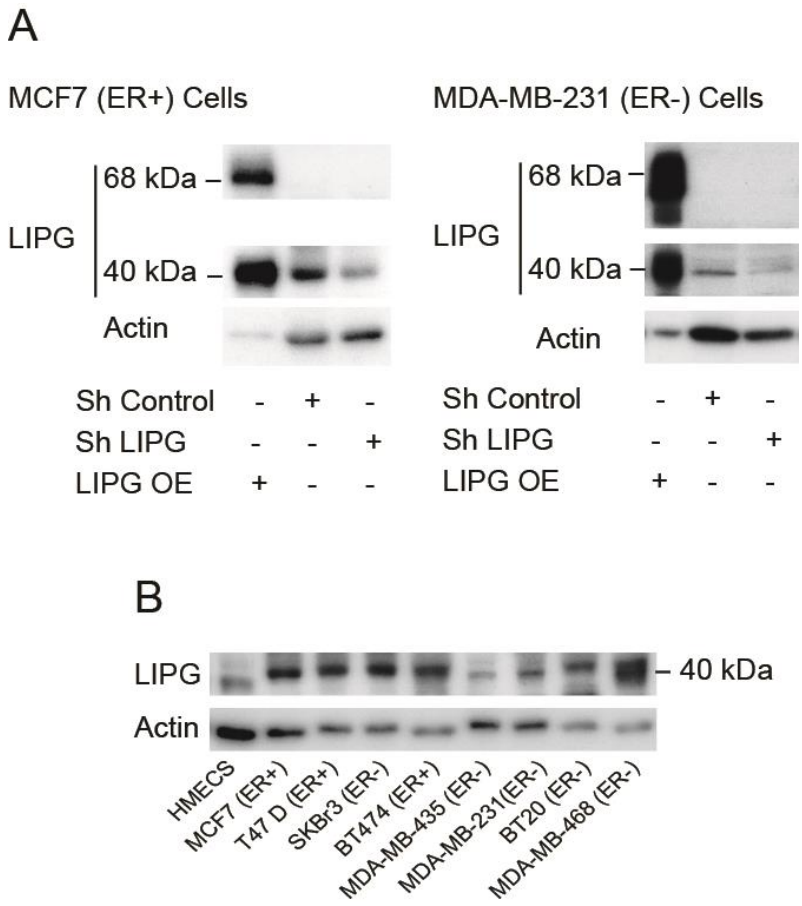

Figure 28.- 40 KDa LIPG isoform is expressed in breast cancer cell lines. A) Cell extracts from MDA-MB-231 and MCF7 cells transduced with sh control sequence, a LIPG short hairpin sequence and LIPG cDNA were inmunobloted with an antibody against LIPG. **B)** Extract of 8 breast cancer cell lines and Human Mammary Epithelial cells were immunobloted using a LIPG antibody.

2.3 LIPG is necessary for breast cancer growth *in vitro*

Next, we studied whether LIPG was involved in tumor growth regulation. To this end, we used LIPG-depleted MCF7 and MDA-MD-231 cells. First, we confirmed that LIPG mRNA and protein expression was reduced in MCF7 and MDA-MB-231 knock-down cells compared with sh controls **(Figure 29 A and B)**.

Interestingly, LIPG depleted cells displayed growth arrest *in vitro*, as previously shown by FoxA1 and FoxA2 depletion (**Figure 29 C**).

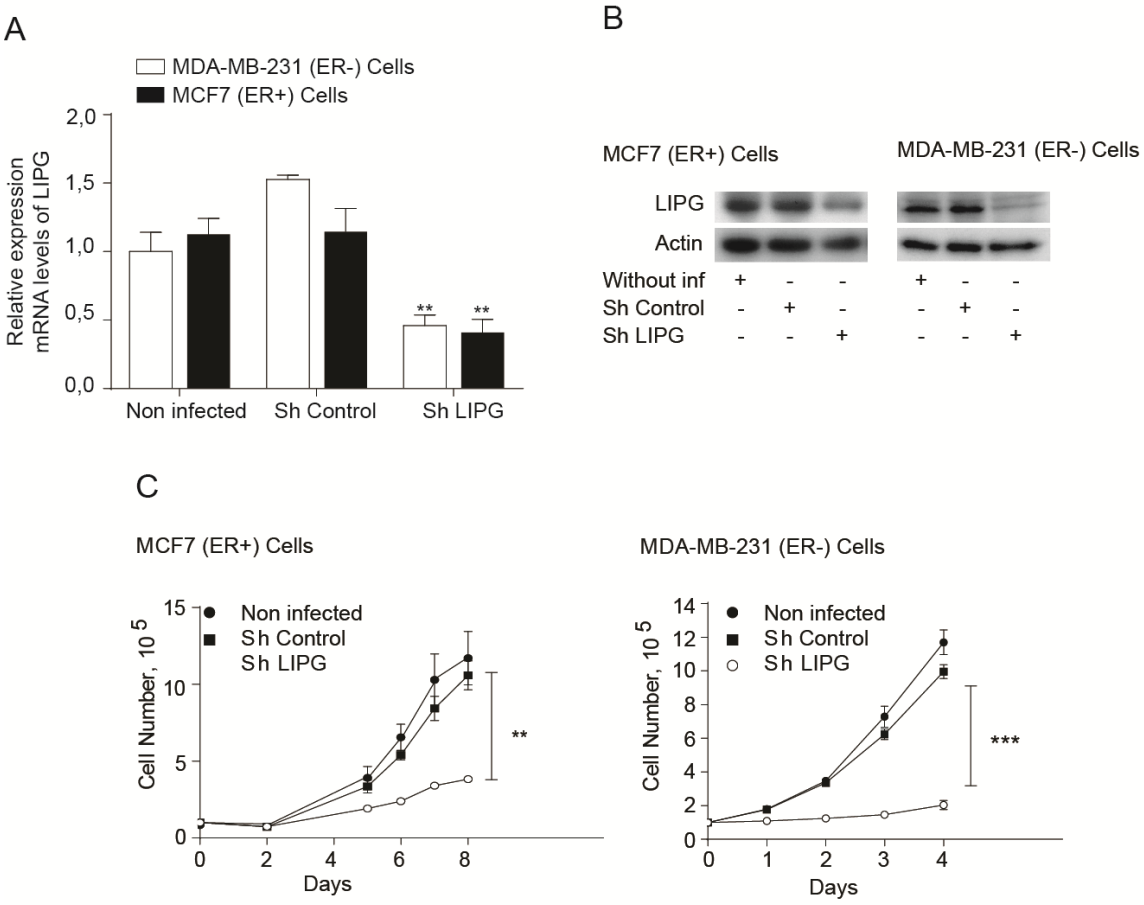

Figure 29.- LIPG reduction reduces MCF7 and MDA-MB-231 cell growth *in vitro*. MCF7 and MDA-MB-231 cells without infection, infected with a sh control sequence and a LIPG sh sequence were grown in complete growth medium. **A)** Total RNA of cells were probed by qRT-PCR with LIPG TaqMan probe and normalized to 18S expression levels, data is normalized to non-infected cells, data are mean +/- SD (n=3) and T-test was calculated using mRNA from cells carrying the sh control sequence as control. **B)** Western blot analysis from cell lysates inmunobloted with LIPG antibody and actin. **C)** Cells were infected, selected with puromycin and plated $1X10^5$ cells for *in vitro* growth for 8 (MCF7 cells) and 4 days (MDA-MB-231 cells) without antibiotic, data are mean +/- SD (n=3) and T-test was calculated for the last point of the curve using cells carrying the scr sequence as control.

2.4 LIPG FoxA depleted growth rescue is dependent on lipase activity

LIPG depleted cells showed cell growth arrest *in vitro*, next we assessed the capacity of LIPG to rescue the tumor growth reduction of FoxA1 or FoxA2 depleted cells. For this reasons, we transduced MCF7 and MDA-MB-231 cells that have the doxycycline–driven FoxA1 or FoxA2 shRNA expression system,

with either a WT LIPG construct or a catalytically inactive LIPG construct (**Table VI and VII**). The substitution of a glutamine by an asparagine drives the expression of a catalytically inactive LIPG isoform, as previously shown (Strauss et al., 2002).

Table VI and VII.- FoxA1, FoxA2 and LIPG expression in MCF7 and MDA-MB-231 engineered cells

Table VI

MCF7 cells (ER+)	**FoxA1 expression**	**FoxA2 expression**	**LIPG overexpression**
Sh control (Dox-/+)	**yes**	**no**	**no**
Sh FoxA1 (Dox-)	**yes**	**no**	**no**
Sh FoxA1 (Dox+)	**no**	**no**	**no**
Sh FoxA1+LIPG (Dox-)	**yes**	**no**	**yes**
Sh FoxA1+LIPG (Dox+)	**no**	**no**	**yes**
Sh FoxA1+LIPG Inactive (Dox-)	**down**	**no**	**yes**
Sh FoxA1+LIPG Inactive (Dox+)	**no**	**no**	**yes**

Table VII

MDA-MB-231 cells (ER+)	**FoxA1 expression**	**FoxA2 expression**	**LIPG overexpression**
Sh Control (Dox-/+)	**no**	**yes**	**no**
Sh FoxA2 (Dox-)	**no**	**yes**	**no**
Sh FoxA2 (Dox+)	**no**	**no**	**no**
Sh FoxA2+LIPG (Dox-)	**no**	**yes**	**yes**
Sh FoxA2+LIPG (Dox+)	**no**	**no**	**yes**
Sh FoxA2+LIPG Inactive (Dox-)	**no**	**down**	**yes**
Sh FoxA2+LIPG Inactive (Dox+)	**no**	**no**	**yes**

After establishing our cell line systems, we induced the expression of the short hairpins on incubating cells for 144 hrs with doxycycline. As controls, we used a doxycycline–driven shRNA sequence that does not target any specific mRNA (sh control). Doxycycline administration to cells expressing the exogenous WT

LIPG or catalytically inactive LIPG, depleted the expression of FoxA1 in MCF7 cells and FoxA2 in MDA-MB-231 cells but not in sh control cells (**Figure 30 A and B**). Interestingly, exogenous inactive LIPG expression in MCF7 and MDA-MB-231 cells reduced FoxA1 and FoxA2 levels, respectively. This reduction was observed without doxycycline treatment. The above observation did not occur in exogenous WT LIPG expressing cells (**Figure 30 A, B, C and D**).

To analyze tumor growth *in vivo*, $1X10^6$ cells cultured without doxycycline were injected subcutaneously in mice pretreated with or without doxycycline for 2 weeks prior injection and maintained during the experiment. We used doxycycline–driven sh FoxA MCF7 and MDA-MB-231 cells injected in animals without doxycycline treatment as controls. Remarkably, FoxA depleted tumors that expressed exogenous WT LIPG grew like the control counterparts. On the contrary, cells that expressed exogenous inactive LIPG did not rescue the growth phenotype, suggesting that LIPG activity is essential to rescue FoxA depletion (**Figure 31A**). Of note, MDA-MB-231 tumors with FoxA2 expression and exogenous WT LIPG expression had an increased growth rate when compared to controls, which was significant at 28 days post-inoculation (**Figure 31B**).

To confirm these results, we evaluated FoxA1, FoxA2 and LIPG mRNA content in 35 days post-inoculation tumors. As expected, doxycycline treated tumors reduced FoxA1 and FoxA2 levels. Similarly, LIPG mRNA levels were reduced in cells that did not have exogenous LIPG (**Figure 32 A and B**).

In summary, these results demonstrate that LIPG is essential in order to rescue FoxA depletion, and its effect is mediated by its enzymatic activity.

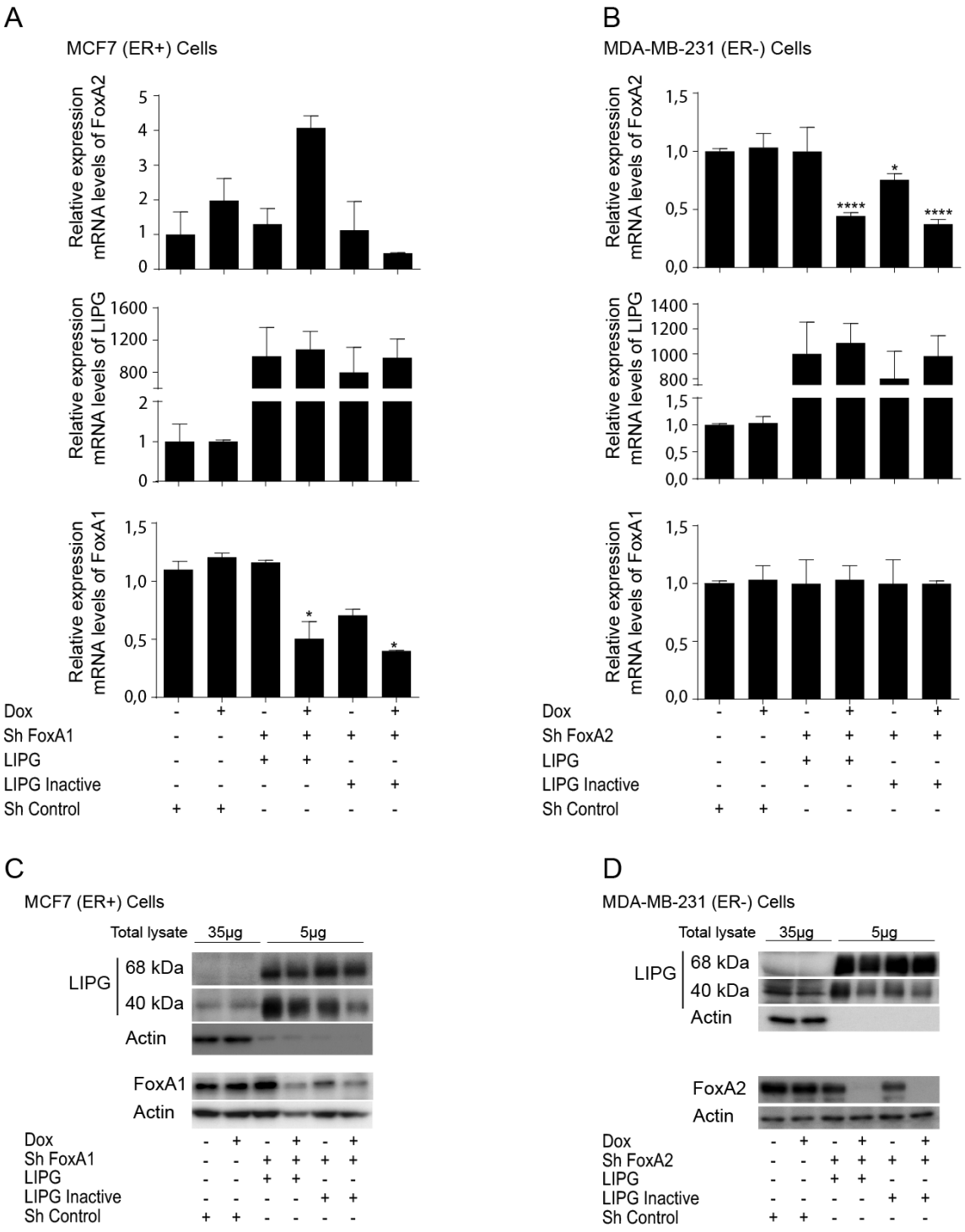

Figure 30.- 144 hrs of doxycycline treatment induces the down-regulation of FoxA1 and FoxA2 in non- and overexpressing LIPG cells. MCF7 and MDA-MB-231 cells containing a non-targeting mRNA sequence or an inducible FoxA1 or FoxA2 short hairpin sequence with WT LIPG or LIPG inactive overexpression incubated for 144 hrs with 2µg of doxycycline or without doxycycline. **A)** Total MCF7 RNA was extracted and qRT-PCR analysis was performed with the corresponding TaqMan probes and normalized to 18S expression levels, data is normalized to cells containing the non-targeting sequence without doxycycline, data are mean +/- SD (n=3). **B)** Total MDA-MB-231 RNA was probed by qRT-PCR with the corresponding TaqMan probes and normalized to 18S expression levels, data is normalized to cells containing the non-

targeting sequence incubated without doxycycline, data are mean +/- SD (n=3). **B** and **C)** P-value were calculated using T-test, comparing each group with MDA-MB-231 Sh FoxA2 (Dox-). **C)** and **D)** MCF7 and MDA-MB-231 lysates were subjected to immunoblotting with the corresponding antibodies. For LIPG immune detection, 35 µg of total protein of cells without WT or inactive LIPG overexpression was used. For cell overexpressing the WT or inactive LIPG, 5 ug of lysates was used.

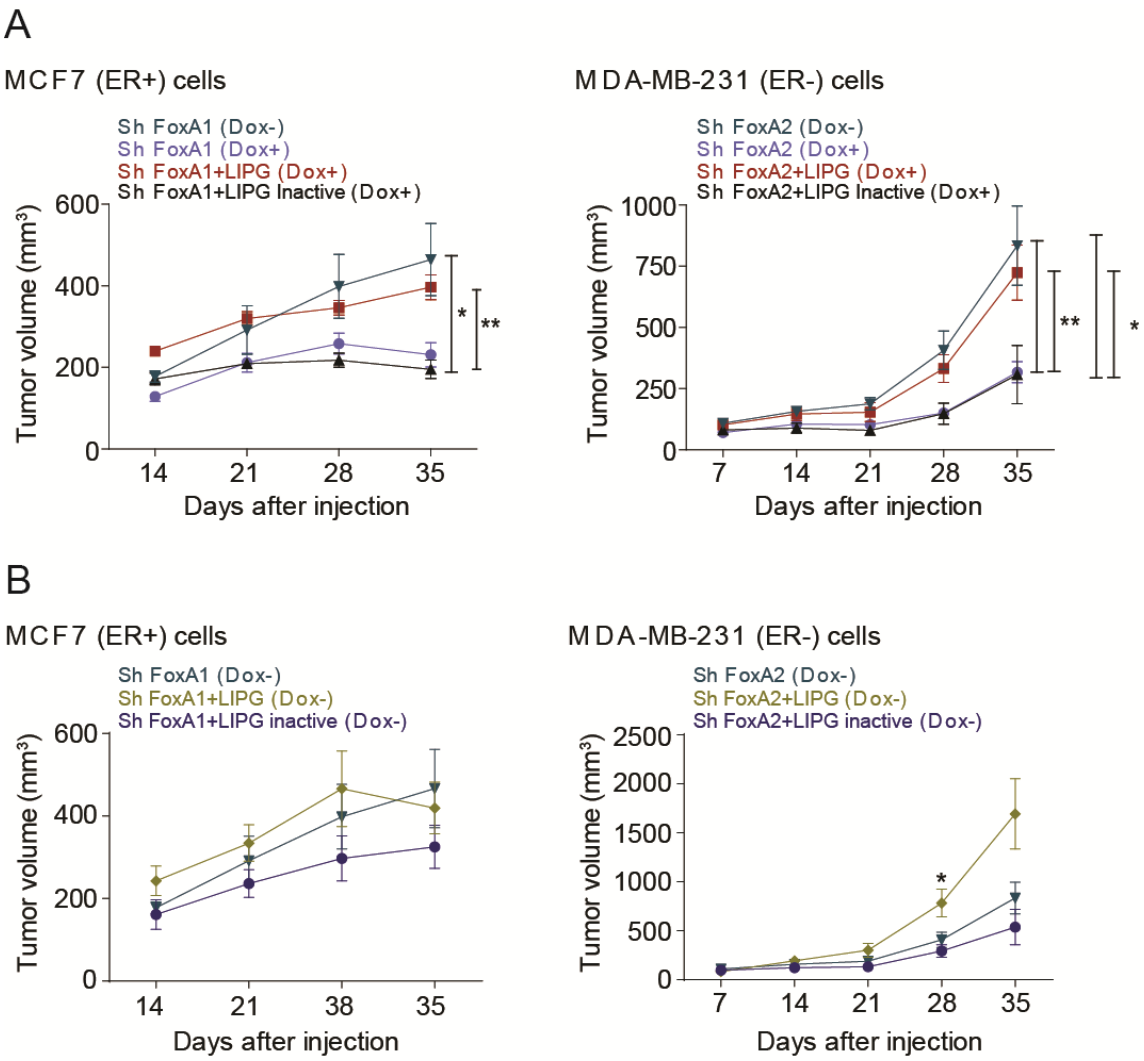

Figure 31.- WT LIPG overexpression, and not the inactive isoform, is able to rescue MDA-MB-231 and MCF7 growth reduction *in vivo*. Tumor growth curves of cells injected subcutaneously in NUD mice with or without doxycycline administration. **A)** MCF7 Sh FoxA1 and MDA231 Sh FoxA2 (Dox-) control tumors (**green lines**); MCF7 Sh FoxA1 and MDA-MB-231 Sh FoxA2 (Dox+), FoxA transcription factors short hairpins expressing tumors (**blue lines**); MCF7 ShFoxA1+LIPG and MDA-MB-231 ShFoxA2+LIPG (Dox+), FoxA transcription factors short hairpins expressing tumors with overexpression of WT LIPG (**red lines**) and MCF7 Sh FoxA1+LIPG Inactive and MDA-MB-231 Sh FoxA2+LIPG inactive (Dox+), FoxA transcription factors short hairpins expressing tumors with overexpression of inactive LIPG (**Black lines**). **B)** Growth of tumors without doxycycline treatment as controls; MCF7 Sh FoxA1 and MDA-MB-231 Sh FoxA2 (Dox-) control tumors (**green lines**); MCF7 Sh FoxA1+LIPG and MDA-MB-231 Sh FoxA2+LIPG (Dox-), cells overexpressing WT LIPG (**green pale lines**) and MCF7 Sh FoxA1+LIPG inactive and MDA-MB-231 Sh FoxA2+LIPG inactive (Dox-), cells overexpressing inactive LIPG (**blue lines**). Each data point represents the mean tumor volume +/- SEM (n=3-8) and T-test was calculated for each point using MCF7 Sh Foxa1 or MDA-MB-231 Sh FoxA2 (Dox-) as controls.

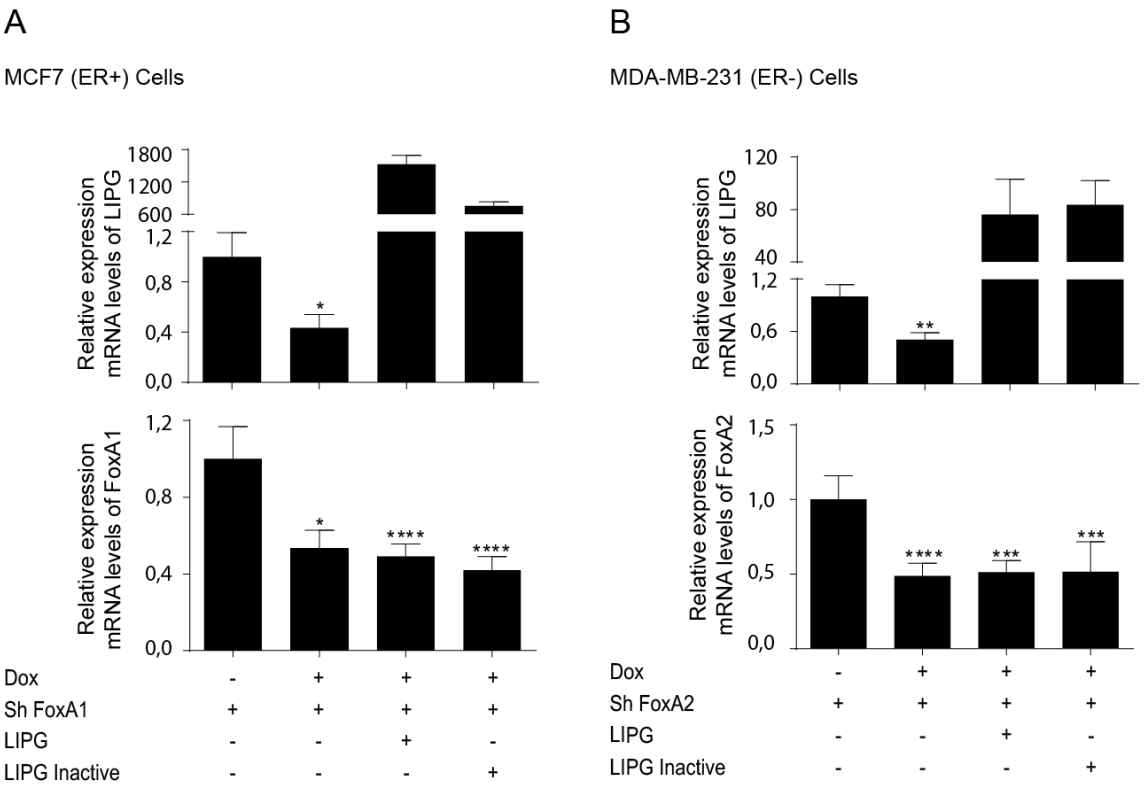

Figure 32.- ***Ex-vivo*** **analysis of tumor at 35 days of growth.** Total RNA of MCF7 or MDA-MB-231 tumors at day 35 were probed with FoxA1, FoxA2 or LIPG TaqMan probes and normalized to 18S expression levels. **A)** MCF7 Sh FoxA1 (Dox-), control tumors; MCF7 Sh FoxA1 (Dox+), FoxA1 short hairpin expressing tumors; MCF7 Sh FoxA1+LIPG (Dox+), FoxA1 short hairpin expressing tumors with overexpression of WT LIPG and MCF7 Sh FoxA1+ LIPG inactive, FoxA1 short hairpin expressing tumors with overexpression of LIPG Inactive. Data is normalized to MCF7 Sh FoxA1 (Dox-) tumors, data are mean +/- SD (n=3-5). P-value was calculated using T-test, comparing each group with MDA-MB-231 Sh FoxA2 (Dox-). **B)** MDA-MB-213 Sh FoxA2 (Dox-), control tumors; MDA-MB-231 ShFoxA2 (Dox+), FoxA2 short hairpin expressing tumors; MDA-MB-231 ShFoxA2+LIPG (Dox+), FoxA2 short hairpin expressing tumors with overexpression of WT LIPG and MDA-MB-231 Sh FoxA2+ LIPG inactive, FoxA2 short hairpin expressing tumors with overexpression of LIPG Inactive . Data is normalized to tumors MDA-MB-231 Sh FoxA2 (Dox-), data are mean +/- SD (n=3-8). P-value was calculated using T-test, comparing each group with MDA-MB-231 Sh FoxA2 (Dox-).

3. LIPG regulates a lipid network enriched in MCF7 and MDA-MB-231 cells

3.1 Untargeted metabolomics reveal differentially lipid levels in LIPG-depleted breast cancer cells

We sought to find metabolites regulated by LIPG in MCF7 and MDA-MB-231 cells. For this reason we used an untargeted lipidomic analysis to reveal deregulated metabolites in LIPG-depleted cells compared with sh control cells. We analyzed organic extracts using untargeted liquid chromatography mass spectrometry (LC-MS) to profile lipids. LIPG cell depletion induced a general reduction of lipids species in both MCF7 and MDA-MB-231 cells. This depletion is represented by the total number of detected metabolic features that were significantly altered (**Figure 33 A**). Lipids reduction is higher in MDA-MB-231 cells (15% of total lipids) than MCF7 cells (1% of total lipids) (**Figure 33 B**). This suggests that LIPG may regulate different types and/or quantities of lipids between different breast cancer cell lines.

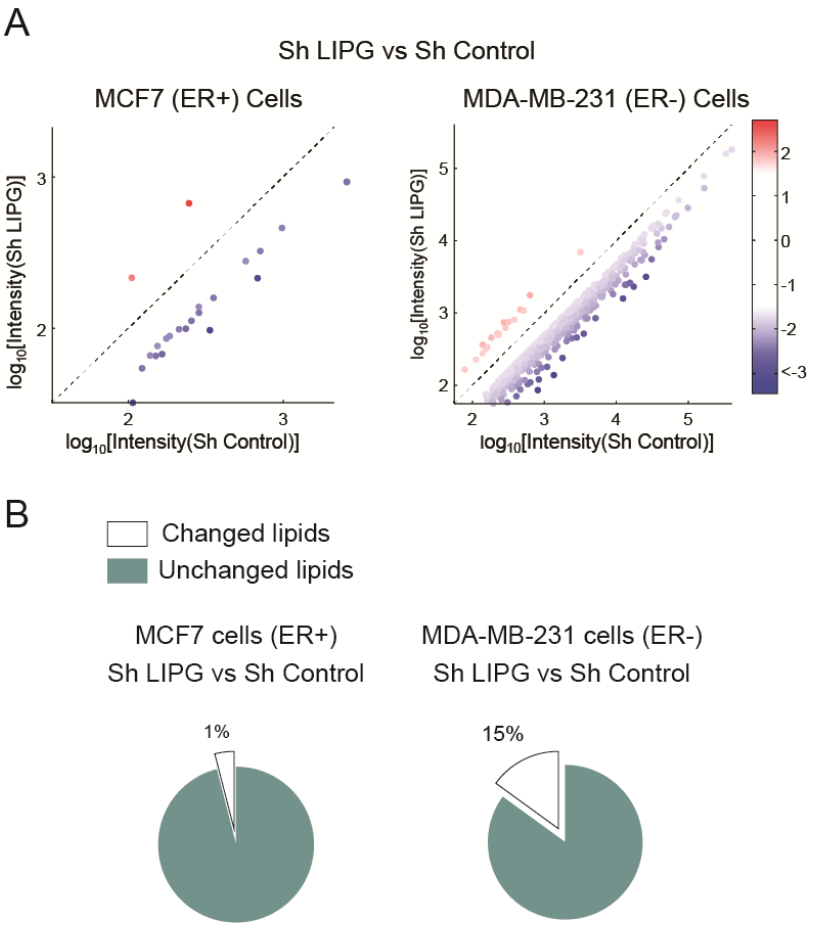

Figure 33.- Reduction of lipids species in both MCF7 and MDA-MB-231 LIPG-depleted cells. MCF7 and MDA-MB-231 cells infected with sh control and sh LIPG were grown in complete growth medium during 4 (MCF7) and 2 (MDA-MB-231) days and extracts were analyzed by LC-MS. **A)** Down-regulated (blue dots) and up-regulated (red dots) metabolic features. **B)** Percentages of altered lipids in MCF7 and MDA-MB-231 by LIPG depletion that were identified in the analysis. **A)** and **B)** n=5.

As previously mentioned, we determined lower number of down-regulated lipids in LIPG-depleted MCF7 cells. Specific lipids families from DG (p value < 0,01) and MG, PE and LPC (p value < 0,05) were statistically reduced (**Figure 34A**). Phosphatyl ethanolamines (PE), phosphatyl cholines (PC), phosphatyl glycerols (PG), lysophosphatidyl cholines (LPC), diacylglycerols (DG) and ether lipids showed reduced levels in MDA-MB-231 LIPG-depleted cells. Moreover, the family of ether lipids was also reduced (**Figure 34 B**). It is interesting to note that decreased lipid families in both cell types were shown to be indispensable in cancer malignancy as they contribute to membrane synthesis (PE, PC and PG) or activating signaling cascades (DG) (Mulvihill and Nomura, 2013; Nomura et al., 2010).

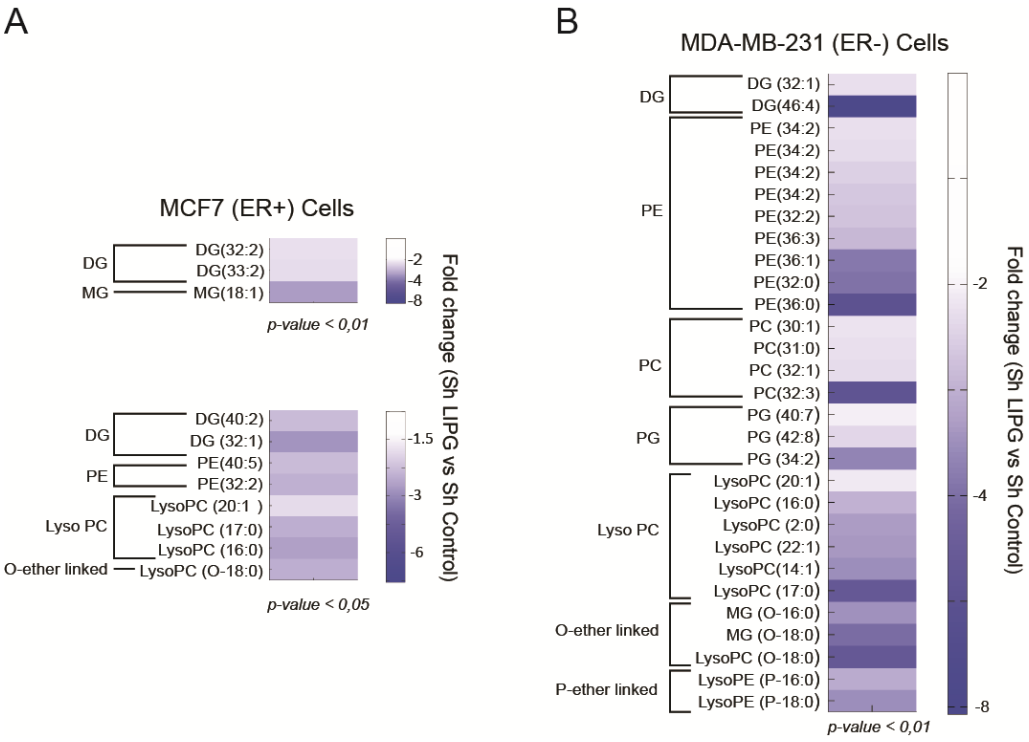

Figure 34.- LIPG lipid signature in breast cancer cells. Down-regulated lipids are represented as the fold change when sh LIPG cells were compared with sh control cells. P-values are represented in the figure and calculated by T-test, n=5.

The common LIPG lipid signature in MCF7 and MDA-MB-231 cells was composed of lysophosphatidyl cholines (LPC), phosphatyl ethanolamines (PE) and diacylglycerols (DG) families (**Figure 34 A and B**). Furthermore, specific lipids had reduced levels in both cell types. These include, DG (32:1), PE (32:2), LPC (O-18:0), LPC (17:0), LPC (20:1) and LPC (20:1) (**Figure 35**).

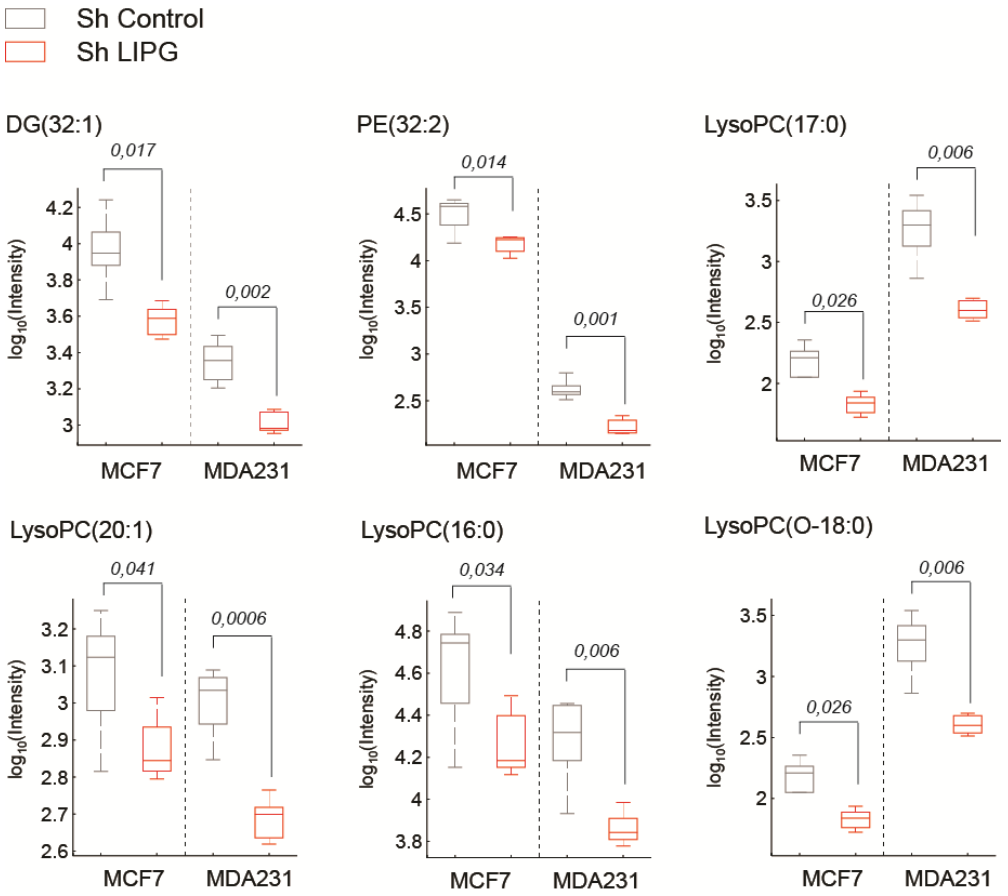

Figure 35.- Specific down-regulated lipids in LIPG silenced cells. Down-regulated lipids are represented in box plots as the log_{10} intensity in sh control and sh LIPG cells. P-values are represented in the figure and calculated by T-test, n=5.

4. Regulation of luminal and basal genes by FoxA1 and FoxA2

4.1. Gene expression analysis highlight a malignant gene regulation

We have previously shown that FoxA1 and FoxA2 transcription factors regulate LIPG mRNA expression, and ultimately tumor growth, in MDA-MB-231 and in MCF7 cells. Nevertheless, there are many genes regulated by either FoxA1 in MCF7 cells or FoxA2 in MDA-MB-231 cells (**supplementary Table 1**). It has been shown that MDA-MB-231 cells are a known triple negative breast cancer subtype with a basal phenotype, whereas MCF7 cells are ER+ breast cancer subtype exhibiting a luminal phenotype. Regarding breast cancer pathogenesis, it has been postulated that the induction of an EMT program confers the acquisition of motility, invasiveness and self-renewal traits to normal and immortalized epithelial cells of the mammary gland (Mani et al., 2008). The signals responsible for inducing this EMT/stem cell transition and maintain this phenotype depend the on transforming growth factor beta (TGF-β) and the canonical and non-canonical Wnt signaling pathways (Scheel et al., 2011). In this context, we asked ourselves whether FoxA1 and FoxA2 controlled EMT and stem cell genes in MCF7 and MDA-MB-231 cells, thus reflecting tumor malignancy. Because FoxA depletion in MCF7 and MDA-MB-231 cells drives tumor growth reduction, we were especially interested in the EMT/stem cell gene expression in FoxA1-depleted MCF7 cells with exogenous FoxA2 and in FoxA2-depleted MDA-MB-231 cells with exogenous FoxA1.

The microarray expression analysis of the same samples in section 2.1 revealed that FoxA1-depleted cells had increased transcript levels of EMT/Stem cell genes compared to control cells. FoxA2 overexpression in FoxA1-depleted MCF7 cells present similar EMT/stem expression pattern (**Figure 36A**). On the contrary, FoxA2 depletion as well as FoxA1 expression in FoxA2-depleted MDA-MB-231 cells induced EMT/stem gene signature reduction (**Figure 36B**).

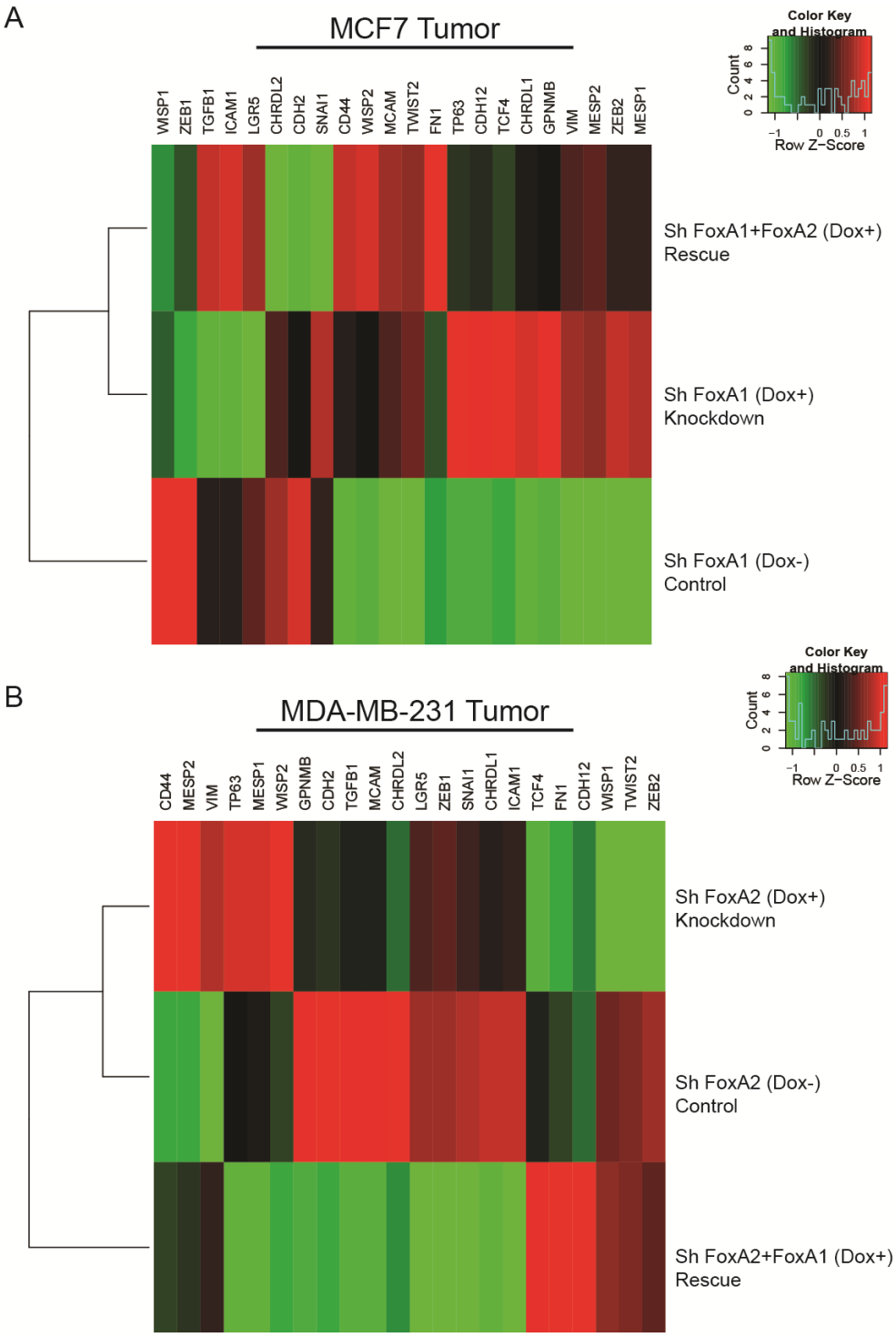

Figure 36: EMT/Stem cell gene expression controlled by FoxA1 or FoxA2. Heatmap shows the differential expression of 22 known EMT/stem cell genes regulated in MCF7 or MDA-MB-231 cells when FoxA transcription factors expression are modified. RNA was obtained from cells isolated from tumors in section 2.1 at 39 days of xenograft growth. Each column represents one gene, and each row one generated cell line. Varying expression levels are represented on a scale from dark green (lowest expression) to dark red (highest expression). **A)** MCF7 cells with the corresponding genotype: Sh FoxA1 (Dox-), control cells; Sh FoxA1 (Dox+), short hairpin

expressing cells and Sh FoxA1+ FoxA2 (Dox+), short hairpin expressing cells in a FoxA2 overexpression background. **B)** MDA-MB-231 cells with the corresponding genotype: Sh FoxA2 (Dox-), control cells; Sh FoxA2 (Dox+), short hairpin expressing cells and Sh FoxA2+ FoxA1 (Dox+), short hairpin expressing cells in a FoxA1 overexpression background.

Next, we investigated β-catenin localization by immunofluorescence in the engineered cell lines upon doxycycline administration. MCF7 control cells (sh FoxA1 (Dox-)) showed a weak β-catenin signal, preferentially located in the cell membrane. The β-catenin signal increased in FoxA1-depleted cells as well as in FoxA1-depleted cells with exogenously FoxA2 expression, whereas Contrary, MDA-MB-231 control cells (sh FoxA2 (Dox-)) expressed β-catenin in the nucleus and cytoplasm. Interestingly, β-catenin mainly localized in the cytoplasm of FoxA2-depleted cells, as did in FoxA2-depleted cells with exogenous FoxA1 (**Figure 37B**). Remarkably, FoxA2-depleted MDA-MB-231 cells with exogenous FoxA1 displayed morphological changes: they were more spindle-like and exhibited less fibroblastic morphology (**Figure 37B**).

4.2 FoxA1 and FoxA2 regulate breast cancer cell migration

Since we saw changes in β-catenin localization and in EMT/stem gene expression in Sh FoxA1+FoxA2 expressing MCF7 cells and in Sh FoxA2+FoxA1 MDA-MB-231 expressing cells, we decided to asses scratch wound-healing assays. This showed that FoxA1-depleted MCF7 cells with exogenous FoxA2 were more proficient in closing an artificial wound than FoxA1-depleted MCF7cells and sh control cells (**Figure 38A**). On the contrary, FoxA2-depleted MDA-MB-231 cells with exogenous FoxA1 and FoxA2-depleted MDA-MB-231 cells were less proficient in closing the wound in a confluent monolayer than sh control cells (**Figure 38B**).

Finally, we explored the possibility that the interchange of FoxA1 and FoxA2 in breast cancer cells could affect their lung seeding ability when inoculated in to the tail vein of immune deficient animals. Cells cultured with doxycycline were inoculated in nude mice treated with doxycycline for 2 weeks, and maintained with this regime for the duration of the experiment (**Figure 39A**). MCF7 cells were not able to colonize the lungs in any genetic background (**data not shown**). Sh control MDA-MB-231 cells and FoxA2-depleted MDA-MB-231 cells

with exogenous FoxA1 grew without significant differences in lungs (**Figure 39B**).

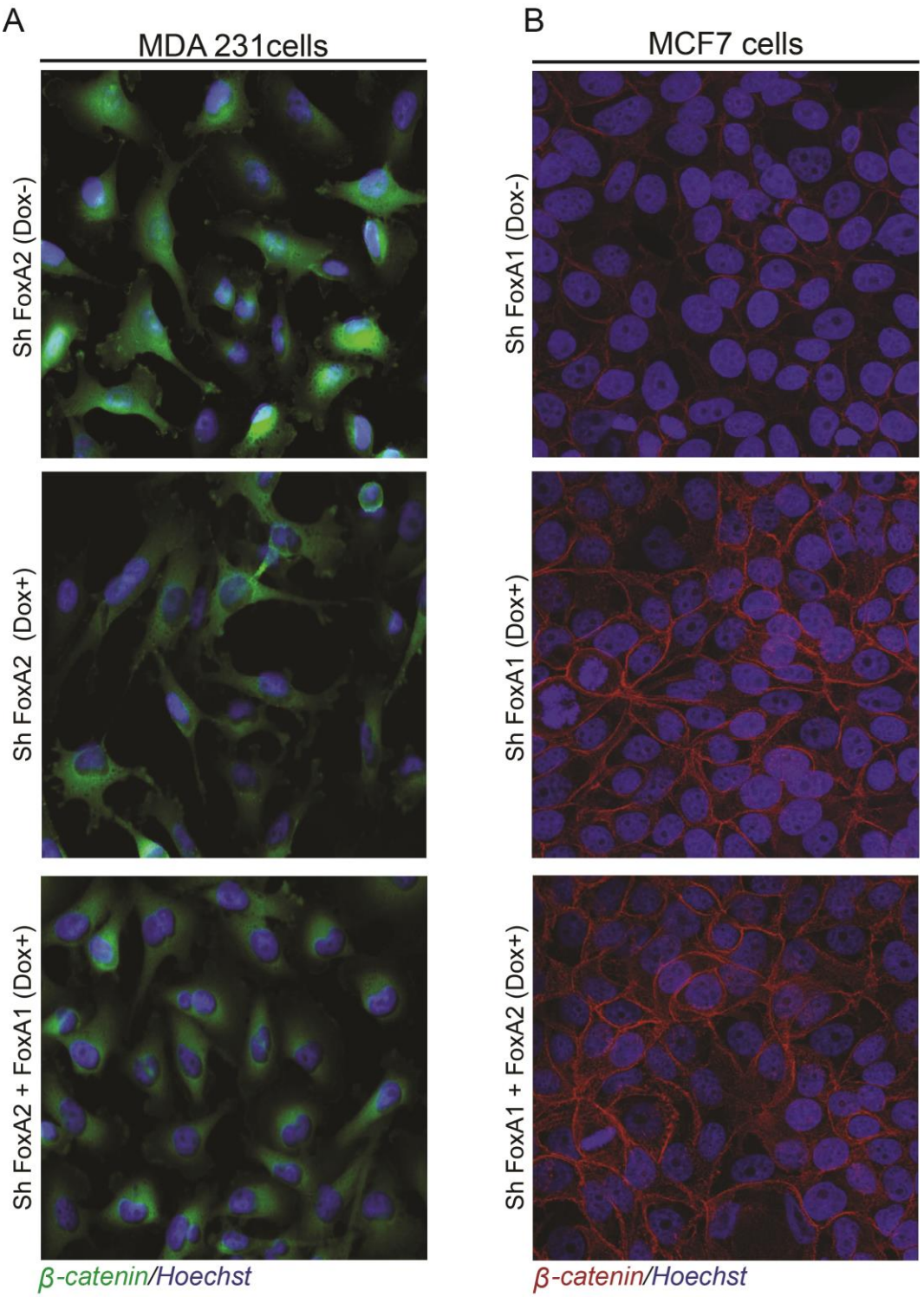

Figure 37: FoxA1 and FoxA2 regulate β-catenin localization. Immunofluorescence of β-catenin in MCF7 and MDA-MB-231 cells with the corresponding genotypes. Hoechst 33342 was utilized to stain nuclei. Cells were incubated with 2μg/mL of doxycycline for 144 hrs. **A)** MCF7 cells with the corresponding genotype: Non-targeting mRNA (Dox+), control cells expressing a

non-targeting sequence; Sh FoxA1 (Dox+), short hairpin expressing cells and Sh FoxA1+ FoxA2 (Dox+), short hairpin expressing cells in a FoxA2 overexpression background. **B)** MDA-MB-231 cells with the corresponding genotype: Non-targeting mRNA (Dox+), control cells expressing a non-targeting sequence; Sh FoxA2 (Dox+), short hairpin expressing cells and Sh FoxA2+ FoxA1 (Dox+), short hairpin expressing cells in a FoxA1 overexpression background. The results are representative of three independent experiments.

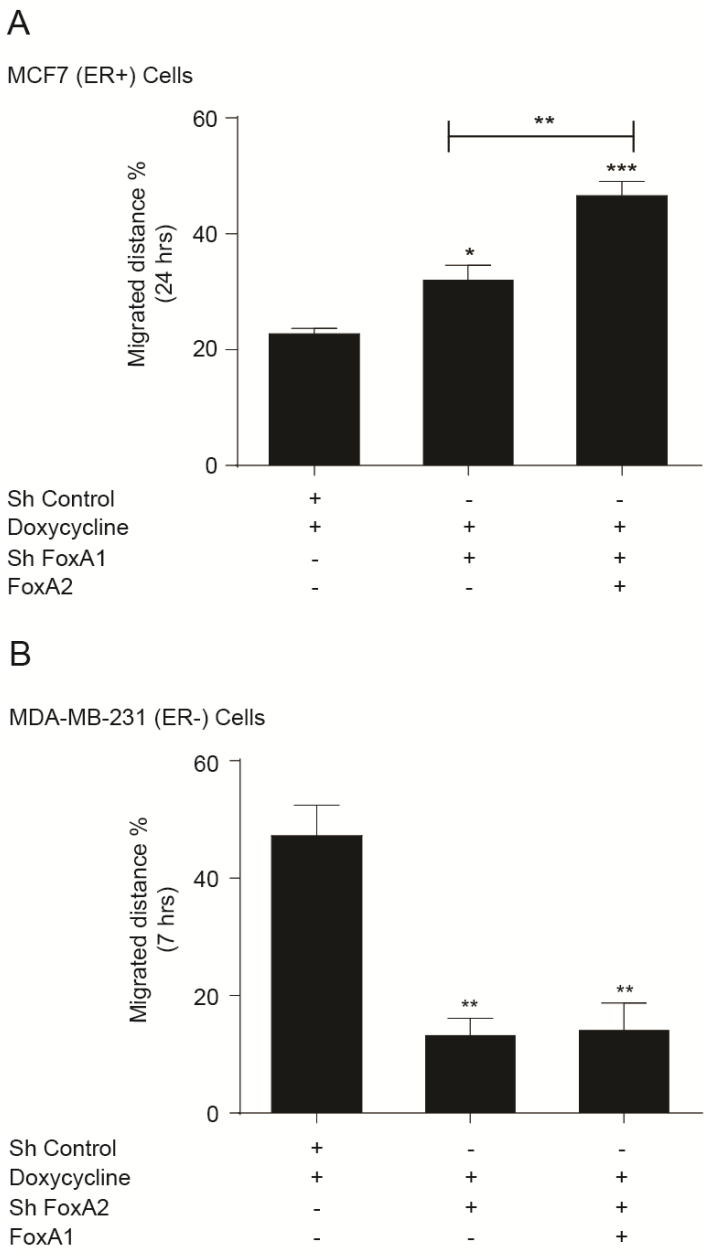

Figure 38: FoxA1 and FoxA2 transcription factors modulate breast cancer cell migration. Wound-healing assay of tumor cells, **A** and **B,** represent the width percentage of remaining open wound measured in relation to time 0 h separation. MCF7 and MDA-MB-231 cells were treated with 2 µg of doxycycline for 7 days to induce the short hairpin expression. Data are mean +/- SD (n=3) and T-test was calculated using control cells. **A)** MCF7 cells with the corresponding genotype: Non-targeting mRNA (Dox+), control cells expressing a non-targeting sequence; Sh FoxA1 (Dox+), short hairpin expressing cells and Sh FoxA1+ FoxA2 (Dox+), short hairpin expressing cells in a FoxA2 overexpression background. **B)** MDA-MB-231 cells with the corresponding genotype: Non-targeting mRNA (Dox+), control cells expressing a non-targeting

sequence; Sh FoxA2 (Dox+), short hairpin expressing cells and Sh FoxA2+ FoxA1 (Dox+), short hairpin expressing cells in a FoxA1 overexpression background.

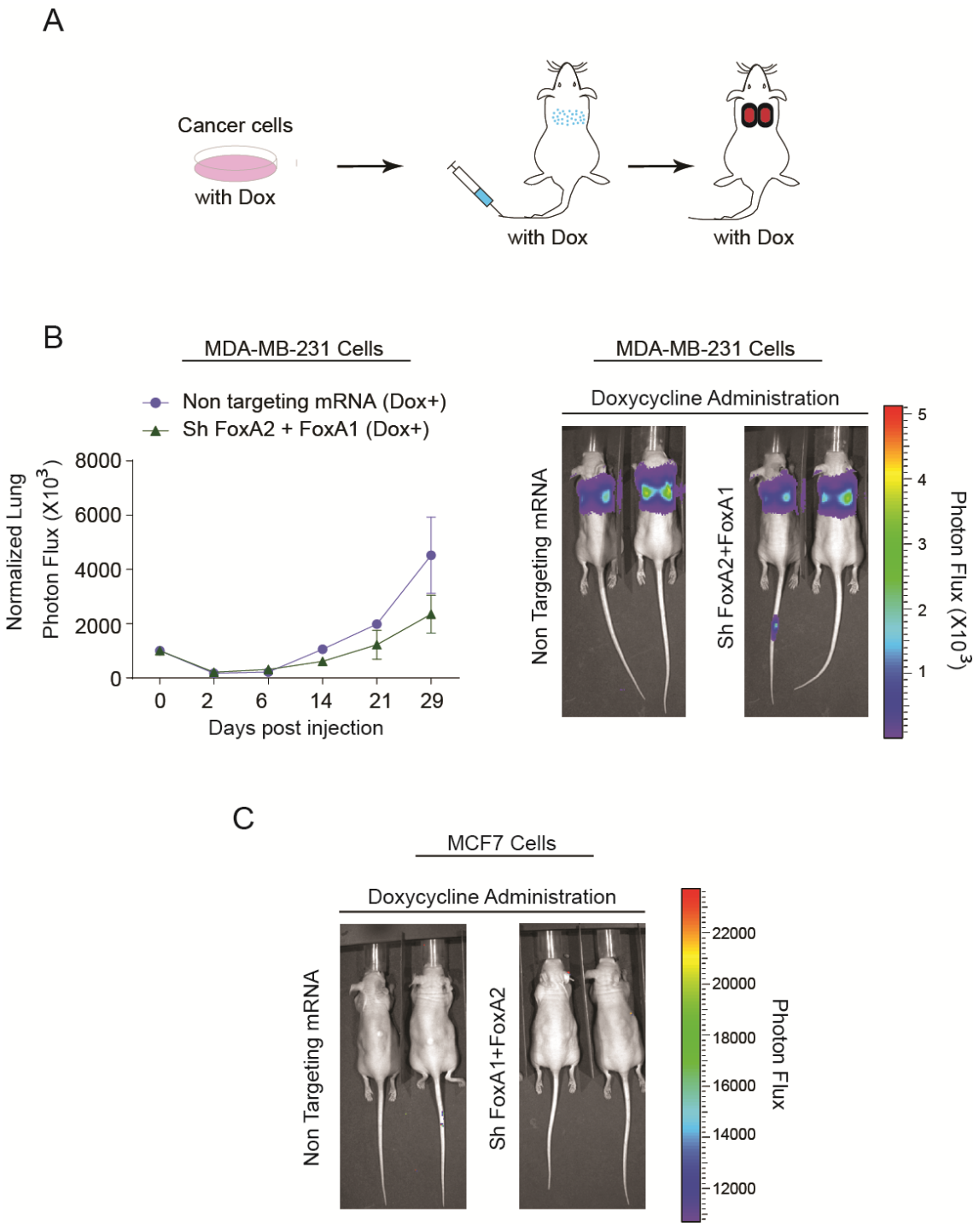

Figure 39: FoxA1 and FoxA2 transcription factors do not exhibit lung seeding capacity *in vivo*. 5X10^5 MCF7 and MDA-MB-231 cells were injected into the tail vein of Balb c/nude mice to assess lung seeding of the different cell groups generated. **A)** Schematic representation of the experiment; cells treated for 7 days with doxycycline were injected in animals administrated with doxycycline. **B)** MDA-MB-231 cells with the corresponding genotype: Non-targeting mRNA (Dox+), control cells expressing a non-targeting sequence; and Sh FoxA2+FoxA1 (Dox+), short hairpin expressing cells in a FoxA1 overexpression background. Total photon flux intensity in the lungs of mice was quantified and normalized to day of injection, data are mean +/- SD (n=5). **C)** MCF7 cells with the corresponding genotype: Non-targeting mRNA (Dox+), control cells

expressing a non-targeting sequence; and Sh FoxA1+FoxA2 (Dox+), short hairpin expressing cells in a FoxA2 overexpression background. MCF7 cells were not able to grow in the lungs, data are mean +/- SD (n=5). Bioluminescence images are representative of each group at day 29.

Discussion

Advances in cancer metabolism research over the last decade have enhanced our understanding of how metabolic alterations in cancer cells support the anabolic requirements associated with tumor growth and proliferation. Growing evidence indicates that modifications in metabolic enzymes, pathways, and metabolites greatly contribute to disease progression and malignancy. It has been postulated that *de novo* lipid synthesis and the generation of specific pro-oncogenic lipids play a major role in cancer. Here, we identified endothelial lipase (LIPG) as a metabolic FoxA-regulated gene. FoxA1 and FoxA2 mediated cell growth *in vitro* and tumor growth *in vivo* through LIPG expression. Interestingly, LIPG activity arose as an indispensable regulator of breast cancer growth generating a broad family of lipids known to promote malignancy. Although breast tumors are classified into a number of distinct biological classes that show relationships with clinical outcome, LIPG emerges as a common growth regulator in different breast cancer subtypes. Together, these findings reveal how breast cancer cells generate a central hub of lipids indispensable for growth.

We studied the involvement of the FoxA family of transcription factors in breast cancer growth. FoxA1 is expressed in ER+ human breast cancer samples as well as in ER+ human cell lines. At the time of the study, it was reported that FoxA1 is expressed in luminal subtype tumors along with ESR1 and GATA 3 (Perou et al., 1999; Sorlie et al., 2001). Moreover, tissue microarrays reveal that FoxA1 expression is associated to better survival and correlates negatively with proliferation markers and high histological grade (Thorat et al., 2008). Moreover, nuclear FoxA1 immunohistochemistry detection is a significant predictor of breast cancer–specific and relapse-free survival (Mehta et al., 2012). FoxA1 is also involved in tissue function by coupling metabolic responses to different stimuli. Furthermore, FoxA1 in the liver activates gluconeogenesis and lipid oxidation (Santisteban et al., 2010), promoting the physiological response to fasting. These observations describe the transcription factor FoxA1 as a predictor of clinical outcome with clear implications in controlling cell fate

differentiation in breast cancer pathogenesis and a central regulator of metabolic responses.

We have seen that FoxA1 mRNA levels stratified patient tumor samples: all ER+ samples have similar FoxA1 mRNA levels, whereas ER- breast cancers can be segregated into either high or low FoxA1 mRNA levels. We observed similar tendencies with respect to FoxA1 expression in breast cancer cell lines: all ER+ cell lines expressed FoxA1 when compared to HMEC, and 3 of 5 ER- cell lines expressed high FoxA1 mRNA levels. Regarding the last, it is known that there is an apocrine breast cancer subtype which does not express estrogen receptor. Despite these tumors being ER-, they express genes typically up-regulated in luminal subtypes which include SPDEF, FoxA1, XBP1, CYB5 (Farmer et al., 2005). Moreover, these tumors grow in an androgen-dependent manner using FoxA1 as a key mediator of the androgen response (Doane et al., 2006; Ni et al., 2011; Robinson and Carroll, 2012; Robinson et al., 2011)

To date, FoxA1 function has been associated with luminal commitment in transformed mammary epithelium. Still, it is poorly understood whether FoxA1 regulates metabolic genes necessary for tumor malignancy. Wolf et al. have described that an overexpression of FoxA1 in MCF7, MDA-MB-231 and SKBR3 cells inhibits clonal proliferation accompanied by an increase in p27 mRNA expression (Wolf et al., 2007). We started by evaluating FoxA1 loss of function in the MCF7 cell line, which presents the highest levels of FoxA1 mRNA, and we observed an arrest of cell proliferation when cells were depleted of FoxA1. While our study was in progress, Hurtado et al. described that FoxA1 is required for almost all ER binding events in MCF7 cell lines and that specific silencing of FoxA1 globally affects the estrogen-mediated transcriptome. Furthermore, FoxA1 silencing results in MCF7 (ER+) and MDA-MB-453 (ER-/AR+) growth arrest (Hurtado et al., 2011; Ni et al., 2011; Robinson et al., 2011). This data highlights the FoxA1 transcription factor as an indispensable tumor growth regulator in ER and AR expressing breast cancer subtypes, which we have confirmed in this study.

Studies in breast cancer tumors position FoxA1 as a key transcription factor in luminal and apocrine subtypes. Nevertheless, it remains unknown whether other members of the FoxA family of transcription factors have relevant functions in breast cancer growth. Global gene expression analyses, detailed in section 1.1, indicated that FoxA2 mRNA levels were up-regulated in MDA-MB-231 cells compared with HMEC and MCF7 cells. On the other hand, similar levels of FoxA3 mRNA were expressed in all cell lines. Also, real time and western blot analysis confirmed FoxA2 up-regulation in MDA-MB-231 cells, whereas FoxA2 depletion resulted in cell growth arrest, as previously observed in FoxA1-depleted MCF7 cells.

We hypothesize that the Affymetrix probes failed to detect the precise levels of FoxA2 mRNA in breast cancer samples for several reasons. First, real time analysis using Taqman technology showed greater differences than Affymetrix probes when comparing FoxA2 mRNA expression levels between MDA-MB-231 and HMEC cells, section 1.1. Second, when FoxA2 was silenced in tumor xenografts, section 2.1, we again observed greater differences between Affymetrix and real time analysis. Finally, in cell lines, we observed that FoxA1 and FoxA2 expression was mutually exclusive, which was not detected in the MSKCC/EMC breast cancer cohort. Thus, FoxA2 mRNA evaluation by Affymetrix probes may have underestimated the role of the transcription factor FoxA2 in breast cancer pathogenesis. To further determine the possible implications of FoxA2 in breast cancer disease, we are studying FoxA2 protein expression in human breast cancer samples. Here, we will attempt to elucidate the presence of FoxA2 in breast cancer samples and whether FoxA2 protein expression is able to stratify patient samples or correlate with clinical outcome. Due to the fact that prostate NE tumors show androgen independency, and that FoxA2 is involved in the development (Qi et al., 2010a) and metastatic capacities of NE cells (Qi et al., 2010b) we consider FoxA2 to be an important factor in hormone-independent breast cancers.

We do not rule out that breast tumors could be heterogeneous for FoxA expression and that in same tumors FoxA1 and FoxA2 expression coexist having both mutually exclusive expression patterns.

FoxA1 and FoxA2 govern a wide range of indispensible genes necessary for the development and function of various tissues. Our data and previously published results support the idea that the FoxA family of transcription factors plays a pivotal function in breast cancer development. Firstly, FoxA1 is a key component in the ER and AR response expressed in ER+ and ER-/AR breast cancer subgroups. Secondly, we demonstrated by real time, western blot and using FoxA2 shRNA, that FoxA2 is expressed in MDA-MB-231 cells (a triple negative breast cancer cell line). And thirdly, we have shown, using *in vitro* and *in vivo* settings, that the loss of FoxA1 and FoxA2 decreased cell proliferation and tumor growth. Taking all of this information into consideration, our results suggest that breast cancer cell lines either express FoxA1 or FoxA2, and that the presence of one or the other is essential for breast cancer development.

Interestingly, in some tissues, FoxA1 is able to fulfill the loss of FoxA2 and vice-versa. The complementary functions of the transcription factors led us to hypothesize that FoxA1 and FoxA2 regulated common essential tumor growth genes in luminal and basal cell types. Furthermore, we wanted to discern whether FoxA1 and FoxA2 regulated the same metabolic pathways in breast cancer cells and if these pathways were necessary for growth. For this reason, we sought to elucidate whether FoxA1 could be replaced by FoxA2 in MCF7 cells or vice-versa in MDA-MB-231 cells.

The FoxA-depleted phenotype was rescued by exogenous FoxA2 expression in MCF7 and exogenous FoxA1 expression in MDA-MB-231 cells, suggesting that MCF7 and MDA-MB-231 cells share common pro-proliferation pathways.

We aimed to mechanistically understand FoxA function in breast cancer by identifying which proteins were regulated by the FoxA1-FoxA2 axis in MCF7 and MDA-MB-231 cells. To solve this question, we analyzed the gene expression profile of cells isolated from tumors described in section 2,1. Interestingly, FoxA1 and FoxA2 factors in both cell types regulated the same metabolic enzyme, LIPG. LIPG was found to be down-regulated in MCF7 and MDA-MB-231 cells when FoxA1 and FoxA2 were depleted. Moreover, LIPG mRNA levels were reestablished to control levels in rescued cells.

We determined the contribution of LIPG to tumor growth, finding that the loss of LIPG protein in both cell types induced *in vitro* cell growth arrest. Next, we attempted to rescue the reduced growth phenotype due to FoxA1 or FoxA2 loss by overexpressing a wild type LIPG isoform and a catalytically inactive one. We observed that overexpression of wild type LIPG was able to rescue the *in vivo* tumor proliferation when FoxA transcription factors were depleted, whereas the catalytically mutant isoform was not. Moreover, in control MDA-MB-231 cells, overexpression of LIPG induced an increase in growth rate. These observations reflect that MCF7 and MDA-MB-231 cell types have a common feature responsible for tumor proliferation. Surprisingly, this characteristic is independent of ER signaling and basal/stem/EMT-like genes. In this regard, LIPG protein becomes a metabolic regulator necessary for breast cancer growth.

LIPG is expressed in almost all tested breast cancer cell lines but not in HMEC. According to LIPG tissue localization studies, LIPG is expressed in several tissues but not in adult mouse mammary glands (Hirata, 1999; Jaye et al., 1999). We are now studying LIPG protein expression in human breast cancer samples and non-tumor breast tissue by immunohistochemistry. With this, we hope to uncover whether LIPG expression is a unique feature of cancer cells. Interestingly, LIPG knockout mouse models are viable and do not present overt defects (Ishida et al., 2003), suggesting that LIPG is dispensable for non-tumor cells, but an essential contributor to breast tumor growth.

Furthermore, we identified the metabolites regulated by LIPG *in vitro* using an untargeted lipidomic approach. Mass spectrometry revealed that around 1 % of total lipids changed in LIPG-depleted MCF7 cells and 15 % of lipids in LIPG depleted MDA-MB-231 cells. The low number of LIPG regulated lipids highlighted the substrate specificity of the enzyme.

We observed a common lipid signature regulated by LIPG in both cell types, which included lysophosphatidyl cholines (LPC), phosphatidyl ethanolamines (PE) and diacylglycerols (DG). However, the aggressive MDA-MB-231 cell line showed more regulated lipids and lipid species than the non-aggressive MCF7: phospho cholines (PC, PG and PE), lysophospho cholines (LPC), and

diacylglycerols (DG) lipid families and ether lipids species were reduced in MDA-MB-231 LIPG depleted cells.

Interestingly, the lipid families regulated by LIPG in MCF7 and MDA-MB-231 cells have been shown to be important in cancer biology. As previously described, monoacylglycerol lipase (MAGL) regulates the hydrolysis of monoacylglycerols to free fatty acids in aggressive cancer cells. Untargeted metabolomics show that MAGL regulates the synthesis of phospholipids (PC, PE and PA), lysophospholipids (LPC, LPA and LPE), ether lipids and prostaglandin E2 (Nomura et al., 2010). Remarkably, MAGL depletion lead to tumor growth reduction, just as LIPG depletion does in our model.

It is worth noting that Nomura et al described lipid species regulated by MAGL only in aggressive cancer lines. However, MAGL is expressed in some non-aggressive cell lines at lower levels, as detected in MCF7 cells. One question that remains unanswered is whether MAGL regulates lipids in non-aggressive cancer cells and if it has an impact on cancer malignancy, as LIPG does. According to this logic, a principal core of lipids should be necessary across diverse cancer lines to allow for proliferation. It is likely that MAGL and LIPG have different cellular distributions and substrate specificities. Nevertheless, the bulk of lipids regulated by both are similar, reinforcing the idea of a central lipid metabolic state for tumor proliferation. For aggressive cancer cells, the same lipid signature is necessary for cell proliferation, however more lipid species are needed to drive more malignant phenotypes, as seen in MDA-MB-231 cells.

Beyond the tumorigenic role of MAGL mediating the production of pro-tumorigenic signaling lipids, MAGL's physiological function is to modulate endocannabinoid signaling (Mulvihill and Nomura, 2013). This evidence suggests that MAGL has different functions and that it processes different precursors in normal tissue when compared to cancer cell lines. We believe that LIPG, as well as MAGL, may control different lipid pathways depending on where and to which extent they are expressed.

In addition, the lipid signature generated by isotopic palmitic acid tracing comparing non-tumor cells and cancer cells was also similar to the lipids

regulated by LIPG and MAGL. These include structural lipids (e.g. PC, LPC, PE, LPE, PS, PG and others), lipids stores (e.g. triacylglycerols and diacylglycerols) and signaling lipids (e.g. LPA, ceramide and DAG) (Louie et al., 2013).

Overall, LIPG promoted the availability of structural lipids and signaling lipids, such as DAG, in breast cancer cell lines. DAG can affect a wide range of processes in cells, and has been shown to be a lipid intermediate in metabolism, a component of membranes and a second messenger (Carrasco and Merida, 2007). DAG can be used for complex lipid synthesis as well as a source of free fatty acids, which in turn, can be used to build signaling lipids. Furthermore, DAG can act as a second messenger activating a broad type of proteins that regulate signaling cascades and gene programs. The most well-known examples are PKC and PKD proteins, shown to be mediators of biological processes such as cell survival, proliferation, migration, differentiation membrane trafficking, inflammation, angiogenesis, cardiac contractility and hypertrophy (Ochi et al., 2011; Rozengurt, 2011). DAG not only regulates PKC and PKD: Vav, Raf, Rock chimaerin, Ras guanine-releasing protein (RasGRP) and myotonic dystrophy kinase-related Cdc42-binding kinase (MRCK) are also modulated by DAG. Remarkably, most of these proteins influence biological processes that could be important for cancer growth (Carrasco and Merida, 2007).

Lastly, most of the pathways in lipid synthesis are interconnected (Aad et al., 2012; Mills and Moolenaar, 2003). This highlights that LIPG-modulated lipids could be further used to generate different lipid classes. One example is the bioactive lipids, LPA and PA, which both have growth factor-like activities which stimulate cell proliferation, migration and survival. LPA and PA can both be synthesized upon DAG or MAG hydrolysis. Another way of generating LPA is through the hydrolysis of LPC by the ATX/lyso PLD enzyme (Mills and Moolenaar, 2003). Interestingly, enhanced ATX/lyso PLD expression, elevated LPA production and increased LPA receptor expression are found in breast and ovarian cancer (Liu et al., 2009a). Furthermore, overexpression of ATX/lyso PLD or LPA receptors in mice induces breast cancer initiation and progression.

Mammary tumors of these animals show more activation of the PI3K, MAPK and Wnt signaling pathways (Liu et al., 2009b).

Little is known about the function and distribution of lipids in cancer cells and, more specifically, in breast cancer. Nevertheless, it is known that LPA and LPS transiently induce an increase of calcium and cell proliferation in breast cancer cell lines (Xu et al., 1995). Moreover, MDA-MB-231 breast tumor xenografts are enriched in PC species in viable tumor regions compared with necrotic ones (Chughtai et al., 2013). Our data highlights the importance of lipid metabolism in cancer cell growth and pathogenesis, and situates LIPG in the regulation of breast cancer growth.

We believe that in breast cancer cells, LIPG is involved in the uptake of extracellular lipids from HDL, LDL and other lipoproteins, as shown in other cell types and tissues. It is worth to mention that LIPG is able to stimulate lipid and free fatty uptake without using its enzymatic activity (Choi, 2002; Yasuda et al., 2010). Here we demonstrated that only active LIPG was able to rescue the proliferation reduction induced by FoxA1-FoxA2 loss. In this sense, we believe that breast cancer cells depend on LIPG`s activity to uptake and process extracellular lipids to promote cancer malignancy.

It has been highlighted that the *de-novo* lipid biosynthesis plays a major role in cancer pathogenesis and that several enzymes involved in the pathway are overexpressed in tumors (Menendez and Lupu, 2007). Collectively our results showed LIPG as an enzyme that regulates the hydrolysis of phospholipids and the uptake of lipids from the extracellular niche. In this context, we describe a new mechanism to fulfill the lipid demands of cancer growth.

It is known that FoxA1 confers a luminal phenotype, and along with estrogen receptors, it regulates a number of luminal commitment genes (Hurtado et al., 2011). As expected, when we knocked down FoxA1 in MCF7 cells, there were an important number of luminal commitment genes that were down-regulated. Furthermore, there was an increase in well-known regulators of EMT/Basal commitment genes such as CD44, vimentin and fibronectin, among others (Mani et al., 2008; Polyak and Weinberg, 2009; Scheel et al., 2011). Despite an

increase in EMT/Basal markers, MCF7 cells were not able to proliferate *in vitro* and *in vivo*. It was only when we overexpressed FoxA2 or LIPG that we observed a recovery in tumor growth. Interestingly, when FoxA2 was substituted for FoxA1, neither the pattern of down-regulated luminal genes, nor that of up-regulated basal genes detected in FoxA1 silenced cells changed. This indicated that FoxA2 in MCF7 cells did not regulate the bulk of the estrogen response, but MCF7 cells were still able to grow. Furthermore, FoxA2 MDA-MB-231 knock down cells showed a down regulation of the previously mentioned EMT/basal genes, and the same behavior was observed in FoxA1 rescues. On the contrary, luminal markers and modulators were increased when FoxA2 was replaced by FoxA1. This reinforces the idea that MCF7 and MDA-MB-231 cells are absolutely dependent on LIPG to grow.

Finally, the modulation of luminal and basal commitment genes driven by FoxA factor variations influenced the migratory capacities of MCF7 and MDA-MB-231 cell lines. FoxA1(-)/FoxA2(+) MCF7 cells had a better migration capacity, whereas FoxA2(-)/FoxA1(+) MDA-MB-231 cells migrated slower than controls. Changes at the molecular level and migration capacities *in vitro* were still not sufficient to change these cells' *in vivo* distant organ seeding ability. When injected into tail veins, MCF7 cells do not grow under any condition, and similar results have been observed in Dr.Gomis' laboratory. In the case of MDA-MB-231 cells, we did not find any differences in lung colonization between FoxA2(-)/FoxA1(+) and control cells. The negative results observed *in vivo* can be explained by several reasons. First, we used a shRNA expression system with which we obtained a decrease of FoxA transcription factors, but this did not completely eliminate them. As a result, these cells most likely showed residual FoxA function. Therefore, genes intrinsic to either luminal or basal cell lines were still present. Second, gene expression regulation observed in these cells could drive a more subtle phenotype. We believe that the self-renewal capacities of these cells are different and that in limiting dilution assays, FoxA1(-)/FoxA2(+) MCF7 cells would be enriched in tumor initiating cells. In the same approach, FoxA2(-)/FoxA1(+) MDA-MB-231 cells would have a decreased ability to initiate tumors. Third, we could assess whether FoxA factors regulated lung seeding using a lung metastatic subpopulation of LM2-

4175 cells isolated by *in vivo* selection of MDA-MB-231 cells in mice (Minn et al., 2005). These cells expressed FoxA2, as did MDA-MB-231 cells (data not shown), and are able to better seed lungs than MDA-MB-231. Last, we could use immortalized human MECs (HMLE) and their spontaneously arising mesenchymal subpopulation (MSP) derivatives (Elenbaas et al., 2001). A first approach would be to check their FoxA1 or FoxA2 mRNA and protein expression and then modulate their levels and evaluate basal and luminal phenotypes. If these cells do not express any FoxA factors, we could induce their expression and analyze HMLE and MSP gene expression and cell behavior.

There are numerous studies trying to elucidate the complex function that the FoxA1 transcription factor plays in breast cancer development. Here, we showed that FoxA1 regulates a lipid pathway involved in cell growth independently of hormone response. Surprisingly, FoxA2 regulates the same lipid network in MDA-MB-231 cells promoting growth, as does FoxA1 in MCF7 cells. This lipid network may be central in growth regulation across all breast cancer subtypes, while highlighting LIPG as a central player. Moreover, the FoxA2 transcription factor may emerge as a regulator of the basal phenotype, but it is necessary to study this function more in depth.

Conclusions

1. FoxA1 and FoxA2 transcription factors regulate cell proliferation and tumor growth when they are expressed in breast cancer cells. Each factor can be replaced by the other one, allowing cell proliferation. Interestingly, FoxA2 expression does not regulate estrogen receptor genes.

2. LIPG mRNA expression is regulated by FoxA1 and FoxA2 in MCF7 and MDA-MB-231 cells, respectively.

3. LIPG and its activity promote proliferation of basal and luminal cancer cell types *in vitro*. Furthermore LIPG is able to mediate the rescue of the *in vivo* growth reduction generated by FoxA1 or FoxA2 depletion.

4. LIPG regulates in cancer cells a lipid network of oncogenic, structural and lipid stores. This network is enriched in phospholipids and lysophospholipids (PE, PC and LPC) and diacylglycerols (DAG).

5. LIPG regulates the hydrolysis of phospholipids and the uptake of lipids from the extracellular niche. In this context, we describe a new mechanism to fulfill the lipid demands of cancer growth.

6. FoxA1 and FoxA2 transcription factors govern features of luminal and basal phenotypes in MCF7 and MDA-MB-231 cell lines. FoxA1-/FoxA2+ MCF7 cells have more basal commitment genes and they have more migration capacities than their parental cells. Instead FoxA2-/FoxA1+ MDA-MB-231 cells have more expression of luminal commitment genes and they have less migration abilities than their parental cells.

7. LIPG is homogeneously distributed across breast cancer subtypes. This expression pattern gives rise to the question of whether LIPG can be an attractive target for breast cancer treatment. Furthermore, it would be

interesting to understand whether LIPG modulates the lipid metabolism in a broader spectrum of cancer types.

Supplementary tables

Supplementary Table I: Top 20 differentially expressed genes in FoxA1 depleted MCF7 cells

MCF7 sh FoxA1 (Dox-) v/s MCF7 sh FoxA1 (Dox+)

Symbol	Fold-Change	Probability of being differentially express	Symbol	Fold-Change	Probability of being differentially express
OLFM4	12,88	1	COL1A1	-19,75	1
EGR4	8,86	1	PPIA	-18,47	1
NR4A3	8,11	1	COX6A1	-15,11	1
CPB1	7,79	1	MAF	-14,91	1
NR5A2	6,35	1	EFEMP1	-14,77	1
AXIN2	6,25	1	ZEB2	-12,20	1
MSMB	5,95	1	---	-11,78	1
LDLR	5,83	1	RPS15	-11,14	1
FOLH1	5,54	1	PRRX1	-11,05	1
EGR1	5,50	1	ANXA1	-10,85	1
IL20	5,38	1	TFPI	-10,16	1
EGR2	5,35	1	TUBB6	-10,06	1
FRMD4B	5,31	1	CALD1	-9,99	1
GEM	5,28	1	PRDM8	-9,96	1
NR4A1	5,23	1	VIM	-9,50	1
MYO3B	5,22	0,99	CELF2	-9,45	1
ITGA8	5,18	0,99	AKT3	-8,22	1
HGD	5,14	0,99	CCDC80	-7,93	1
SCD	5,02	0,99	TCF4	-7,89	1
FAM5C	4,92	0,99	IGDCC4	-7,85	1

Supplementary Table II: Top 20 differentially expressed genes in MCF7 rescues cells

MCF7 sh FoxA1 (Dox+) v/s MCF7 sh FoxA1+FoxA2 (Dox+)

Symbol	Fold-Change	Probability of being differentially express	Symbol	Fold-Change	Probability of being differentially express
DAB2	10,19	1	S100A8	-10,89	1
EPHA3	8,38	1	---	-10,27	1
PPFIA2	8,28	1	PI3	-8,19	1
ATF3	7,67	1	C1orf168	-6,80	1
IL1R1	7,45	1	IGSF1	-6,61	1
ANXA1	7,43	1	RAB31	-6,56	1
FAM129A	7,03	1	FN1	-6,25	1
TNFRSF19	6,78	1	LIPG	-5,94	1
IGDCC4	6,73	1	NAV2	-5,81	0,99
KRT81	6,62	1	XAF1	-5,64	0,99
GRB14	6,62	1	MGP	-5,55	0,99
CD36	6,47	1	KRTAP5-10	-5,38	0,99
ELF5	6,36	1	ATP6V1B1	-5,20	0,99
FOLH1	6,36	1	HMGA2	-5,18	0,99
CYR61	6,21	1	SYTL5	-5,16	0,99
PTPRN2	6,08	1	TMEM45A	-5,05	0,99
ABCC4	6,07	1	WISP2	-5,02	0,99
PCDH10	5,93	1	PLAT	-4,91	0,99
CTGF	5,91	1	MFGE8	-4,86	0,99
HOXB3	5,90	1	RNF183	-4,84	0,99

Supplementary Table III: Top 20 differentially expressed genes in FoxA2 MDA-MB-231 depleted cells

MDA-MB-231 sh FoxA2 (Dox-) v/s MDA-MB-231 sh FoxA2 (Dox+)

Symbol	Fold-Change	Probability of being differentially express	Symbol	Fold-Change	Probability of being differentially express
MCAM	10,70	1	COL3A1	-16,46	1
COX7B2	10,55	1	MGP	-11,87	1
HOOK1	7,05	1	COL1A2	-10,65	1
QPRT	6,93	1	UNC5B	-10,49	1
---	6,81	1	KCTD15	-9,83	1
C6orf223	6,71	1	GNG2	-9,52	1
TIE1	6,65	1	ZNF318	-9,46	1
TBXAS1	5,94	1	TFAP2C	-9,17	1
NRXN3	5,85	1	STRA6	-9,14	1
AGR2	5,78	1	MAGEB1	-8,59	1
SPANXC	5,61	1	TFCP2L1	-8,43	1
PRDM16	5,28	1	TMEM163	-8,37	1
ADAM28	5,25	1	SAMSN1	-8,23	1
LIPG	5,19	1	SUSD2	-8,10	1
EPB41L4B	5,16	1	VIPR1	-7,99	1
ZNF300	5,15	1	PADI4	-7,74	1
SERPINA3	5,08	1	PADI2	-7,71	1
BCL2	4,98	0,99	HLA-F	-7,33	1
PBX1	4,91	0,99	POSTN	-7,26	1
CACNB4	4,89	0,99	NGFR	-7,26	1

Supplementary Table IV: Top 20 differentially expressed genes in MDA-MB-231 rescues cells

MDA-MB-231 sh FoxA2 (Dox+) v/s MDA-MB-231 sh FoxA2+FoxA1 (Dox+)

Symbol	Fold-Change	Probability of being differentially express	Symbol	Fold-Change	Probability of being differentially express
SAMSN1	9,00	1	TFF1	-14,13	1
SPP1	8,26	1	TFF3	-13,16	1
HBE1	8,25	1	AGR2	-11,21	1
MGP	8,10	1	MPZL2	-10,74	1
HBG1	8,00	1	TNS4	-10,41	1
CA9	7,52	1	TMPRSS3	-10,04	1
AQP1	6,57	1	CAPN8	-10,03	1
KCTD15	6,54	1	KIAA1462	-9,00	1
SUSD2	6,51	1	CD24	-8,92	1
PADI2	6,35	1	HNF4A	-8,81	1
KLRK1	6,12	1	MAGEC2	-8,65	1
ADSSL1	5,93	1	TBXAS1	-8,39	1
SLC6A8	5,86	1	RAB3B	-8,20	1
S100B	5,74	1	GATA2	-8,07	1
ZNF318	5,65	1	SHANK2	-7,61	1
DMBT1	5,54	1	RSAD2	-7,59	1
APOBEC3G	5,52	1	MMP1	-7,49	1
FREM2	5,51	1	SEL1L3	-7,47	1
ALOX5AP	5,51	1	GKAP1	-7,47	1
PADI4	5,35	1	FOXA1	-7,46	1

Supplementary Table V: Affymetrix analysis of CDH11, BCL2, LIPG gene expression in MCF7 and MDA-MB-231 engineered cells

MCF7 (ER+) Cells

Sh FoxA1 (Dox-) v/s Sh FoxA1 (Dox+)

Symbol	Fold-Change	Probability of being differentially express
CDH11	-3,715	0,99
BCL2	3,065	0,99
LIPG	3,203	0,99

Sh FoxA1 (Dox+) v/s Sh FoxA1+FoxA2 (Dox+)

Symbol	Fold-Change	Probability of being differentially express
CDH11	2,55	0,89
BCL2	-3,37	0,98
LIPG	-5,94	1

MDA-MB-231 (ER-) Cells

Sh FoxA2 (Dox-) v/s Sh FoxA2 (Dox+)

Symbol	Fold-Change	Probability of being differentially express
CDH11	-5,18	1
BCL2	4,98	0,99
LIPG	5,19	1

Sh FoxA2 (Dox+) v/s Sh FoxA2+FoxA1 (Dox+)

Symbol	Fold-Change	Probability of being differentially express
CDH11	3,74	0,99
BCL2	-3,29	0,99
LIPG	-3,93	0,99

Methods

Breast cancer cell lines

Human Mammary epithelial cells (HMEC) were purchased at Lonza and MDA-MB-468 and MDA-MB-435 were purchased at (ATCC). MDA-MB-231, MCF7, T47D, BT20 and BT474 breast cancer cell lines were a donation from Gomis Lab. All cells except HMEC were maintained in Dulbecco´s modified Eagle´s media (DMEM) supplemented with 10 %FBS, 100mg/mL streptomycin and 100 U/mL penicillin and 2mM L-glutamine. HMEC cells were maintained in mammary epithelial growth media (Lonza).

Cell proliferation assays

Sh LIPG

After puromicyne selection cells were recovered with fresh media for 12 hrs and 10^5 cells were plated in multiwell culture plates of 6. At every time point, cells were trypsinized, collected and counted using Scepter™ 2.0 Cell Counter.

Sh FoxA1 and sh FoxA2.

Cells were seeded in 100 mm plates and treated with or without 2µg/mL doxycycline for 6 days. At day 6, 10^5 cells were plated in multiwell culture plates of 6 and the doxycycline treatment was continued until the end of the experiment. At every time point, cells were trypsinized, collected and counted using Scepter™ 2.0 Cell Counter.

Migration assays

MCF7 and MDA-MB-231 engineered cells were incubated with doxycycline 2µg/mL for 6 days and plated into 60 mm plates, with parallel lines drawn at the underside of the well with marker. These lines will serve as fiducially marks for the wound areas to be analyzed. When cells are absolutely confluent growth media was aspirated and washed with PBS three times. One parallel scratch wound was made perpendicular to the marker lines with a P10 pipet tip (atembio). Pictures were made using a 10× objective and a total of six lines were taken at 0 hrs for both cell types and after 7 hrs (MDA-MB-231 cells) and 12hrs (MCF7 cells). Images were analyzed with the Image J software to

measure the scratch seize. Data was normalized to the measured scratch seize at time 0 hrs.

Site directed mutagenesis

Asp193 was substituted to an Asn to obtain a catalytically inactive LIPG isoform. The kit Quickchange (Stratagene) was utilized following manufacturer´s instructions and the mutation was confirmed by DNA sequencing using Big Dye v3.1 Cycle Sequencing Kit (Applied Biosystems).

Mutation	Primers
LIPG (ASP 193 ASN)	Fw: 5'CGAATCACAGGTTTGAATCCTGCCGGGCC3' Rev: 5'GGCCCGGCAGGATTCAAACCTGTGATTCG3'

FoxA1, FoxA2 and LIPG construct

Human FoxA1, FoxA2 and LIPG (pDONR-223 backbone) were obtained from (Open Biosystem). The gene of interest cDNA fragment was amplified using KOD DNA polymerase (Merck) and specific primers to generate a PCR product with attB sites. The PCR product was isolated from a PCR gel with illustra GFX PCR DNA and Gel Band Purification Kit (GE Healthcare). Next, the fragment was recombined with a donor clone (pDONR-221) using the BP clonase Enxyme Mix (Invitrogene). The pDONR-221 plasmid (containing the cDNA of interest) was cloned by the gateway system into a pDEST/pLlenti-PGK Hygro DEST W530-1 vector (p-lenti) using the LR Clonase Enzyme MIX following manufacturer´s instructions.

Inactive LIPG was generated by site directed mutagenesis of the human LIPG (pDONR-221vector) and cloned into the p-lenti vector using LR Clonase Enzyme MIX.

DNA sequencing confirmed the correct generation of constructs by using Big Dye v3.1 Cycle Sequencing Kit (Applied Biosystems).

Gene	Primers
FoxA1	Fw:: 5'GGGGACAAGTTTGTACAAAAAAGCAGGCTTCACCATGTTAGGAACTGTGAAGATGGAAGG3'
	Rev: 5'GGGGACCACTTTGTACAAGAAAGCTGGGTTCTAGGAAGTGTTTAGGACGGGTCTGG3'
FoxA2	Fw: 5'GGGGACAAGTTTGTACAAAAAAGCAGGCTTCACCATGCTGGGAGCGAGATGGAAGG3'
	Rev: 5'GGGGACCACTTTGTACAAGAAAGCTGGGTTTTAAGAGGAGTTCATAATGGGCCGGGA3'
LIPG	Fw: 5'GGGGACAAGTTTGTACAAAAAAGCAGGCTTCACCATGAGCAACTCCGTTCCTCTGCTCTG3'
	Rev: 5'GGGGACCACTTTGTACAAGAAAGCTGGGTTTCAGGGAAGCTCCACAGTGGGACTGG3'

Generation of inducible sh-RNA systems

The generation of the inducible sh-RNA systems were done as described (Paddison et al., 2004). First, we selected a hairpin sequence from constitutive short hairpins (TRC1 sh clones Sigma Aldrich) known to work for FoxA1 and FoxA2. We design and order a template oligonucleotide by incorporating miR-30 micro RNA sequences between the sense and the antisense sequence of the selected hairpin and amplified the fragment to incorporate *Eco*RI and *Xho*l cloning sites. The PCR product was isolated from a PCR gel with illustra GFX PCR DNA and Gel Band Purification Kit (GE Healthcare) and digested with *Eco*RI and *Xho*l at 15-25 ºC. The digested product was inserted in a p-Triptz vector and the ligation reaction was transform into competent bacteria and selected for growth in the presence of ampicillin.

Short hairpin	Template oligonucleotide
Sh FoxA1	5‘TGCTGTTGACAGTGAGCGCGAACACCTACATGACCATGAATAGTGAAGCCACAGATGTATTCATGGTCATGTAGGTGTTCATGCCTACTGCCTCGGA3’
Sh FoxA2	5‘TGCTGTTGACAGTGAGCGAGCCCATTATGAACTCCTCTTATAGTGAAGCCACAGATGTATAAGAGGAGTTCATAATGGGCCTGCCTACTGCCTCGGA3’

The short hairpin sequence sense and antisense are shown in red and blue

Cloning sites	Primers
5`miR30PCRxhoIF	5'CAGAAGGCTCGAGAAGGTATATTGCTGTTGACAGTGAGCG3'
3`miR30PCREcoRIF	5'CTAAAGTAGCCCCTTGAATTCCGAGGCAGTAGGCA3'

Lentiviral production and infection protocol

Constitutive sh-RNA

HEK293T cells were seeded at 80% confluence and after 8-16 hours, were transfected with lentiviral packaging plasmids RSV, VSV-G, RRE and TRC1 sh clone for LIPGb (Sigma Aldrich) in a ratio 1:1:1. 24 hours post infection, the media was collected, and replace. 24 hours later the media was collected again. Viral supernatants were sterilized by passing through a 0,22 µm filter and then concentrated at 18.000 rpm for 2 hrs. Concentrated supernatants were added to recipient cells (MCF7 and MDA-MB-231) seeded at low confluence (20-30%) and infected for 24 hrs in the presence of 8µg/mL polybrene. Cells were then recovered for 24 hrs with fresh media and the selected by 5µg/mL puromycin to obtain a stable resistant population.

Short hairpin	**Sequence**
Sh LIPG # 5	CCGGGCCGCAAGAACCGTTGTAATACTCGAGTATTACAACGGTTC TTGCGGCTTTTTG

Inducible sh-RNA and ORF systems

HEK293T cells were seeded at 80% confluence and after 8-16 hours, were transfected with third generation lentiviral packaging plasmids RTR2, VSV-G, KGP1R and p-Triptz (sh plasmid) or p-lenti (ORF plasmid; Open Biosystem) in a ratio 1:1:3:5. 24 hours post infection, the media was collected, and replace. 24 hours later the media was collected again. Viral supernatants were sterilized by passing through a 0,22 μm filter and then concentrated at 18.000 rpm for 2 hrs. Concentrated supernatants were added to recipient cells (MCF7 and MDA-MB-231) seeded at low confluence (20-30%) and infected for 24 hrs in the presence of 8μg/mL polybrene. Cells were then recovered for 24 hrs with fresh media and the selected by 5μg/mL puromycin (p-triptz backbone) or 5μg/mL hygromicyn (p-lenti backbone) to obtain a stable resistant population.

RNA extraction, cDNA production and RT qPCR analysis

RNA extractions from breast cancer cells, engineered cells grown *in vitro* and FACS sorted cells were done with the Qiagen RNeasy Mini Kit and quantified by Nanodrop. RNA extractions from isolated tumors were done with Trizol reagent (Invitrogene). The RNA from the aqueous phase was then purified with the Qiagen RNeasy Mini Kit and quantified by Nanodrop. cDNA was produced with SuperScript III First-Strand Kit (Invitrogene) following manufacturer´s instructions.

To asses changes in expression of selected genes qRT-PCR was performed using the comparative CT method and ABI Prism Fast 7900 HT instrument (PE Applied Biosystems). Amplification was performed using taqman Gene Expression Assays (applied Biosystems) following manufacturer's instructions. FoxA1, FoxA2, LIPG and 18 S probes were purchased from Taqman Gene expression assays (Applied Biosystems). All assays were done in triplicate and

18 S mRNA was used as an endogenous control for normalization. Results were analyzed by SDS2.3 software (PE Applied Biosystems).

TaqMan probes	References
FoxA1	Hs00270129-m1
FoxA2	Hs00232764-m1
LIPG	Hs00195812-m1
18S	Hs99999901-s1

Western Blot Analysis

Cells were washed with PBS and frozen. For FoxA1 and FoxA2 detection cells were lysed with a buffer containing (10% SDS, 60 mM Tris pH 6,8 and 7% DTT). For LIPG detection cells were lysed using a buffer containing 25 mM Tris-HCl pH 7.4, 25mM NaCl 1% (v/v), Triton X-100, 0,1% SDS, 10 mM NaF, 10 mM PPi, 1mM sodium orthovanadate, 0.5 mM EGTA, 20nM oxadaic acid supplemented with protease and phosphatase inhibitors (Sigma Aldrich). All cell lysates were pipeted several times and later centrifuged at 13200 rpm for 15 min at 4ºC. The supernant was kept as the protein extract. Equal amounts of protein per sample were separated by standard SDS-PAGE and transferred to immobilon membranes (Millipore). The membranes were incubated with PBS-T 0,1% for FoxA1(Millipore) and LIPG (Abcam) or TBS-T 0,1% supplemented with 5% milk for FoxA2 for 30 min at RT to block unspecific antibody binding. FoxA1 (Millipore), FoxA2 (Cell Signaling) and LIPG (Abcam) primary antibodies were incubated overnight at 4ºC. Mouse or rabbit HRP secondary antibodies were used. After antibody incubations membranes were washed at least 3 times for 10 min. Immuno-complex were visualized with Chemiluminescent HRP Substrate kit (Millipore). All primary antibodies were incubated in a dilution 1:1000.

Immunofluorescence of cultures cells

Cells were seeded in glass slides and fixed for 10 min with 4% PFA at room temperature. After this, 3 washes with PBS were done and the cells were incubated with TRITON x-100 0,25% in PBS for 20 min at room temperature. Once again 3 washes were done with PBS and cells were blocked with PBS-BSA 1% for 30 min at room temperature. β-catenin (Transduction Laboratories) primary antibody was diluted in PBS-BSA 1% and added to the cells overnight at 4ºC. After this incubation the cells were washed with PBS 3 times and the secondary antibody was added (in PBS-BSA 1%) and incubated at room temperature for 90 min in the dark. Finally, cells were washed twice with PBS, stained with DAPI, washed once again and mounted for viewing by epifluorescence in a vertical Nikon E1000 microscope and an objective of 60X/1.4 was utilized.

Transcriptomic analysis

RNA sample collection and generation of biotinylated complementary RNA (cRNA) probe were carried out essentially as described in the standard Affymetrix (Santa Clara, CA) GeneChip protocol. Ten micrograms of total RNA was used to prepare cRNA probe using a Custom Superscript Kit (Invitrogen). For expression profiling 25ng of RNA per sample was processed using isothermal amplification SPIA Biotin System (NuGEN technologies). Each sample of the first batch of arrays was hybridized with an Affymetrix Human Gene 1.0 ST microarray at the IRB Barcelona Functional Genomics Laboratory. GeneAtlas Human Genome U-219 array was used in the second batch of arrays.All microarray statistical analyses were performed using Bioconductor (Gentleman et al., 2004). Background correction, quantile normalization and RMA summarization was performed as implemented in bioconductor's affy package.

In the first set of arrays we considered several expression patterns, and classified each gene into one of those expression patterns. The expression pattern analysis presented was performed by fitting the GaGa model (Rossell, 2009). The model was fit to data in via an Expectation-Maximization scheme, as implemented in the Bioconductor gaga package. The Bayesian FDR was

controlled using the optimal Bayesian rule described in (P. Müller, 2004).

In the second set of arrays we a semi-parametric empirical Bayes (Rossell et al., 2008) procedure based on moderated t-tests (Smyth, 2005) as implemented in the limma package was performed to select the differentially expressed genes setting the Bayesian FDR at 5% (Rossell et al., 2008). Additionally, only genes with an absolute fold change value bigger than 2 were considered differentially expressed.

Patient gene expression data sets

The patients' information is publically available and has been downloaded from GEO (Barrett et al. (2007)). The following cohorts was used: MSKCC/EMC. Pooled GSE2603, GSE2034 and GSE12276. This union cohort has 560 patients. In order to remove systematic biases, the expression measurements were converted to z-scores for all genes prior to merging. ER+ patients were selected based on the bimodality of gene ESR1.

FACS sorting of MCF7 and MDA-MB-231 cells

Subcutaneously tumors were removed from mice and a fraction of the tumor was cut into pieces and incubated in buffer containing Collagenase IV (Sigma Aldrich) for 30 min at 37ºC. Samples were further homogenized using an 18G needle and then filtered through a 70 µm mesh filter and centrifuged at 1200 rpm for 5 min at 4ºC. The pellet obtained was incubated in an ammonium chloride buffer for 3 min at room temperature to lyse erythrocytes and then washed and resuspended in DMEM 10% FBS containing 10 µg/mL PI and sorted in a FACS Aria 2.0 (BD). Cells were sorted based on GFP and RFP expression and collected in DMEM 10% FBS. After cell collection total RNA was extracted (Merlos-Suarez et al., 2011).

Metabolomic analysis

Lipid extraction method

The culture medium was removed from cells and the dishes were placed on top of dry ice. Cells were scrapped immediately and metabolites extracted into the extraction solvent by adding 2 mL of a cold mixture of

dichloromethane/methanol (2:1 v/v). The resulting suspension was vortexed and bath-sonicated for 5 minutes. We subsequently added 2 mL of cold water, vortex samples again and organic and aqueous layers were allowed to equilibrate for 10 min at room temperature. Cell lysates were centrifuged (5000 × g, 15 min at 4 °C) and the organic phase (lipidic) was collected and it was dried under a nitrogen stream. For LC-MS analysis lipid pellets were resuspended in 300 µL (acetonitrile: isopropanol: water (65:30:5 v/v).

LC/MS analyses

Untargeted LC/MS analyses were performed using an UHPLC system (1200 series, Agilent Technologies) coupled to a 6540 ESI-QTOF MS (Agilent Technologies) operated in positive (ESI+) or negative (ESI–) electrospray ionization mode. Lipids were separated by reverse phase chromatography with Aquity UPLC C8 (150 x 2.1 mm, 1.8 µm). Mobile phase A = water:acetonitrile (60:40) (10mM ammonium formate and 0.1% formic acid) and B = isopropanol:acetonitrile (95:5) (10mM ammonium formate, 0.1% formic acid and 0.1%H2O). Solvent modifiers such as 0.1% formic acid and 10 mM ammonium formate were used to assist ionization as well as to improve the LC resolution in both positive and negative ionization modes. The elution gradient started at 32% B (time 0–1 min), increased to 60% of B (time 1-4 min) and increased again to 100% B over 11 minutes (time 4-15 min). The injection volume was 2 µL. ESI conditions: gas temperature, 150 °C; drying gas, 13 L min–1; nebulizer, 35 psig; fragmentor, 400 V; and skimmer, 65 V. The instrument was set to acquire over the m/z range 50–1200 with an acquisition rate of 3 spectra/sec.

For compound identification, MS/MS analyses were performed in targeted mode, and the instrument set to acquire over the m/z range 50–1000, with a default iso width (the width half-maximum of the quadrupole mass bandpass used during MS/MS precursor isolation) of 4 m/z. The collision energy was fixed at 20 V.

Data analysis

LC/MS (ESI+ and ESI− mode) data were processed using the XCMS (Smith et al., 2006) software to detect and align features. A feature is defined as a

molecular entity with a unique m/z and a specific retention time. XCMS analysis of these data provided a matrix containing the retention time, m/z value, and integrated peak area of each feature for every cell sample. This matrix was subsequently imported into Matlab (version 6.5.1, Release 13, The Mathworks, 2003) where we constrained the initial number of features according to the following criteria: only features detected in 80% of samples in at least one group above an intensity threshold of 500 counts were retained for further statistical analysis. We normalized peak intensities to cell fresh weight to account for cell number differences. Then, based on metabolic features intensities we compared sh LIPG and sh control groups using Welch's t-test in either MCF7 or MDA cell types. Those metabolic features resulting differentially regulated in any of the cell types were ($p<0.01$ and fold>2) were retained for further tandem MS characterization. Identification of lipidic structures was performed by matching tandem MS spectra against reference standards in LIPIDMAPS (Fahy et al., 2007), database. Additionally, to expand our database of tandem MS spectra for lipids, we used LipidBlast (Kind et al., 2013), a recently launched computer-generated in-silico MS/MS spectral database.

Animal studies

All animal work was done in accordance with a protocol approved by the institutional Animal Care and Use committee.

Subcutaneous xenograft transplantation assay

For subcutaneous implanted tumor assays, cells were harvested by trypsinization, washed twice with PBS, and counted. Cells were resuspended in 50 µl growth factor reduced Mtrigel. Female nude-beige (NIH-bg-nu-xidBR) mice 4-6 weeks old were administrated with and without doxycycline in drinking water all over the experiment. After the first week of doxycyline treatment mice were anesthetized using a cocktail of 100mg/kg ketamine and 10 mg/kg xylazine. A cell suspension of $1X10^6$ cells resuspended in matrix growth factor reduced (BD Bioscience) were inoculated subcutaneously, 4 tumor per mice in the FoxA rescues experiments and 2 tumors per animal in the LIPG rescues. Tumor growth was monitored weekly. An estrogen pellet was implanted in mice injected with MCF7 cells (ER+).

Tumor growth rates were analyzed by measuring tumor length (L) and width (W), and calculating tumor volume based on the formula$Volume = \pi LW^2/6$.

Mice were sacrificed and tumors were extracted. A fraction of the tumor was fixed with 4% of paraformaldehyde and paraffin-embedded for immunohistologic staining. Another fraction was directly frozen in dry ice for protein and RNA extraction.

Lung seeding injections and bioluminescent imaging and analysis

Cells were harvested by trypsinization, washed twice with PBS, and counted. Cells were resuspended PBS and cells were injected into the lateral tail vein from Female nude-beige (NIH-bg-nu-xidBR) mice 4-6 weeks old administrated with doxycycline in drinking water one week before the injection and all over the experiment. Growth rate in the lung/pleura was measured as a function of lung photon flux normalized to day 0 in live animals. In order to detect luciferase activity, 1,5 mg of d-luciferin (luciferase substrate at 15mg/mL in serum) was injected retro-orbital. Imaging was completed between 2-5 min after injection with a Xenogen IVIS-2000 imaging system coupled to living Image acquisition and analysis software (Xenogen). At day 0 mice were imaged for luciferase activity immediately after injection to exclude any that were not successfully xenografted. Tumor development and metastasis was monitored by weekly bioluminescence imaging as previously described. For bioluminescence plots, photon flux was calculated for each mouse by using a circular region of interest encompassing the lung of the mouse. This value was scaled to a comparable background value (from an area of the mouse without lesion), and then normalized to the value obtained immediately after xenografting at the same area (day 0). An arbitrary starting Bioluminiscence signal of 1000 was established in all assays. Each mouse was counted as 1 sample of a total of 5.

Sadistic analysis

All values were expressed as the mean ± SD, and the p-value was calculated by T-test.

References

Aad, G., Abajyan, T., Abbott, B., Abdallah, J., Abdel Khalek, S., Abdelalim, A.A., Abdinov, O., Aben, R., Abi, B., Abolins, M.*, et al.* (2012). Search for magnetic monopoles in sqrt[s]=7 TeV pp collisions with the ATLAS detector. Phys Rev Lett *109*, 261803.

Algire, C., Amrein, L., Bazile, M., David, S., Zakikhani, M., and Pollak, M. (2011). Diet and tumor LKB1 expression interact to determine sensitivity to anti-neoplastic effects of metformin in vivo. Oncogene *30*, 1174-1182.

Altenberg, B., and Greulich, K.O. (2004). Genes of glycolysis are ubiquitously overexpressed in 24 cancer classes. Genomics *84*, 1014-1020.

Anderson, W.F., Chatterjee, N., Ershler, W.B., and Brawley, O.W. (2002). Estrogen receptor breast cancer phenotypes in the Surveillance, Epidemiology, and End Results database. Breast cancer research and treatment *76*, 27-36.

Anisimov, V.N., Berstein, L.M., Egormin, P.A., Piskunova, T.S., Popovich, I.G., Zabezhinski, M.A., Kovalenko, I.G., Poroshina, T.E., Semenchenko, A.V., Provinciali, M.*, et al.* (2005). Effect of metformin on life span and on the development of spontaneous mammary tumors in HER-2/neu transgenic mice. Experimental gerontology *40*, 685-693.

Baselga, J., Perez, E.A., Pienkowski, T., and Bell, R. (2006). Adjuvant trastuzumab: a milestone in the treatment of HER-2-positive early breast cancer. The oncologist *11 Suppl 1*, 4-12.

Bauer, D.E., Hatzivassiliou, G., Zhao, F., Andreadis, C., and Thompson, C.B. (2005). ATP citrate lyase is an important component of cell growth and transformation. Oncogene *24*, 6314-6322.

Bensaad, K., Tsuruta, A., Selak, M.A., Vidal, M.N., Nakano, K., Bartrons, R., Gottlieb, E., and Vousden, K.H. (2006). TIGAR, a p53-inducible regulator of glycolysis and apoptosis. Cell *126*, 107-120.

Bernardo, G.M., Lozada, K.L., Miedler, J.D., Harburg, G., Hewitt, S.C., Mosley, J.D., Godwin, A.K., Korach, K.S., Visvader, J.E., Kaestner, K.H.*, et al.* (2010). FOXA1 is an essential determinant of ERalpha expression and mammary ductal morphogenesis. Development *137*, 2045-2054.

Bochkis, I.M., Schug, J., Rubins, N.E., Chopra, A.R., O'Malley, B.W., and Kaestner, K.H. (2009). Foxa2-dependent hepatic gene regulatory networks depend on physiological state. Physiological genomics *38*, 186-195.

Broedl, U.C., Maugeais, C., Marchadier, D., Glick, J.M., and Rader, D.J. (2003). Effects of nonlipolytic ligand function of endothelial lipase on high density lipoprotein metabolism in vivo. The Journal of biological chemistry *278*, 40688-40693.

Brusselmans, K., De Schrijver, E., Verhoeven, G., and Swinnen, J.V. (2005). RNA interference-mediated silencing of the acetyl-CoA-carboxylase-alpha gene induces growth inhibition and apoptosis of prostate cancer cells. Cancer research *65*, 6719-6725.

Buzzai, M., Bauer, D.E., Jones, R.G., Deberardinis, R.J., Hatzivassiliou, G., Elstrom, R.L., and Thompson, C.B. (2005). The glucose dependence of Akt-transformed cells can be reversed by pharmacologic activation of fatty acid beta-oxidation. Oncogene *24*, 4165-4173.

Cairns, R.A., Harris, I.S., and Mak, T.W. (2011). Regulation of cancer cell metabolism. Nature reviews Cancer *11*, 85-95.

Cantor, J.R., and Sabatini, D.M. (2012). Cancer cell metabolism: one hallmark, many faces. Cancer discovery *2*, 881-898.

Carlsson, P., and Mahlapuu, M. (2002). Forkhead transcription factors: key players in development and metabolism. Developmental biology *250*, 1-23.

Carrasco, S., and Merida, I. (2007). Diacylglycerol, when simplicity becomes complex. Trends in biochemical sciences *32*, 27-36.

Cui, X., Schiff, R., Arpino, G., Osborne, C.K., and Lee, A.V. (2005). Biology of progesterone receptor loss in breast cancer and its implications for endocrine therapy. Journal of clinical oncology : official journal of the American Society of Clinical Oncology *23*, 7721-7735.

(CGAN) The Cancer Genome Atlas Network, (2012). Comprehensive molecular portraits of human breast tumours. Nature *490*, 61-70.

Chajes, V., Cambot, M., Moreau, K., Lenoir, G.M., and Joulin, V. (2006). Acetyl-CoA carboxylase alpha is essential to breast cancer cell survival. Cancer research *66*, 5287-5294.

Chaneton, B., and Gottlieb, E. (2012). Rocking cell metabolism: revised functions of the key glycolytic regulator PKM2 in cancer. Trends in biochemical sciences *37*, 309-316.

Choi, S.Y. (2002). Endothelial lipase: a new lipase on the block. The Journal of Lipid Research *43*, 1763-1769.

Christofk, H.R., Vander Heiden, M.G., Harris, M.H., Ramanathan, A., Gerszten, R.E., Wei, R., Fleming, M.D., Schreiber, S.L., and Cantley, L.C. (2008). The M2 splice isoform of pyruvate kinase is important for cancer metabolism and tumour growth. Nature *452*, 230-233.

Chughtai, K., Jiang, L., Greenwood, T.R., Glunde, K., and Heeren, R.M. (2013). Mass spectrometry images acylcarnitines, phosphatidylcholines, and sphingomyelin in MDA-MB-231 breast tumor models. Journal of lipid research *54*, 333-344.

Davies, H., Bignell, G.R., Cox, C., Stephens, P., Edkins, S., Clegg, S., Teague, J., Woffendin, H., Garnett, M.J., Bottomley, W.*, et al.* (2002). Mutations of the BRAF gene in human cancer. Nature *417*, 949-954.

De Schrijver, E., Brusselmans, K., Heyns, W., Verhoeven, G., and Swinnen, J.V. (2003). RNA interference-mediated silencing of the fatty acid synthase gene attenuates growth and induces morphological changes and apoptosis of LNCaP prostate cancer cells. Cancer research *63*, 3799-3804.

DeBerardinis, R.J., Lum, J.J., Hatzivassiliou, G., and Thompson, C.B. (2008). The biology of cancer: metabolic reprogramming fuels cell growth and proliferation. Cell metabolism *7*, 11-20.

Doane, A.S., Danso, M., Lal, P., Donaton, M., Zhang, L., Hudis, C., and Gerald, W.L. (2006). An estrogen receptor-negative breast cancer subset characterized by a hormonally regulated transcriptional program and response to androgen. Oncogene *25*, 3994-4008.

Dowling, R.J., Niraula, S., Stambolic, V., and Goodwin, P.J. (2012). Metformin in cancer: translational challenges. Journal of molecular endocrinology *48*, R31-43.

Duvel, K., Yecies, J.L., Menon, S., Raman, P., Lipovsky, A.I., Souza, A.L., Triantafellow, E., Ma, Q., Gorski, R., Cleaver, S.*, et al.* (2010). Activation of a metabolic gene regulatory network downstream of mTOR complex 1. Molecular cell *39*, 171-183.

Dykens, J.A., Jamieson, J., Marroquin, L., Nadanaciva, S., Billis, P.A., and Will, Y. (2008). Biguanide-induced mitochondrial dysfunction yields increased lactate production and cytotoxicity of aerobically-poised HepG2 cells and human hepatocytes in vitro. Toxicology and applied pharmacology *233*, 203-210.

Edinger, A.L., and Thompson, C.B. (2002). Akt maintains cell size and survival by increasing mTOR-dependent nutrient uptake. Molecular biology of the cell *13*, 2276-2288.

Egan, D.F., Shackelford, D.B., Mihaylova, M.M., Gelino, S., Kohnz, R.A., Mair, W., Vasquez, D.S., Joshi, A., Gwinn, D.M., Taylor, R.*, et al.* (2011). Phosphorylation of ULK1 (hATG1) by AMP-activated protein kinase connects energy sensing to mitophagy. Science *331*, 456-461.

El-Mir, M.Y., Nogueira, V., Fontaine, E., Averet, N., Rigoulet, M., and Leverve, X. (2000). Dimethylbiguanide inhibits cell respiration via an indirect effect targeted on the respiratory chain complex I. The Journal of biological chemistry *275*, 223-228.

El Mjiyad, N., Caro-Maldonado, A., Ramirez-Peinado, S., and Munoz-Pinedo, C. (2011). Sugar-free approaches to cancer cell killing. Oncogene *30*, 253-264.

Elenbaas, B., Spirio, L., Koerner, F., Fleming, M.D., Zimonjic, D.B., Donaher, J.L., Popescu, N.C., Hahn, W.C., and Weinberg, R.A. (2001). Human breast

cancer cells generated by oncogenic transformation of primary mammary epithelial cells. Genes & development *15*, 50-65.

Elstrom, R.L., Bauer, D.E., Buzzai, M., Karnauskas, R., Harris, M.H., Plas, D.R., Zhuang, H., Cinalli, R.M., Alavi, A., Rudin, C.M*., et al.* (2004). Akt stimulates aerobic glycolysis in cancer cells. Cancer research *64*, 3892-3899.

Fabiana Schwartzenberg-Bar-Yoseph F, A.M., Karnieli E (2004). The tumor supressor p53 down regulates glucose transporters GLUT1 and GLUT4 gene expression. Cancer research *64*, 2627-2633.

Fahy, E., Sud, M., Cotter, D., and Subramaniam, S. (2007). LIPID MAPS online tools for lipid research. Nucleic acids research *35*, W606-612.

Farmer, P., Bonnefoi, H., Becette, V., Tubiana-Hulin, M., Fumoleau, P., Larsimont, D., Macgrogan, G., Bergh, J., Cameron, D., Goldstein, D*., et al.* (2005). Identification of molecular apocrine breast tumours by microarray analysis. Oncogene *24*, 4660-4671.

Ferri, A.L., Lin, W., Mavromatakis, Y.E., Wang, J.C., Sasaki, H., Whitsett, J.A., and Ang, S.L. (2007). Foxa1 and Foxa2 regulate multiple phases of midbrain dopaminergic neuron development in a dosage-dependent manner. Development *134*, 2761-2769.

Friedman, J.R., and Kaestner, K.H. (2006). The Foxa family of transcription factors in development and metabolism. Cellular and molecular life sciences : CMLS *63*, 2317-2328.

Fujimori, K., and Amano, F. (2011). Forkhead transcription factor Foxa1 is a novel target gene of C/EBPbeta and suppresses the early phase of adipogenesis. Gene *473*, 150-156.

Fuki, I.V., Blanchard, N., Jin, W., Marchadier, D.H., Millar, J.S., Glick, J.M., and Rader, D.J. (2003). Endogenously produced endothelial lipase enhances binding and cellular processing of plasma lipoproteins via heparan sulfate proteoglycan-mediated pathway. The Journal of biological chemistry *278*, 34331-34338.

Gao, N., Le Lay, J., Qin, W., Doliba, N., Schug, J., Fox, A.J., Smirnova, O., Matschinsky, F.M., and Kaestner, K.H. (2010). Foxa1 and Foxa2 maintain the metabolic and secretory features of the mature beta-cell. Mol Endocrinol *24*, 1594-1604.

Gao, N., LeLay, J., Vatamaniuk, M.Z., Rieck, S., Friedman, J.R., and Kaestner, K.H. (2008). Dynamic regulation of Pdx1 enhancers by Foxa1 and Foxa2 is essential for pancreas development. Genes & development *22*, 3435-3448.

Gao, N., Zhang, J., Rao, M.A., Case, T.C., Mirosevich, J., Wang, Y., Jin, R., Gupta, A., Rennie, P.S., and Matusik, R.J. (2003). The role of hepatocyte nuclear factor-3 alpha (Forkhead Box A1) and androgen receptor in transcriptional regulation of prostatic genes. Mol Endocrinol *17*, 1484-1507.

Gao, P., Tchernyshyov, I., Chang, T.C., Lee, Y.S., Kita, K., Ochi, T., Zeller, K.I., De Marzo, A.M., Van Eyk, J.E., Mendell, J.T.*, et al.* (2009). c-Myc suppression of miR-23a/b enhances mitochondrial glutaminase expression and glutamine metabolism. Nature *458*, 762-765.

Garten, A., Petzold, S., Korner, A., Imai, S., and Kiess, W. (2009). Nampt: linking NAD biology, metabolism and cancer. Trends in endocrinology and metabolism: TEM *20*, 130-138.

Gaudet, J., and Mango, S.E. (2002). Regulation of organogenesis by the Caenorhabditis elegans FoxA protein PHA-4. Science *295*, 821-825.

Gentleman, R.C., Carey, V.J., Bates, D.M., Bolstad, B., Dettling, M., Dudoit, S., Ellis, B., Gautier, L., Ge, Y., Gentry, J.*, et al.* (2004). Bioconductor: open software development for computational biology and bioinformatics. Genome biology *5*, R80.

Gingras, A.C., Raught, B., and Sonenberg, N. (2001). Regulation of translation initiation by FRAP/mTOR. Genes & development *15*, 807-826.

Guo, J.Y., Chen, H.Y., Mathew, R., Fan, J., Strohecker, A.M., Karsli-Uzunbas, G., Kamphorst, J.J., Chen, G., Lemons, J.M., Karantza, V.*, et al.* (2011). Activated Ras requires autophagy to maintain oxidative metabolism and tumorigenesis. Genes & development *25*, 460-470.

Gupta, G.P., Nguyen, D.X., Chiang, A.C., Bos, P.D., Kim, J.Y., Nadal, C., Gomis, R.R., Manova-Todorova, K., and Massague, J. (2007). Mediators of vascular remodelling co-opted for sequential steps in lung metastasis. Nature *446*, 765-770.

Hanahan, D., and Weinberg, R.A. (2011). Hallmarks of cancer: the next generation. Cell *144*, 646-674.

Hatzivassiliou, G., Zhao, F., Bauer, D.E., Andreadis, C., Shaw, A.N., Dhanak, D., Hingorani, S.R., Tuveson, D.A., and Thompson, C.B. (2005). ATP citrate lyase inhibition can suppress tumor cell growth. Cancer cell *8*, 311-321.

Hawley, S.A., Ross, F.A., Chevtzoff, C., Green, K.A., Evans, A., Fogarty, S., Towler, M.C., Brown, L.J., Ogunbayo, O.A., Evans, A.M.*, et al.* (2010). Use of cells expressing gamma subunit variants to identify diverse mechanisms of AMPK activation. Cell metabolism *11*, 554-565.

Hemminki, A., Markie, D., Tomlinson, I., Avizienyte, E., Roth, S., Loukola, A., Bignell, G., Warren, W., Aminoff, M., Hoglund, P.*, et al.* (1998). A serine/threonine kinase gene defective in Peutz-Jeghers syndrome. Nature *391*, 184-187.

Hirata, K., Ishida, T., Matsushita, H., Tsao, P.S., and Quertermous, T. (2000). Regulated expression of endothelial cell-derived lipase. Biochemical and biophysical research communications *272*, 90-93.

Hirata, K.i. (1999). Cloning of a Unique Lipase from Endothelial Cells Extends the Lipase Gene Family. Journal of Biological Chemistry *274*, 14170-14175.

Hirsch, E., Ciraolo, E., Franco, I., Ghigo, A., and Martini, M. (2013). PI3K in cancer-stroma interactions: bad in seed and ugly in soil. Oncogene.

Hitosugi, T., Zhou, L., Elf, S., Fan, J., Kang, H.B., Seo, J.H., Shan, C., Dai, Q., Zhang, L., Xie, J.*, et al.* (2012). Phosphoglycerate mutase 1 coordinates glycolysis and biosynthesis to promote tumor growth. Cancer cell *22*, 585-600.

Holness, M.J., and Sugden, M.C. (2003). Regulation of pyruvate dehydrogenase complex activity by reversible phosphorylation. Biochemical Society transactions *31*, 1143-1151.

Huang, X., Wullschleger, S., Shpiro, N., McGuire, V.A., Sakamoto, K., Woods, Y.L., McBurnie, W., Fleming, S., and Alessi, D.R. (2008). Important role of the LKB1-AMPK pathway in suppressing tumorigenesis in PTEN-deficient mice. The Biochemical journal *412*, 211-221.

Hurtado, A., Holmes, K.A., Ross-Innes, C.S., Schmidt, D., and Carroll, J.S. (2011). FOXA1 is a key determinant of estrogen receptor function and endocrine response. Nature genetics *43*, 27-33.

Inoki, K., Zhu, T., and Guan, K.L. (2003). TSC2 mediates cellular energy response to control cell growth and survival. Cell *115*, 577-590.

Isaacs, J.S., Jung, Y.J., Mole, D.R., Lee, S., Torres-Cabala, C., Chung, Y.L., Merino, M., Trepel, J., Zbar, B., Toro, J.*, et al.* (2005). HIF overexpression correlates with biallelic loss of fumarate hydratase in renal cancer: novel role of fumarate in regulation of HIF stability. Cancer cell *8*, 143-153.

Ishida, T., Choi, S., Kundu, R.K., Hirata, K.-i., Rubin, E.M., Cooper, A.D., and Quertermous, T. (2003). Endothelial lipase is a major determinant of HDL level. Journal of Clinical Investigation *111*, 347-355.

Jain, R.K., Mehta, R.J., Nakshatri, H., Idrees, M.T., and Badve, S.S. (2011). High-level expression of forkhead-box protein A1 in metastatic prostate cancer. Histopathology *58*, 766-772.

Jaye, M., Lynch, K.J., Krawiec, J., Marchadier, D., Maugeais, C., Doan, K., South, V., Amin, D., Perrone, M., and Rader, D.J. (1999). A novel endothelial-derived lipase that modulates HDL metabolism. Nature genetics *21*, 424-428.

Jemal, A., Bray, F., Center, M.M., Ferlay, J., Ward, E., and Forman, D. (2011). Global cancer statistics. CA: a cancer journal for clinicians *61*, 69-90.

Jemal, A., Siegel, R., Ward, E., Hao, Y., Xu, J., Murray, T., and Thun, M.J. (2008). Cancer statistics, 2008. CA: a cancer journal for clinicians *58*, 71-96.

Jeon, S.M., Chandel, N.S., and Hay, N. (2012). AMPK regulates NADPH homeostasis to promote tumour cell survival during energy stress. Nature *485*, 661-665.

Jiang, J.K., Boxer, M.B., Vander Heiden, M.G., Shen, M., Skoumbourdis, A.P., Southall, N., Veith, H., Leister, W., Austin, C.P., Park, H.W.*, et al.* (2010). Evaluation of thieno[3,2-b]pyrrole[3,2-d]pyridazinones as activators of the tumor cell specific M2 isoform of pyruvate kinase. Bioorganic & medicinal chemistry letters *20*, 3387-3393.

Jiang, P., Du, W., Wang, X., Mancuso, A., Gao, X., Wu, M., and Yang, X. (2011). p53 regulates biosynthesis through direct inactivation of glucose-6-phosphate dehydrogenase. Nature cell biology *13*, 310-316.

Jin, W., Fuki, I.V., Seidah, N.G., Benjannet, S., Glick, J.M., and Rader, D.J. (2005). Proprotein convertases [corrected] are responsible for proteolysis and inactivation of endothelial lipase. The Journal of biological chemistry *280*, 36551-36559.

Jin, W., Millar, J.S., Broedl, U., Glick, J.M., and Rader, D.J. (2003a). Inhibition of endothelial lipase causes increased HDL cholesterol levels in vivo. J Clin Invest *111*, 357-362.

Jin, W., Sun, G.S., Marchadier, D., Octtaviani, E., Glick, J.M., and Rader, D.J. (2003b). Endothelial cells secrete triglyceride lipase and phospholipase activities in response to cytokines as a result of endothelial lipase. Circulation research *92*, 644-650.

Jin, W., Wang, X., Millar, J.S., Quertermous, T., Rothblat, G.H., Glick, J.M., and Rader, D.J. (2007). Hepatic proprotein convertases modulate HDL metabolism. Cell metabolism *6*, 129-136.

Kaestner, K.H. (2000). The hepatocyte nuclear factor 3 (HNF3 or FOXA) family in metabolism. Trends in endocrinology and metabolism: TEM *11*, 281-285.

Kaestner, K.H. (2010). The FoxA factors in organogenesis and differentiation. Current opinion in genetics & development *20*, 527-532.

Kaestner, K.H., Katz, J., Liu, Y., Drucker, D.J., and Schutz, G. (1999). Inactivation of the winged helix transcription factor HNF3alpha affects glucose homeostasis and islet glucagon gene expression in vivo. Genes & development *13*, 495-504.

Kelly, P.N., and Strasser, A. (2011). The role of Bcl-2 and its pro-survival relatives in tumourigenesis and cancer therapy. Cell death and differentiation *18*, 1414-1424.

Khoor, A., Stahlman, M.T., Johnson, J.M., Olson, S.J., and Whitsett, J.A. (2004). Forkhead box A2 transcription factor is expressed in all types of neuroendocrine lung tumors. Human pathology *35*, 560-564.

Kim, J., and DeBerardinis, R.J. (2013). Cancer. Silencing a metabolic oncogene. Science *340*, 558-559.

Kind, T., Liu, K.H., Lee do, Y., DeFelice, B., Meissen, J.K., and Fiehn, O. (2013). LipidBlast in silico tandem mass spectrometry database for lipid identification. Nature methods *10*, 755-758.

Kittappa, R., Chang, W.W., Awatramani, R.B., and McKay, R.D. (2007). The foxa2 gene controls the birth and spontaneous degeneration of dopamine neurons in old age. PLoS biology *5*, e325.

Kondoh, H., Lleonart, M.E., Gil, J., Wang, J., Degan, P., Peters, G., Martinez, D., Carnero, A., and Beach, D. (2005). glycoloytic enzymes can modulate cellular life span. Cancer research *65*.

Koppenol, W.H., Bounds, P.L., and Dang, C.V. (2011). Otto Warburg's contributions to current concepts of cancer metabolism. Nature reviews Cancer *11*, 325-337.

Kroemer, G., and Pouyssegur, J. (2008). Tumor cell metabolism: cancer's Achilles' heel. Cancer cell *13*, 472-482.

Laplante, M., and Sabatini, D.M. (2012). mTOR signaling in growth control and disease. Cell *149*, 274-293.

Le, A., Lane, A.N., Hamaker, M., Bose, S., Gouw, A., Barbi, J., Tsukamoto, T., Rojas, C.J., Slusher, B.S., Zhang, H.*, et al.* (2012). Glucose-independent glutamine metabolism via TCA cycling for proliferation and survival in B cells. Cell metabolism *15*, 110-121.

Lee, C.S., Friedman, J.R., Fulmer, J.T., and Kaestner, K.H. (2005). The initiation of liver development is dependent on Foxa transcription factors. Nature *435*, 944-947.

Lehner, F., Kulik, U., Klempnauer, J., and Borlak, J. (2007). The hepatocyte nuclear factor 6 (HNF6) and FOXA2 are key regulators in colorectal liver metastases. FASEB journal : official publication of the Federation of American Societies for Experimental Biology *21*, 1445-1462.

Li, L., Ying, J., Li, H., Zhang, Y., Shu, X., Fan, Y., Tan, J., Cao, Y., Tsao, S.W., Srivastava, G.*, et al.* (2012). The human cadherin 11 is a pro-apoptotic tumor suppressor modulating cell stemness through Wnt/beta-catenin signaling and silenced in common carcinomas. Oncogene *31*, 3901-3912.

Lim, E., Vaillant, F., Wu, D., Forrest, N.C., Pal, B., Hart, A.H., Asselin-Labat, M.L., Gyorki, D.E., Ward, T., Partanen, A.*, et al.* (2009). Aberrant luminal progenitors as the candidate target population for basal tumor development in BRCA1 mutation carriers. Nature medicine *15*, 907-913.

Lin, W., Metzakopian, E., Mavromatakis, Y.E., Gao, N., Balaskas, N., Sasaki, H., Briscoe, J., Whitsett, J.A., Goulding, M., Kaestner, K.H.*, et al.* (2009). Foxa1 and Foxa2 function both upstream of and cooperatively with Lmx1a and Lmx1b in a feedforward loop promoting mesodiencephalic dopaminergic neuron development. Developmental biology *333*, 386-396.

Liu, S., Murph, M., Panupinthu, N., and Mills, G.B. (2009a). ATX-LPA receptor axis in inflammation and cancer. Cell Cycle *8*, 3695-3701.

Liu, S., Umezu-Goto, M., Murph, M., Lu, Y., Liu, W., Zhang, F., Yu, S., Stephens, L.C., Cui, X., Murrow, G.*, et al.* (2009b). Expression of autotaxin and lysophosphatidic acid receptors increases mammary tumorigenesis, invasion, and metastases. Cancer cell *15*, 539-550.

Locasale, J.W., Grassian, A.R., Melman, T., Lyssiotis, C.A., Mattaini, K.R., Bass, A.J., Heffron, G., Metallo, C.M., Muranen, T., Sharfi, H.*, et al.* (2011). Phosphoglycerate dehydrogenase diverts glycolytic flux and contributes to oncogenesis. Nature genetics *43*, 869-874.

Louie, S.M., Roberts, L.S., Mulvihill, M.M., Luo, K., and Nomura, D.K. (2013). Cancer cells incorporate and remodel exogenous palmitate into structural and oncogenic signaling lipids. Biochimica et biophysica acta.

Lum, J.J., Bui, T., Gruber, M., Gordan, J.D., DeBerardinis, R.J., Covello, K.L., Simon, M.C., and Thompson, C.B. (2007). The transcription factor HIF-1alpha plays a critical role in the growth factor-dependent regulation of both aerobic and anaerobic glycolysis. Genes & development *21*, 1037-1049.

Lunt, S.Y., and Vander Heiden, M.G. (2011). Aerobic glycolysis: meeting the metabolic requirements of cell proliferation. Annual review of cell and developmental biology *27*, 441-464.

Luo, W., Hu, H., Chang, R., Zhong, J., Knabel, M., O'Meally, R., Cole, R.N., Pandey, A., and Semenza, G.L. (2011). Pyruvate kinase M2 is a PHD3-stimulated coactivator for hypoxia-inducible factor 1. Cell *145*, 732-744.

Ma, K., Cilingiroglu, M., Otvos, J.D., Ballantyne, C.M., Marian, A.J., and Chan, L. (2003). Endothelial lipase is a major genetic determinant for high-density lipoprotein concentration, structure, and metabolism. Proceedings of the National Academy of Sciences of the United States of America *100*, 2748-2753.

Mani, S.A., Guo, W., Liao, M.J., Eaton, E.N., Ayyanan, A., Zhou, A.Y., Brooks, M., Reinhard, F., Zhang, C.C., Shipitsin, M.*, et al.* (2008). The epithelial-mesenchymal transition generates cells with properties of stem cells. Cell *133*, 704-715.

Mardis, E.R., Ding, L., Dooling, D.J., Larson, D.E., McLellan, M.D., Chen, K., Koboldt, D.C., Fulton, R.S., Delehaunty, K.D., McGrath, S.D.*, et al.* (2009). Recurring mutations found by sequencing an acute myeloid leukemia genome. The New England journal of medicine *361*, 1058-1066.

Maugeais, C., Tietge, U.J., Broedl, U.C., Marchadier, D., Cain, W., McCoy, M.G., Lund-Katz, S., Glick, J.M., and Rader, D.J. (2003). Dose-dependent acceleration of high-density lipoprotein catabolism by endothelial lipase. Circulation *108*, 2121-2126.

McCoy, M.G., Sun, G.S., Marchadier, D., Maugeais, C., Glick, J.M., and Rader, D.J. (2002). Characterization of the lipolytic activity of endothelial lipase. Journal of lipid research *43*, 921-929.

Mehta, R.J., Jain, R.K., Leung, S., Choo, J., Nielsen, T., Huntsman, D., Nakshatri, H., and Badve, S. (2012). FOXA1 is an independent prognostic marker for ER-positive breast cancer. Breast cancer research and treatment *131*, 881-890.

Memmott, R.M., Mercado, J.R., Maier, C.R., Kawabata, S., Fox, S.D., and Dennis, P.A. (2010). Metformin prevents tobacco carcinogen--induced lung tumorigenesis. Cancer Prev Res (Phila) *3*, 1066-1076.

Menendez, J.A., and Lupu, R. (2007). Fatty acid synthase and the lipogenic phenotype in cancer pathogenesis. Nature reviews Cancer *7*, 763-777.

Merlos-Suarez, A., Barriga, F.M., Jung, P., Iglesias, M., Cespedes, M.V., Rossell, D., Sevillano, M., Hernando-Momblona, X., da Silva-Diz, V., Munoz, P.*, et al.* (2011). The intestinal stem cell signature identifies colorectal cancer stem cells and predicts disease relapse. Cell stem cell *8*, 511-524.

Mills, G.B., and Moolenaar, W.H. (2003). The emerging role of lysophosphatidic acid in cancer. Nature reviews Cancer *3*, 582-591.

Minn, A.J., Gupta, G.P., Siegel, P.M., Bos, P.D., Shu, W., Giri, D.D., Viale, A., Olshen, A.B., Gerald, W.L., and Massague, J. (2005). Genes that mediate breast cancer metastasis to lung. Nature *436*, 518-524.

Molyneux, G., Geyer, F.C., Magnay, F.A., McCarthy, A., Kendrick, H., Natrajan, R., Mackay, A., Grigoriadis, A., Tutt, A., Ashworth, A.*, et al.* (2010). BRCA1 basal-like breast cancers originate from luminal epithelial progenitors and not from basal stem cells. Cell stem cell *7*, 403-417.

Morad, S.A., and Cabot, M.C. (2013). Ceramide-orchestrated signalling in cancer cells. Nature reviews Cancer *13*, 51-65.

Moya, M., Benet, M., Guzman, C., Tolosa, L., Garcia-Monzon, C., Pareja, E., Castell, J.V., and Jover, R. (2012). Foxa1 reduces lipid accumulation in human hepatocytes and is down-regulated in nonalcoholic fatty liver. PloS one *7*, e30014.

Mulvihill, M.M., and Nomura, D.K. (2013). Therapeutic potential of monoacylglycerol lipase inhibitors. Life sciences *92*, 492-497.

Network, T.C.G.A. (2012). Comprehensive molecular portraits of human breast tumours. Nature *490*, 61-70.

Ni, M., Chen, Y., Lim, E., Wimberly, H., Bailey, S.T., Imai, Y., Rimm, D.L., Liu, X.S., and Brown, M. (2011). Targeting androgen receptor in estrogen receptor-negative breast cancer. Cancer cell *20*, 119-131.

Nijstad, N., Wiersma, H., Gautier, T., van der Giet, M., Maugeais, C., and Tietge, U.J. (2009). Scavenger receptor BI-mediated selective uptake is required for the remodeling of high density lipoprotein by endothelial lipase. The Journal of biological chemistry *284*, 6093-6100.

Nomura, D.K., Long, J.Z., Niessen, S., Hoover, H.S., Ng, S.W., and Cravatt, B.F. (2010). Monoacylglycerol lipase regulates a fatty acid network that promotes cancer pathogenesis. Cell *140*, 49-61.

Ochi, N., Tanasanvimon, S., Matsuo, Y., Tong, Z., Sung, B., Aggarwal, B.B., Sinnett-Smith, J., Rozengurt, E., and Guha, S. (2011). Protein kinase D1 promotes anchorage-independent growth, invasion, and angiogenesis by human pancreatic cancer cells. Journal of cellular physiology *226*, 1074-1081.

Owen, M.R., Doran, E., and Halestrap, A.P. (2000). Evidence that metformin exerts its anti-diabetic effects through inhibition of complex 1 of the mitochondrial respiratory chain. The Biochemical journal *348 Pt 3*, 607-614.

P. Müller, G.P., C. Robert, and J. Rousseau (2004). Optimal sample size for multiple testing: the case of gene expression microarrays. Journal of the American Statistical Association, 990–1001.

Paddison, P.J., Cleary, M., Silva, J.M., Chang, K., Sheth, N., Sachidanandam, R., and Hannon, G.J. (2004). Cloning of short hairpin RNAs for gene knockdown in mammalian cells. Nature methods *1*, 163-167.

Papandreou, I., Cairns, R.A., Fontana, L., Lim, A.L., and Denko, N.C. (2006). HIF-1 mediates adaptation to hypoxia by actively downregulating mitochondrial oxygen consumption. Cell metabolism *3*, 187-197.

Parsons, D.W., Jones, S., Zhang, X., Lin, J.C., Leary, R.J., Angenendt, P., Mankoo, P., Carter, H., Siu, I.M., Gallia, G.L.*, et al.* (2008). An integrated genomic analysis of human glioblastoma multiforme. Science *321*, 1807-1812.

Perou, C.M., Jeffrey, S.S., van de Rijn, M., Rees, C.A., Eisen, M.B., Ross, D.T., Pergamenschikov, A., Williams, C.F., Zhu, S.X., Lee, J.C.*, et al.* (1999). Distinctive gene expression patterns in human mammary epithelial cells and breast cancers. Proceedings of the National Academy of Sciences of the United States of America *96*, 9212-9217.

Perou, C.M., Sorlie, T., Eisen, M.B., van de Rijn, M., Jeffrey, S.S., Rees, C.A., Pollack, J.R., Ross, D.T., Johnsen, H., Akslen, L.A.*, et al.* (2000). Molecular portraits of human breast tumours. Nature *406*, 747-752.

Pizer, E.S., Thupari, J., Han, W.F., Pinn, M.L., Chrest, F.J., Frehywot, G.L., Townsend, C.A., and Kuhajda, F.P. (2000). Malonyl-coenzyme-A is a potential mediator of cytotoxicity induced by fatty-acid synthase inhibition in human breast cancer cells and xenografts. Cancer research *60*, 213-218.

Pizer, E.S., Wood, F.D., Heine, H.S., Romantsev, F.E., Pasternack, G.R., and Kuhajda, F.P. (1996). Inhibition of fatty acid synthesis delays disease

progression in a xenograft model of ovarian cancer. Cancer research *56*, 1189-1193.

Polyak, K., and Weinberg, R.A. (2009). Transitions between epithelial and mesenchymal states: acquisition of malignant and stem cell traits. Nature reviews Cancer *9*, 265-273.

Prat, A., Parker, J.S., Karginova, O., Fan, C., Livasy, C., Herschkowitz, J.I., He, X., and Perou, C.M. (2010). Phenotypic and molecular characterization of the claudin-low intrinsic subtype of breast cancer. Breast cancer research : BCR *12*, R68.

Prat, A., and Perou, C.M. (2011). Deconstructing the molecular portraits of breast cancer. Molecular oncology *5*, 5-23.

Qi, J., Nakayama, K., Cardiff, R.D., Borowsky, A.D., Kaul, K., Williams, R., Krajewski, S., Mercola, D., Carpenter, P.M., Bowtell, D.*, et al.* (2010a). Siah2-dependent concerted activity of HIF and FoxA2 regulates formation of neuroendocrine phenotype and neuroendocrine prostate tumors. Cancer cell *18*, 23-38.

Qi, J., Pellecchia, M., and Ronai, Z.A. (2010b). The Siah2-HIF-FoxA2 axis in prostate cancer - new markers and therapeutic opportunities. Oncotarget *1*, 379-385.

Rajagopalan, H., Bardelli, A., Lengauer, C., Kinzler, K.W., Vogelstein, B., and Velculescu, V.E. (2002). Tumorigenesis: RAF/RAS oncogenes and mismatch-repair status. Nature *418*, 934.

Rakha, E.A., El-Sayed, M.E., Green, A.R., Paish, E.C., Powe, D.G., Gee, J., Nicholson, R.I., Lee, A.H., Robertson, J.F., and Ellis, I.O. (2007). Biologic and clinical characteristics of breast cancer with single hormone receptor positive phenotype. Journal of clinical oncology : official journal of the American Society of Clinical Oncology *25*, 4772-4778.

Rakha, E.A., Reis-Filho, J.S., Baehner, F., Dabbs, D.J., Decker, T., Eusebi, V., Fox, S.B., Ichihara, S., Jacquemier, J., Lakhani, S.R.*, et al.* (2010). Breast cancer prognostic classification in the molecular era: the role of histological grade. Breast cancer research : BCR *12*, 207.

Riederer, M., Kofeler, H., Lechleitner, M., Tritscher, M., and Frank, S. (2012). Impact of endothelial lipase on cellular lipid composition. Biochimica et biophysica acta *1821*, 1003-1011.

Rivenbark, A.G., O'Connor, S.M., and Coleman, W.B. (2013). Molecular and Cellular Heterogeneity in Breast Cancer: Challenges for Personalized Medicine. The American journal of pathology.

Robbins, C.M., Tembe, W.A., Baker, A., Sinari, S., Moses, T.Y., Beckstrom-Sternberg, S., Beckstrom-Sternberg, J., Barrett, M., Long, J., Chinnaiyan, A.*, et al.* (2011). Copy number and targeted mutational analysis reveals novel somatic events in metastatic prostate tumors. Genome research *21*, 47-55.

Robinson, J.L., and Carroll, J.S. (2012). FoxA1 is a key mediator of hormonal response in breast and prostate cancer. Frontiers in endocrinology *3*, 68.

Robinson, J.L., Macarthur, S., Ross-Innes, C.S., Tilley, W.D., Neal, D.E., Mills, I.G., and Carroll, J.S. (2011). Androgen receptor driven transcription in molecular apocrine breast cancer is mediated by FoxA1. The EMBO journal *30*, 3019-3027.

Rohle, D., Popovici-Muller, J., Palaskas, N., Turcan, S., Grommes, C., Campos, C., Tsoi, J., Clark, O., Oldrini, B., Komisopoulou, E.*, et al.* (2013). An inhibitor of mutant IDH1 delays growth and promotes differentiation of glioma cells. Science *340*, 626-630.

Roos, S., Jansson, N., Palmberg, I., Saljo, K., Powell, T.L., and Jansson, T. (2007). Mammalian target of rapamycin in the human placenta regulates leucine transport and is down-regulated in restricted fetal growth. The Journal of physiology *582*, 449-459.

Rossell, D. (2009). GaGa: a simple and flexible hierarchical model for microarray data analysis. Annals of Applied Statistics, 1035–1051.

Rossell, D., Guerra, R., and Scott, C. (2008). Semi-parametric differential expression analysis via partial mixture estimation. Statistical applications in genetics and molecular biology *7*, Article15.

Rozengurt, E. (2011). Protein kinase D signaling: multiple biological functions in health and disease. Physiology (Bethesda) *26*, 23-33.

Russo, J., and Russo, I.H. (2004). Development of the human breast. Maturitas *49*, 2-15.

Sanchez-Cespedes, M., Parrella, P., Esteller, M., Nomoto, S., Trink, B., Engles, J.M., Westra, W.H., Herman, J.G., and Sidransky, D. (2002). Inactivation of LKB1/STK11 is a common event in adenocarcinomas of the lung. Cancer research *62*, 3659-3662.

Santisteban, P., Recacha, P., Metzger, D.E., and Zaret, K.S. (2010). Dynamic expression of Groucho-related genes Grg1 and Grg3 in foregut endoderm and antagonism of differentiation. Developmental dynamics : an official publication of the American Association of Anatomists *239*, 980-986.

Schafer, Z.T., Grassian, A.R., Song, L., Jiang, Z., Gerhart-Hines, Z., Irie, H.Y., Gao, S., Puigserver, P., and Brugge, J.S. (2009). Antioxidant and oncogene rescue of metabolic defects caused by loss of matrix attachment. Nature *461*, 109-113.

Scheel, C., Eaton, E.N., Li, S.H., Chaffer, C.L., Reinhardt, F., Kah, K.J., Bell, G., Guo, W., Rubin, J., Richardson, A.L.*, et al.* (2011). Paracrine and autocrine signals induce and maintain mesenchymal and stem cell states in the breast. Cell *145*, 926-940.

Selak, M.A., Armour, S.M., MacKenzie, E.D., Boulahbel, H., Watson, D.G., Mansfield, K.D., Pan, Y., Simon, M.C., Thompson, C.B., and Gottlieb, E. (2005). Succinate links TCA cycle dysfunction to oncogenesis by inhibiting HIF-alpha prolyl hydroxylase. Cancer cell *7*, 77-85.

Shackelford, D.B., Abt, E., Gerken, L., Vasquez, D.S., Seki, A., Leblanc, M., Wei, L., Fishbein, M.C., Czernin, J., Mischel, P.S.*, et al.* (2013). LKB1 inactivation dictates therapeutic response of non-small cell lung cancer to the metabolism drug phenformin. Cancer cell *23*, 143-158.

Siegel, R., Naishadham, D., and Jemal, A. (2013). Cancer statistics, 2013. CA: a cancer journal for clinicians *63*, 11-30.

Smith, C.A., Want, E.J., O'Maille, G., Abagyan, R., and Siuzdak, G. (2006). XCMS: processing mass spectrometry data for metabolite profiling using nonlinear peak alignment, matching, and identification. Analytical chemistry *78*, 779-787.

Smyth, G.K.R.G., Carey, V., Dudoit, S., Irizarry, R. and Huber W (2005). Limma: linear models for microarray data. In Bioinformatics and Computational Biology Solutions using R and Bioconductor. In New York: Springer, pp. pp. 397-420.

Song, Y., Washington, M.K., and Crawford, H.C. (2010). Loss of FOXA1/2 is essential for the epithelial-to-mesenchymal transition in pancreatic cancer. Cancer research *70*, 2115-2125.

Sorlie, T., Perou, C.M., Tibshirani, R., Aas, T., Geisler, S., Johnsen, H., Hastie, T., Eisen, M.B., van de Rijn, M., Jeffrey, S.S.*, et al.* (2001). Gene expression patterns of breast carcinomas distinguish tumor subclasses with clinical implications. Proceedings of the National Academy of Sciences of the United States of America *98*, 10869-10874.

Spoden, G.A., Mazurek, S., Morandell, D., Bacher, N., Ausserlechner, M.J., Jansen-Durr, P., Eigenbrodt, E., and Zwerschke, W. (2008). Isotype-specific inhibitors of the glycolytic key regulator pyruvate kinase subtype M2 moderately decelerate tumor cell proliferation. International journal of cancer Journal international du cancer *123*, 312-321.

Srere, P.A. (1972). The citrate enzymes: their structures, mechanisms, and biological functions. Current topics in cellular regulation *5*, 229-283.

Stam, J.C., Michiels, F., van der Kammen, R.A., Moolenaar, W.H., and Collard, J.G. (1998). Invasion of T-lymphoma cells: cooperation between Rho family GTPases and lysophospholipid receptor signaling. The EMBO journal *17*, 4066-4074.

Strauss, J.G., Zimmermann, R., Hrzenjak, A., Zhou, Y., Kratky, D., Levak-Frank, S., Kostner, G.M., Zechner, R., and Frank, S. (2002). Endothelial cell-derived lipase mediates uptake and binding of high-density lipoprotein (HDL) particles and the selective uptake of HDL-associated cholesterol esters independent of its enzymic activity. The Biochemical journal *368*, 69-79.

Sugden, M.C., and Holness, M.J. (2003). Recent advances in mechanisms regulating glucose oxidation at the level of the pyruvate dehydrogenase complex by PDKs. American journal of physiology Endocrinology and metabolism *284*, E855-862.

Sullivan, A.C., Triscari, J., Hamilton, J.G., Miller, O.N., and Wheatley, V.R. (1974). Effect of (-)-hydroxycitrate upon the accumulation of lipid in the rat. I. Lipogenesis. Lipids *9*, 121-128.

Tang, Y., Shu, G., Yuan, X., Jing, N., and Song, J. (2011). FOXA2 functions as a suppressor of tumor metastasis by inhibition of epithelial-to-mesenchymal transition in human lung cancers. Cell research *21*, 316-326.

Taubes, G. (2012). Cancer research. Cancer prevention with a diabetes pill? Science *335*, 29.

Thorat, M.A., Marchio, C., Morimiya, A., Savage, K., Nakshatri, H., Reis-Filho, J.S., and Badve, S. (2008). Forkhead box A1 expression in breast cancer is associated with luminal subtype and good prognosis. Journal of clinical pathology *61*, 327-332.

Vander Heiden, M.G. (2011). Targeting cancer metabolism: a therapeutic window opens. Nature reviews Drug discovery *10*, 671-684.

Vander Heiden, M.G., Cantley, L.C., and Thompson, C.B. (2009). Understanding the Warburg effect: the metabolic requirements of cell proliferation. Science *324*, 1029-1033.

Vazquez-Martin, A., Colomer, R., Brunet, J., and Menendez, J.A. (2007). Pharmacological blockade of fatty acid synthase (FASN) reverses acquired autoresistance to trastuzumab (Herceptin by transcriptionally inhibiting 'HER2 super-expression' occurring in high-dose trastuzumab-conditioned SKBR3/Tzb100 breast cancer cells. International journal of oncology *31*, 769-776.

Visvader, J.E. (2009). Keeping abreast of the mammary epithelial hierarchy and breast tumorigenesis. Genes & development *23*, 2563-2577.

von Meyenn, F., Porstmann, T., Gasser, E., Selevsek, N., Schmidt, A., Aebersold, R., and Stoffel, M. (2013). Glucagon-induced acetylation of Foxa2 regulates hepatic lipid metabolism. Cell metabolism *17*, 436-447.

Vousden, K.H., and Lu, X. (2002). Live or let die: the cell's response to p53. Nature reviews Cancer *2*, 594-604.

Vousden, K.H., and Ryan, K.M. (2009). p53 and metabolism. Nature reviews Cancer *9*, 691-700.

Walsh, M.J., Brimacombe, K.R., Anastasiou, D., Yu, Y., Israelsen, W.J., Hong, B.S., Tempel, W., Dimov, S., Veith, H., Yang, H.*, et al.* (2010). ML265: A potent PKM2 activator induces tetramerization and reduces tumor formation and size

in a mouse xenograft model. In Probe Reports from the NIH Molecular Libraries Program (Bethesda (MD)).

Wan, H., Dingle, S., Xu, Y., Besnard, V., Kaestner, K.H., Ang, S.L., Wert, S., Stahlman, M.T., and Whitsett, J.A. (2005). Compensatory roles of Foxa1 and Foxa2 during lung morphogenesis. The Journal of biological chemistry *280*, 13809-13816.

Wang, F., Travins, J., DeLaBarre, B., Penard-Lacronique, V., Schalm, S., Hansen, E., Straley, K., Kernytsky, A., Liu, W., Gliser, C.*, et al.* (2013). Targeted inhibition of mutant IDH2 in leukemia cells induces cellular differentiation. Science *340*, 622-626.

Wang, X., Jin, W., and Rader, D.J. (2007). Upregulation of macrophage endothelial lipase by toll-like receptors 4 and 3 modulates macrophage interleukin-10 and -12 production. Circulation research *100*, 1008-1015.

Ward, P.S., Patel, J., Wise, D.R., Abdel-Wahab, O., Bennett, B.D., Coller, H.A., Cross, J.R., Fantin, V.R., Hedvat, C.V., Perl, A.E.*, et al.* (2010). The common feature of leukemia-associated IDH1 and IDH2 mutations is a neomorphic enzyme activity converting alpha-ketoglutarate to 2-hydroxyglutarate. Cancer cell *17*, 225-234.

Ward, P.S., and Thompson, C.B. (2012). Metabolic reprogramming: a cancer hallmark even warburg did not anticipate. Cancer cell *21*, 297-308.

Weinberg, F., Hamanaka, R., Wheaton, W.W., Weinberg, S., Joseph, J., Lopez, M., Kalyanaraman, B., Mutlu, G.M., Budinger, G.R., and Chandel, N.S. (2010). Mitochondrial metabolism and ROS generation are essential for Kras-mediated tumorigenicity. Proceedings of the National Academy of Sciences of the United States of America *107*, 8788-8793.

Wiersma, H., Gatti, A., Nijstad, N., Kuipers, F., and Tietge, U.J. (2009). Hepatic SR-BI, not endothelial lipase, expression determines biliary cholesterol secretion in mice. Journal of lipid research *50*, 1571-1580.

Wise, D.R., DeBerardinis, R.J., Mancuso, A., Sayed, N., Zhang, X.Y., Pfeiffer, H.K., Nissim, I., Daikhin, E., Yudkoff, M., McMahon, S.B.*, et al.* (2008). Myc regulates a transcriptional program that stimulates mitochondrial glutaminolysis and leads to glutamine addiction. Proceedings of the National Academy of Sciences of the United States of America *105*, 18782-18787.

Wolf, I., Bose, S., Williamson, E.A., Miller, C.W., Karlan, B.Y., and Koeffler, H.P. (2007). FOXA1: Growth inhibitor and a favorable prognostic factor in human breast cancer. International journal of cancer Journal international du cancer *120*, 1013-1022.

Wolfrum, C., Asilmaz, E., Luca, E., Friedman, J.M., and Stoffel, M. (2004). Foxa2 regulates lipid metabolism and ketogenesis in the liver during fasting and in diabetes. Nature *432*, 1027-1032.

Wolfrum, C., Shih, D.Q., Kuwajima, S., Norris, A.W., Kahn, C.R., and Stoffel, M. (2003). Role of Foxa-2 in adipocyte metabolism and differentiation. Journal of Clinical Investigation *112*, 345-356.

Wolfrum, C., and Stoffel, M. (2006). Coactivation of Foxa2 through Pgc-1beta promotes liver fatty acid oxidation and triglyceride/VLDL secretion. Cell metabolism *3*, 99-110.

Wymann, M.P., and Schneiter, R. (2008). Lipid signalling in disease. Nature reviews Molecular cell biology *9*, 162-176.

Xu, R.H., Pelicano, H., Zhang, H., Giles, F.J., Keating, M.J., and Huang, P. (2005). Synergistic effect of targeting mTOR by rapamycin and depleting ATP by inhibition of glycolysis in lymphoma and leukemia cells. Leukemia *19*, 2153-2158.

Xu, Y., Fang, X.J., Casey, G., and Mills, G.B. (1995). Lysophospholipids activate ovarian and breast cancer cells. The Biochemical journal *309 (Pt 3)*, 933-940.

Yamamoto, T., Seino, Y., Fukumoto, H., Koh, G., Yano, H., Inagaki, N., Yamada, Y., Inoue, K., Manabe, T., and Imura, H. (1990). Over-expression of facilitative glucose transporter genes in human cancer. Biochemical and biophysical research communications *170*, 223-230.

Yan, H., Parsons, D.W., Jin, G., McLendon, R., Rasheed, B.A., Yuan, W., Kos, I., Batinic-Haberle, I., Jones, S., Riggins, G.J.*, et al.* (2009). IDH1 and IDH2 mutations in gliomas. The New England journal of medicine *360*, 765-773.

Yang, W., Xia, Y., Hawke, D., Li, X., Liang, J., Xing, D., Aldape, K., Hunter, T., Alfred Yung, W.K., and Lu, Z. (2012). PKM2 phosphorylates histone H3 and promotes gene transcription and tumorigenesis. Cell *150*, 685-696.

Yasuda, T., Ishida, T., and Rader, D.J. (2010). Update on the Role of Endothelial Lipase in High-Density Lipoprotein Metabolism, Reverse Cholesterol Transport, and Atherosclerosis. Circulation Journal *74*, 2263-2270.

Yecies, J.L., and Manning, B.D. (2010). Chewing the fat on tumor cell metabolism. Cell *140*, 28-30.

Young, S.G., and Zechner, R. (2013). Biochemistry and pathophysiology of intravascular and intracellular lipolysis. Genes & development *27*, 459-484.

Yun, J., Rago, C., Cheong, I., Pagliarini, R., Angenendt, P., Rajagopalan, H., Schmidt, K., Willson, J.K., Markowitz, S., Zhou, S.*, et al.* (2009). Glucose deprivation contributes to the development of KRAS pathway mutations in tumor cells. Science *325*, 1555-1559.

Zhang, L., Rubins, N.E., Ahima, R.S., Greenbaum, L.E., and Kaestner, K.H. (2005). Foxa2 integrates the transcriptional response of the hepatocyte to fasting. Cell metabolism *2*, 141-148.